To the Graduate Council:

I am submitting herewith a dissertation written by Clarence Richard Wobbe entitled "Studies on the Structure of the Virion and Replicative Form DNA of Kilham Rat Virus." I have examined the final copy of this dissertation for form and content and recommend that it be accepted in partial fulfillment of the requirements for the degree of Doctor of Philosophy, with a major in Biomedical Sciences.

Sankar Mitra

Sankar Mitra, Major Professor

We have read this dissertation
and recommend its acceptance:

Elliot Vallen

K Bruce Jacobson

Wen-Kung Yang

Fred C. Hartman

Accepted for the Council:

Lewis Winkel

Vice Provost
and Dean of the Graduate School

STUDIES ON THE STRUCTURE OF THE VIRION AND REPLICATIVE FORM DNA OF KILHAM RAT VIRUS

A Dissertation

Presented for the

Doctor of Philosophy

Degree

The University of Tennessee, Knoxville

Clarence Richard Wobbe

December 1984

DEDICATION

To Mom and Dad for their love and support.

To Archy and Mehitabel--they and their ancestors gave their all so that parvovirology could forge on.

ACKNOWLEDGMENTS

In preparing this section I have come to the realization that, although a scientist (or aspiring scientist) may, at times, feel lonely, he is never alone. This feeling is perhaps best summed up by Lewis Thomas, who, in his book The Lives of a Cell, compares scientists at a national meeting to ". . . assemblages of social insects" and later points out that although "We like to think of science as a lonely meditative business, . . . sooner or later we call to each other, communicate, publish, send letters to the editor, present papers, cry out on finding." To those to whom I have cried out, I would like to give thanks. Above all, my sincerest gratitude goes to my advisor, Dr. Sankar Mitra, for the time, advice, and guidance he has given to me over these past four (or so) years. Although it may not show, he has taught me more than I ever thought I was capable of learning and challenged me to be better than I thought I could be; I hope that my growth in these areas will continue.

For the vast majority of Chapter II of this dissertation, I am greatly indebted to Dr. Venki Ramakrishnan, an Oak Ridge alumnus currently at Brookhaven National Lab, without whom this work would have been, quite literally, impossible. His enthusiasm, intelligence, and sense of humor tricked me into an interest in, if not an understanding of, the field of biophysics. His close friendship has been one of my happiest memories of Oak Ridge.

I thank my dissertation committee, Drs. Fred C. Hartman, K. Bruce Jacobson, Elliot (Ken) Volkin, and Wen K. Yang, for their counsel. If it seemed I had a few too many committee meetings, it is only indicative of the value I place in their individual and collective knowledge and wisdom.

I would like to thank the members of my lab group, past and present, including Buzzy Morse, Liza Snow, Cathy Snyder, Joyce Feezell, Margaret Yette, Bill Dunn, and Bob Foote, who have helped me, technically and otherwise, over the years. Dr. Salil K. Niyogi has been a good friend, soccer teammate, goalie coach, and surrogate advisor in times of need. I also thank Drs. Audrey Stevens and Robert K. Fujimura for their advice, encouragement, and gifts of "materials and methods" when I came begging. In particular, I would like to express my thanks to Scott Fleming, who, in addition to helping with the phosphate and polyamine analyses, was a valuable friend and helped me maintain my sanity over the past year.

A number of members of the Biology Division have helped me over the years. Dr. K. Bruce Jacobson has reviewed manuscripts and listened to me "cry out" with a patience and insight that is little short of saintly. Dave Allison has been most gracious in taking electron micrographs and in allowing the use of his darkroom. Nette Crowe, Esther Thompson, and Willena Carter of the Division editorial staff, biology computer system manager Connie Schmidt, and our secretary, Marie Pickard, gave valuable assistance in the preparation of this manuscript and others.

I have also been greatly helped by many people from outside of Oak Ridge. To Drs. Robert C. Bates and Muriel Lederman of Virginia Tech, I say thanks for welcoming me into your lab and your homes when I visited. It was there that I first isolated the RF terminal proteins and learned how to do Cleveland peptide analysis. Other people cited in the following pages have been most generous in donating materials and technical advice, and have reinforced my belief in views of Lewis Thomas cited above.

For the many close friends I have made here, including Ellen Weiss, Alfred Johnson, Kris Nelson, Buzzy Morse, Jordan Fishman, Scott Fleming, Becky Furkes, and many others too numerous to mention, I am grateful. They have shared the best, and some of the worst, times of the past few years with me. I can honestly say that if it hadn't been for friends like them, I don't know if any of this would have been worth it.

Finally, I would like to express my sincere gratitude to Dr. Ben T. Feese of the Biology faculty of Centre College of Kentucky. Although our contacts over the past few years have been sporadic at best, he has never been far from my heart and he has always been willing to listen and share his valued insight and inspiration with me. After knowing people like these, I can only hope that my future in science will be as good a verification of Dr. Thomas' views as the past five years have been.

ABSTRACT

Three aspects of the chemistry and biology of Kilham rat virus (KRV), an autonomous parvovirus with a linear, single-stranded DNA genome of 5000 nucleotides, were examined. The structure of empty capsids of KRV was investigated by small-angle neutron scattering. The molecular weight was determined to be 4.0×10^6 and the radius of gyration was found to be 105 Å in D_2O and 104 Å in H_2O. The icosahedral capsid consists of two shells of protein: an inner shell, containing 11% of the capsid scattering mass and extending from 60-90 Å in D_2O and 50-91 Å in H_2O, which, based on its lower scattering density in D_2O than H_2O, appears to have a high content of basic amino acids, and an outer shell extending to 121 Å in H_2O and D_2O. We propose that the basic inner shell serves DNA binding and partial charge neutralization functions.

The second study showed that KRV viral and double-stranded replicative form (RF) DNA's lack methylated bases (less than 0.1 m^5C and m^6A per genome), while the host (normal rat kidney cell) DNA had 3% of its cytosines methylated. Both DNA's were methylated *in vitro* by the host DNA methyltransferase.

In the third study, evidence was presented that KRV RF DNA has protein covalently bound at its 5' termini. Three proteins, of 66, 64, and 55 kDa, are tightly but not covalently bound to purified RF DNA, two of which (66 and 64 kDa) cross-react with antibody to nuclear lamina proteins. After electrophoresis in

SDS/agarose, two proteins, of 90 and 40 kDa, are left bound to the DNA that are released only after nuclease treatment. Both of these proteins are associated, in a mutually exclusive manner, with terminal restriction fragments of the RF DNA and appear to share extensive sequence homology based on peptide analysis. One or both of them may represent the putative covalently bound 5'-terminal protein of the autonomous parvoviruses (Revie et al., 1979). None of these proteins cross-react with antibodies to any of the virus' gene products: the capsid proteins or an 85-90 kDa non-structural protein of unknown function.

TABLE OF CONTENTS

CHAPTER		PAGE
I.	GENERAL INTRODUCTION	1
	Classification and Properties of the Parvoviruses	1
	Autonomous Parvovirus Replication in Tissue Culture	7
	Infection	8
	Replication I--ss to Parental RF DNA Synthesis	11
	Replication II--RF DNA Replication	13
	Replication III--RF to ss DNA Synthesis	15
	Encapsidation and Virion Maturation	17
	Aims of the Dissertation	17
II.	STUDIES ON THE STRUCTURE OF THE CAPSID OF KILHAM RAT VIRUS	19
	Introduction	19
	Materials and Methods	24
	Materials	24
	Cells and Virus	24
	Virus Infection and Purification of Empty Capsids	24
	Amino Acid Analysis	25
	Phosphate Analysis	32
	Polyamine Analysis	32
	Electron Microscopy	33
	Neutron Scattering	33
	Data Analysis--Radius of Gyration and Forward Scatter	35
	Data Analysis--Calculation of Radial Density by Fourier Transformation	35
	Data Analysis--Contrast Variation for KRV Full Capsids	38
	Model Building	41
	Results	41
	Amino Acid Analysis	41
	Phosphate Analysis and Extinction Coefficient of KRV	41
	Polyamine Content of KRV	43
	Electron Microscopy of Empty and Full Capsids	43
	Neutron Scattering--Molecular Weight and Radius of Gyration	43
	Neutron Scattering--Radial Density Function	48
	Model Building	51
	Contrast Variation and Radius of Gyration of DNA	57
	Discussion	57
III.	METHYLATION OF KRV VIRAL AND REPLICATIVE FORM DNA	70
	Introduction	70
	Materials and Methods	71

CHAPTER PAGE

III. (Continued)

Virus Growth and Labeling. 71
Isolation of Viral and Cellular DNAs 71
Hydrolysis of DNA to Bases or Nucleosides. 74
Thin Layer Chromatography. 74
Separation of Methylated Nucleosides by High-performance Liquid Chromatography. 75
Purification of Regenerating Rat Liver DNA Methyltransferase and In Vitro Methylation of DNA. 75
Results. 78
5-methylcytosine Content of KRV Viral and RF DNA and NRK Cell DNA 78
Methylation of KRV DNA In Vitro. 81
Discussion 81

IV. ISOLATION AND CHARACTERIZATION OF PROTEINS TIGHTLY BOUND TO THE REPLICATIVE FORM DNA OF KRV 93
Introduction 93
Materials and Methods. 95
Materials. 95
Cells and Virus. 95
Infection of Cells and Purification of RF DNA. 95
Alkaline CsCl Sedimentation. 101
Labeling and Isolation of NRK Cell DNA 101
Nuclease Digestions. 102
Radioiodination of Proteins. 102
Peptide Analysis 103
Results. 103
Rate of Synthesis of KRV RF DNA and NRK Cell DNA 103
Restriction Digestion. 107
Gel Electrophoresis. 107
Electrophoretic Transfer and Immunoblotting. 108
Evidence for Proteins Covalently Bound to KRV RF DNA--Electrophoretic Mobility 109
Evidence for Proteins Covalently Bound to KRV RF DNA--Isopycnic Sedimentation. 114
Evidence for Proteins Covalently Bound to KRV RF DNA--Copurification of ^{35}S and ^{3}H Label 119
Exonuclease Sensitivity of RF DNA. 119
Proteins Associated with CsCl-purified RF DNA. 130
Binding of Uninfected Cellular Proteins to Deproteinized RF 135
Proteins Associated with Electrophoretically Purified RF. 136
Association of Protein with Terminal Restriction Fragments. 136

CHAPTER PAGE

IV. (Continued)

Immunoblot Analysis of Covalently and Non-covalently Bound Proteins 139
Peptide Analysis 149
Alkaline Agarose Gel Electrophoresis of PstI-digested RF DNA 149
Discussion 154

V. SUMMARY AND PERSPECTIVES 161

BIBLIOGRAPHY. 169

VITA. 179

LIST OF TABLES

TABLE		PAGE
1.	Nucleic acid phosphate charge neutralization mechanisms of various viruses.	21
2.	Amino acid analysis of KRV empty capsids.	42
3.	Structural parameters for one- and two-shell models of KRV.	52
4.	Parameters for contrast variation of KRV full capsids . .	58
5.	In vitro methylation of KRV mature viral and RF DNA . . .	79
6.	Transfer of methyl-^{3}H from [methyl-^{3}H]methionine to DNA bases	80

LIST OF FIGURES

FIGURE		PAGE
1.	Replication model for Kilham rat virus	9
2.	Electron micrographs of empty and full KRV capsids at various pH's	26
3.	Ultraviolet spectrum of KRV empty capsids	28
4.	Ultraviolet spectrum of KRV full capsids	30
5.	Guinier plot (ln(I) vs. k^2) for KRV empty capsids in D_2O	36
6.	Separation of dansylated polyamines by high-performance liquid chromatography	44
7.	Ratio of stain-permeable to stain-impermeable particles of KRV	46
8.	Radial density function for KRV empty capsids in H_2O and D_2O	49
9.	Desmeared experimental scattering values for KRV empty capsids (16.6 mg/ml) in H_2O (a) and D_2O (b) compared to model theoretical scattering curves for single- and double-shelled capsids with properties described in Table III	53
10.	Cross section of model for the structure of KRV	55
11.	R_g^2 vs. reciprocal contrast for KRV full capsids in 10 mM Tris-HCl, pH 8.0	59
12.	Schematic illustration of KRV capsid proteins A, B, and C showing location of basic amino acids predicted from nucleotide sequence of H-1 capsid protein genes of Rhode and Paradiso (1983)	65
13.	Equilibrium sedimentation in neutral CsCl of KRV full virions from cells labeled with [methyl-^{3}H]methionine or [6-^{3}H]uridine	72
14.	Schematic diagram of thin layer chromatogram of bases A, C. T, G, m^5C, and m^6A	76

FIGURE PAGE

15. High-pressure liquid chromatogram of nucleosides from [6-^{3}H]uridine labeled NRK cell DNA 82

16. High-pressure liquid chromatogram of nucleosides from [6-^{3}H]uridine-label KRV virion DNA 84

17. High-pressure liquid chromatogram of nucleosides from [6-^{3}H]uridine-labeled KRV RF DNA 86

18. One percent agarose gel electrophoresis of [^{3}H]thymidine-labeled RF DNA and RF DNA methylated *in vitro* by regenerating rat liver DNA methyltransferase and [methyl-^{3}H]S-adenosylmethionine. 88

19. One percent agarose gel electrophoresis of KRV viral DNA labeled *in vitro* with regenerating rat liver DNA methyltransferase and [methyl-^{3}H]S-adenosylmethionine. . . 90

20. Guanidine-HCl/sucrose gradient of intracellular replicative form DNA's of KRV 97

21. One percent agarose gel electrophoresis of guanidine-HCl/sucrose gradient-purified KRV intracellular RF DNA's . . . 99

22. Rate of synthesis of NRK cell DNA and KRV RF DNA infection time 104

23. One percent agarose gel electrophoresis of KRV RF DNA after: (A) no treatment; (B) phenol extraction in the presence of 2% 2-mercaptoethanol; and (C) proteinase K digestion. 110

24. One percent agarose gel electrophoresis of KRV RF DNA after exposure to alkali 112

25. One percent agarose gel electrophoresis of PstI digested RF DNA before and after proteinase K digestion. 115

26. Neutral CsCl gradient sedimentation of KRV RF DNA before and after digestion with proteinase K 117

27. Guanidine-HCl/sucrose gradient of [^{35}S]methionine and [^{3}H]thymidine labeled KRV RF DNA 120

28. Neutral CsCl gradient sedimentation of [^{35}S]methionine and [^{3}H]thymidine labeled KRV RF DNA 122

FIGURE PAGE

29. Alkaline CsCl gradient sedimentation of KRV RF DNA from [^{35}S]methionine and [^{3}H]thymidine labeled cells 124

30. SDS/agarose gel electrophoresis of KRV RF DNA from cells labeled with [^{35}S]methionine and [^{3}H]thymidine . . . 126

31. Sensitivity of KRV RF DNA and bacteriophase T5 DNA to λ exonuclease and E. coli exonuclease III. 128

32. Autoradiogram of 1% SDS/agarose gel of ^{125}I-labeled KRV RF DNA before and after digestion with proteinase K. 131

33. Autoradiogram of SDS/polyacrylamide gels of ^{125}I-labeled proteins associated with KRV RF DNA. 133

34. Autoradiogram of SDS/polyacrylamide gel of ^{125}I-labeled proteins associated with electrophoretically purified RF DNA. 137

35. Autoradiogram of SDS/polyacrylamide gel of ^{125}I-labeled proteins associated with electrophoretically purified HpaII restriction fragments of RF DNA 140

36. Autoradiogram of "Western" immunoblot of KRV capsid proteins and nuclease-treated CsCl-purified KRV RF DNA incubated with rabbit anti-KRV capsid antiserum and ^{125}I protein A 142

37. Autoradiogram of "Western" immunoblot of KRV infected NRK cell lysate and nuclease-digested CsCl-purified KRV RF DNA incubated with PPV-infected pig or H-1-infected hamster antiserum and ^{125}I protein A 145

38. Autoradiogram of "Western" immunoblot of uninfected NRK cell lysate and CsCl-purified KRV RF DNA incubated with guinea pig anti-rat lamin C and ^{125}I protein A. . . . 147

39. Autoradiogram of 15% SDS/polyacrylamide gel of partial proteolytic digests of ^{125}I RF TP-90 and RF TP-40 150

40. Alkaline SDS/agarose gel (1.5%) electrophoresis of PstI-digested KRV RF DNA before and after digestion with proteinase K. 152

CHAPTER I

GENERAL INTRODUCTION

1. CLASSIFICATION AND PROPERTIES OF THE PARVOVIRUSES

Parvoviruses, belonging to the family Parvoviridae, are among the smallest known DNA-containing animal viruses and are the only known animal viruses with a single-stranded genome (Frankel-Conrat, 1974). With an icosahedral capsid 20-25 nm in diameter and a linear single-stranded (ss) DNA genome of 4500-5000 bases they are, in fact, among the smallest of all viruses.

The first parvovirus isolated was the feline panleukopenia virus, etiologic agent of one of the most deadly diseases of cats (Lepine and Pavilanis, 1948), although at the time no characterization of the virus was made and the family designation had not yet been proposed. The first cultivation of parvoviruses in tissue culture came with the isolation of Kilham rat viruses (KRV) from two rat tumor cell lines by Kilham and Oliver (1959). This was the first detailed effort at characterization of these viruses as a distinct group. KRV is currently regarded as one of the prototype members of Parvoviridae (Siegl, 1976).

The apparent governing principle in the pathobiology of this family is perhaps best described by Margolis and Kilham (1975b) as follows: ". . . the dynamics of cell proliferation is the major determinant of viral replication and localization of cytopathic

effects . . . where tissue growth has been the most active, viral involvement has been the heaviest." This is reflected in a preferential infection of fetuses and neonates and mitotically active tissues of older animals (Margolis and Kilham, 1975 a,b), usually leading to extensive tissue damage due to the highly cytopathic nature of the parvoviruses. In older cats, feline panleukopenia virus has been observed to attack mitotically active support tissues surrounding the cerebellum, resulting in ataxia and, ultimately, death (Margolis and Kilham, 1970). Parvovirus infections have also been observed in regenerating tissues of older animals after partial hepatectomy (Ruffolo et al., 1966) and in healing bone fractures (Engler et al., 1966). The first parvovirus etiologic agent of a human disease, B19, was recently isolated from children with a mild form of anemia known as fifth disease of children (Marx, 1984).

There are three genera within the family Parvoviridae, based on their host range specificity and requirement for coinfection by a helper virus. One genus is designated adeno-associated virus (AAV) or dependovirus, also sometimes referred to as the defective parvoviruses (reviewed by Berns and Hauswirth, 1979). These viruses are dependent upon coinfection with adenovirus helper for replication and almost any cell line that can support adenovirus replication can also be productively infected with AAV. Although each virion encapsidates a single strand of DNA, both strands are packaged with approximately equal frequency in separate virions. In the absence of helper, no AAV DNA is replicated and no AAV protein is produced.

A second genus, Densonucleosis virus (DNV), first reported in insect larvae by Meynadier et al. (1964), is found exclusively in arthropods. Unlike AAV, they have no helper requirement and hence are termed non-defective, or autonomous, parvoviruses. Like AAV, these viruses package complementary DNA single strands in separate virions with equal frequency. The DNV isolated thus far have been found to have four capsid proteins instead of the three found in most other parvoviruses (Tijssen et al., 1976).

The third and largest genus of the family is designated simply as Parvovirus. It includes a number of viruses infecting a wide variety of vertebrate hosts: KRV, minute virus of mice (MVM), H-1 parvovirus, LuIII parvovirus, canine, bovine, and porcine parvoviruses, feline panleukopenia virus, and B19. These viruses are all non-defective and, unlike DNV and AAV, most of them package a unique DNA strand into the virion, the minus strand, or the strand complementary to their messenger RNA. Exceptions to the unique packaging rule are LuIII, which packages both strands with equal frequency (Bates et al., 1984), and bovine parvovirus (BPV) in which approximately 30% of the virions contain a plus strand (R. C. Bates, personal communication).

Despite the wide variety of hosts they infect, the parvoviruses share a large number of characteristics in common. They all have icosahedral, non-enveloped capsids containing about 60 protein molecules (Tattersall, 1978). Based on buoyant density in CsCl, four types of capsids have been observed during a productive

infection (Tattersall, 1978). Empty capsids banding at 1.30-1.32 g/cc usually have an $s_{20,w}$ of 70S and are devoid of DNA. Three classes of DNA-containing, full capsids have been reported. Particles banding at 1.38-1.43 g/cc and 1.46-1.48 g/cc sediment at 110S and have a full-length complement of genomic DNA, while particles banding at 1.32-1.38 g/cc have sedimentation coefficients intermediate between empty capsids and full capsids and contain shorter than full-sized DNA molecules. As will be discussed in detail later, the heavier of the two complete-genome-containing full capsids is probably a precursor to the lighter during the maturation of the virion.

The capsid of the parvoviruses is comprised of three or four different proteins (Tattersall, 1978). In Chapter II, evidence will be reviewed demonstrating that these proteins share a great deal of primary sequence homology, in agreement with the common coding sequences for these proteins, illustrating the remarkably efficient use of the limited coding capacity of these viral genomes. The precise three-dimensional arrangement of these proteins in the capsid is not known; observations presented in Chapter II pertain to this area.

In addition to its simplicity, the parvovirus capsid is also known to be quite stable to a number of harsh conditions such as high temperatures and exposure to ether, chloroform, low pH and ionic detergents for extended periods (Kilham and Oliver, 1959). Studies on the structure of these viruses such as those presented

in Chapter II should give not only insights into how this stability is maintained, but also into some of the more general principles of how viruses are organized.

As mentioned above, parvoviruses encapsidate a linear single-stranded DNA genome 5000-5500 bases in length (Berns and Hauswirth, 1978; Snyder et al., 1982). Physical and enzymatic analysis of the viral DNA suggests there are 110-130 nucleotide long base-paired hairpin structures at both the 5' and 3' termini (Bougignon et al., 1976; Rhode, 1977b; Salzman, 1977; Lavelle and Mitra, 1978). DNA sequence data (Fife et al., 1978; Astell et al., 1979) has shown that palindromes do exist at the termini and that the sequences involved are highly conserved among the parvoviruses. A distinguishing feature of AAV DNA is that it possesses inverted terminal repeats in addition to palindromes so that "panhandled" molecules can be formed by hydrogen-bonding of the 5' and 3' terminal regions of a given DNA molecule (Koczot et al., 1973). It is thought that these hairpins are used for the initiation of DNA replication as will be discussed below.

Several studies have pointed out the limited coding capacity of the genomes of these viruses (Rhode and Paradiso, 1983; Astell 1983; Pintel et al., 1983). Only two overlapping transcription units have been identified, one initiating at 4 map units on the DNA (the genome defined as having 100 map units starting from the 3' end of the viral strand, complementary to the mRNA), and the other at 38 map units. Both are transcribed off of the minus strand, which

is in most cases the DNA of the mature virion. Sequence data indicate that only two open translational reading frames exist in the genome, one in the 3' proximal half and one in the 5' proximal half (Rhode and Paradiso, 1983; Astell et al., 1983; Pintel et al., 1983). The 4 map unit primary transcript spans the entire genome and includes both of these reading frames but alternative RNA processing events give rise to two mRNAs. The longer of these two mRNAs still contains both reading frames, but in vitro translation data indicate that only the genomic 3'-proximal reading frame is utilized, giving rise to an 80-90 kilodalton (kDa) non-capsid protein of unknown function (Rhode and Paradiso, 1983; Pintel et al., 1983; Cottmore et al., 1983; Paradiso, 1984). The other mRNA generated from this primary transcript contains only the 5'-proximal open reading frame plus a small portion of a third, very short reading frame and is translated in vitro to give the largest of the capsid proteins, the A protein (Rhode and Paradiso, 1983; Pintel et al., 1983; Paradiso et al., 1984). The second primary transcript is processed to give an mRNA that contains only the 5'-proximal reading frame and coding for the other two capsid proteins, B and C (Rhode and Paradiso, 1983; Pintel et al., 1983; Paradiso et al., 1984).

Two interesting properties of the genome of autonomous rodent parvoviruses are worthy of note. First, the inverted repeats of the termini are non-identical and thus the DNA cannot form "pandandle" structures, analogous to adenovirus (Stillman, 1983). This difference in structure from AAV may portend key differences in the DNA

replication mechanisms of viruses in these two genera. Secondly, there is a high degree of DNA sequence conservation among the rodent parvoviruses particularly in the 3' half of the viral genome (Banerjee et al., 1983). This conservation would explain the strong antigenic cross-reactivity of the autonomous parvovirus non-capsid proteins (Cottmore et al., 1983; Rhode and Paradiso, 1983), which are encoded by this region, and may imply that this protein plays some vital, common role in the replication of the autonomous parvoviruses. Moreover, replication-deficient deletion mutants of H-1 which lack this region can be complemented by wild-type KRV and MVM (Rhode, 1982). The sequence divergence in the 5' half of the viral genome (Banerjee et al., 1983), the region which encodes the capsid proteins (Rhode and Paradiso, 1983; Pintel et al., 1983), could explain the rather stringent host range specificity of these viruses.

2. AUTONOMOUS PARVOVIRUS REPLICATION IN TISSUE CULTURE

One of the conclusions from the pathobiology of parvovirus infections is that highly mitotic tissues are required for virus replication. This requirement was shown to exist for parvovirus infections in tissue culture as well by Tennant et al. (1969, 1970). Growth-arrested or quiescent cells were shown to be incapable of supporting the growth of KRV, but when the block to cell growth was removed, viral DNA replication and progeny virus production were resumed.

The following discussion is intended to review briefly the major steps in the parvovirus life cycle with particular emphasis

given to events associated with the DNA replication and assembly of the virus. The DNA replication model to be presented is a variation of the "hairpin transfer" model of Cavalier-Smith (1974) for the replication of the ends of linear DNA molecules. This model has been adapted to the parvoviruses by a number of authors (Tattersall et al., 1976; Berns and Hauswirth, 1979; Mitra, 1980; Astell et al., 1982), but for the purposes of this discussion, only the model of Mitra (1980), as modified and presented in Figure 1, will be considered in detail. Since no known DNA polymerase can initiate DNA synthesis in the absence of an RNA or ribonucleotide primer, the priming and synthesis of DNA complementary to the 3' end of linear DNA molecules, such as eukaryotic chromosomes and the genome of KRV, presents a mechanistic problem. This model explains how the problem has been oversome in the case of parvoviruses and has been invoked, in necessarily altered form, for eukoryotic chromosomal replication as well (Szostak and Blackburn, 1982).

Infection

After addition of KRV to host cells, there is a very rapid endocytosis of the virus in which more than 80% of the virus is removed from the medium in the first 60 minutes (Salzman et al., 1972). The virus is then transported to nucleus, where the DNA is replicated and transcribed. Shortly thereafter, the first detectable virus antigen is seen in the cytoplasm, in some cases within 5 hours post-infection in asychronous cultures (Cole and Nathanson, 1969).

Figure 1. Replication model for Kilham rat virus. Structure I represents an infecting DNA molecule; a, b, c, d, e, f, g, h represent cucleotides with complements a', b', c', d', e', f', g', h'. Cross-hatched rectangles represent blockage of pathways due to mutations indicated (see text for description). Wavy and boldfaced lines represent newly synthesized DNA. O- represents the covalently bound 5' terminal protein. KRV_{heavy} and KRV_{light} refer to the high and low buoyant density forms of KRV full capsids, respectively.

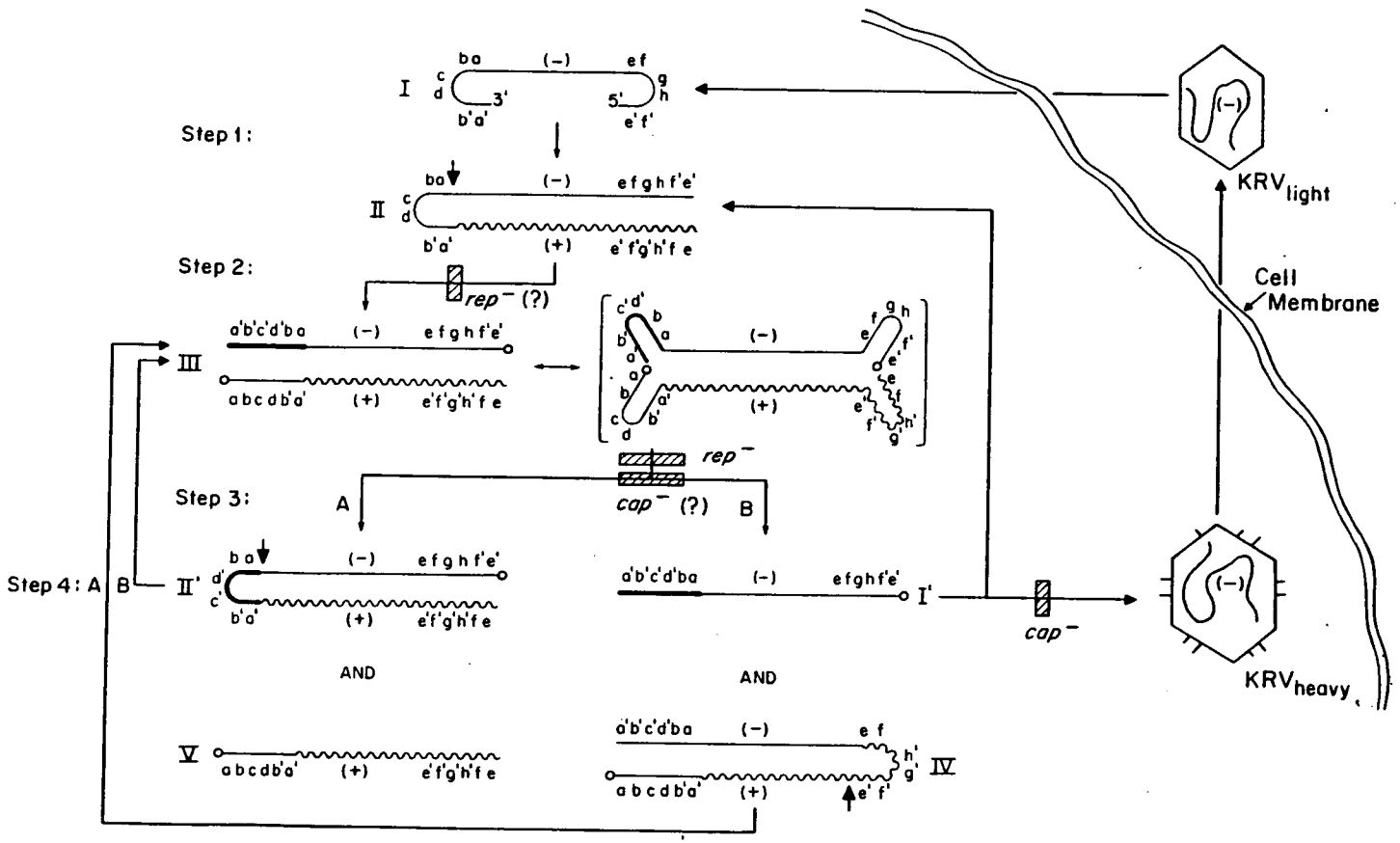
Step 1:
Step 2:
Step 3:
Step 4: A B
I
II
III
II'
I'
IV
V
rep⁻ (?)
rep⁻
cap⁻ (?)
cap⁻
AND
AND
KRV light
KRV heavy
Cell Membrane

Figure 1

Replication I--ss to Parental RF DNA Synthesis

The first step, following infection, in parvovirus replication involves the conversion of the ss viral DNA molecule to a linear double-stranded (ds) replicative form (RF) DNA (step 1, Figure 1) (Rhode, 1973, 1974a,b; Dobson and Helleiner, 1973; Salzman and White, 1973) which can then be used as a template for the production of progeny ss viral DNA. This step will be referred to as parental RF DNA replication to emphasize that it is directed by the infecting DNA molecule.

In experiments where asynchronously growing cells were infected with ^{3}H-labeled KRV, parental RF DNA synthesis was observed as early as 1 hour post-infection (Salzman and White, 1973). Later attempts to demonstrate this rapid conversion in synchronous cultures were unsuccessful (Rhode, 1974b). Instead, RF DNA synthesis was observed to initiate 8-10 hours after host S-phase had commenced, which, in these experiments, was several hours post-infection, leading to the proposal that some cellular factor expressed "late" in S-phase was required for parental RF DNA synthesis (Rhode, 1974a,b; Siegl and Gautschi, 1976). As will be discussed later, RF DNA synthesis can be detected much closer to the start of S-phase and problems with high particle-to-infectivity ratios and low signal-to-noise ratios for RF DNA detection may have led some workers to observe initial RF DNA synthesis at a time much later than it actually occurred. Moreover, since parental RF DNA must be synthesized before transcription can take place (Rhode, 1973, 1974a) and since the first viral

proteins can be detected within 5 hours post-infection (Cole and Nathanson, 1969), it is clear that at least a few RF DNA molecules can be synthesized very early after infection.

According to the generally accepted models of parvovirus DNA replication, and as depicted in Figure 1, the first event in the conversion of the ss viral DNA to a ds RF DNA is the use of the 3' terminal hairpin as a primer-template for replication primed by the free 3'-hydroxyl group. Two pieces of evidence make this self-priming initiation mechanism seem likely. First, the 3'-OH can be utilized by a number of prokaryotic DNA polymerases in vitro to generate a full-length duplex molecule in the absence of RNA priming (Bourgignon et al., 1976; Banerjee et al., 1981). Second, some RF DNA molecules have been found to contain covalently linked viral and complementary strands (structure II, Figure 1) (Rhode, 1977a). However, direct kinetic evidence showing the use of the viral 3' terminus as a replication origin has not been presented.

The next step in parental RF DNA synthesis is believed to be the introduction of a nick near the 3' end of the viral strand by an as yet undiscovered site-specific endonuclease. The 3'-OH terminus of this nick would then be extended by displacement synthesis (step 2, Figure 1) giving rise to a full-length duplex DNA molecule (structure III, Figure 1). Most of the RF DNA isolated from infected cells has this fully extended configuration (Rhode, 1977a; Banerjee et al., 1981). As will be discussed later, most of this RF DNA also appears to have a protein covalently bound to its 5' termini (Revie et al., 1979; Astell et al., 1982).

It is not yet clear which cellular DNA polymerase(s) catalyze(s) the replication of the viral DNA. Based on the synthesis of BPV RF DNA in a crude lysate in the presence of various inhibitors, Pritchard et al. (1981) concluded that DNA polymerase α alone is necessary and sufficient. In similar studies using H-1, however, it was concluded that both DNA polymerases α and γ are required for H-1 RF DNA synthesis (Kolleck et al., 1982). The latter studies further argued that, because DNA polymerase α cannot use a single-stranded template while DNA polymerase γ can, the latter is probably used in vivo for the initial ss to RF DNA synthesis while polymerase α is used for the subsequent displacement synthesis reactions. The fact that DNA polymerase γ is used almost exclusively for mitochondrial DNA replication (Bolden et al., 1977) (parvovirus replication takes place strictly in the nucleus) and the recent discovery of forms of DNA polymerase α which can, in the presence of ATP, fully replicate ss parvoviral DNA (Faust et al., 1984) cast doubt on the physiological significance of experiments involving DNA polymerase γ.

Replication II--RF DNA Replication

As with the replicative cycle of ϕX174 (Sims et al., 1978), the next stage in KRV DNA replication is considered to be RF DNA replication, also known as progeny RF DNA synthesis. Since both ends of the DNA can form stable hairpins as depicted in Figure 1, it would appear that this synthesis could originate at both termini giving two RF DNA's. However, the results of Rhode (1977a) and

Singer and Rhode (1977a,b) indicate that only one hairpin, at the 3' end of the complementary strand, is used preferentially (step 3B, Figure 1). This would give rise to RF DNA plus a displaced viral (minus) strand as depicted in step 3A in Figure 1. The difficulty in interpreting these results, as will be seen shortly, is in distinguishing the net synthesis of dsRF DNA from pre-existing RF DNA molecules (RF DNA replication), which would still use both termini as replication origins, from ss viral DNA synthesis (step 3B, Figure 1).

As in ss to RF DNA synthesis, a site-specific nicking endonuclease would be used to generate full-length duplexes after extension by DNA polymerase. One consequence of the repeated use of the plus strand 3' terminus as a replication origin in the manner indicated is that half of the RF DNA ends would have one orientation ("flip") while the other half would have the opposite orientation ("flop") due to the transfer of the hairpin from the plus strand to the minus strand as a result of the nicking reaction and because of a lack of perfect complementarity of the hairpin sequences. This sequence alternation has been observed at the 5' end but not at the 3' end of mature virion DNA (Rhode and Klaassen, 1982; Astell et al., 1982) again suggesting selective use of the complementary strand 3' terminus as a replication origin.

Two classes of mutants of H-1, designated rep$^-$ mutants, have been isolated that appear to be defective in this stage of replication. A cis-acting temperature sensitive mutation has been isolated which

presumably has a defect in some sequence which regulates replication (Rhode, 1978). Deletion mutants of H-1 have also been obtained which can be complemented in trans by a number of parvoviruses (Rhode, 1982). It has not been established whether parental and progeny RF DNA synthesis or just progeny RF DNA synthesis is blocked by these mutations, but it is likely that only the latter is affected since parental RF DNA synthesis must take place prior to virus transcription (see above). All of these mutations are located in the highly conserved 3' half of the viral genome, in the coding sequence for the 90 kDa non-structural protein, suggesting that this protein is required for RF synthesis, although its function remains unknown.

Replication III--RF to ss DNA Synthesis

Repetitive initiations at the 3'-OH of the complementary strand are responsible for the net synthesis of ss viral DNA as depicted in step 3B of Figure 1. Although the mechanisms by which the two processes take place appear to be identical, RF to RF DNA replication and RF to ss DNA replication can be distinguished in mutants which appear to selectively depress the production of progeny ssDNA. Both temperature sensitive (Rhode, 1976) and deletion mutants (Merchlinski et al., 1983) have been isolated in which the accumulation of progeny RF appears normal or slightly above normal but the synthesis of ss viral DNA has been reduced or eliminated. In both cases, the mutations have been localized to the 5' half of the viral genome, the region encoding the capsid proteins, and consequently they are designated cap$^-$ mutations. This situation would be analogous to

ØX174 where progeny ssDNA synthesis is blocked by mutants defective in capsid protein synthesis (Fujisawa and Hayashi, 1977; Sims et al., 1978).

There are at least three possible explanations for the apparent lack of accumulation of progeny viral DNA in the capsid mutants: (a) the capsid proteins or capsid assembly intermediates may be required for the initiation of ssDNA synthesis; (b) the capsid proteins may protect the viral DNA from degradation and in their absence the half-life of the viral DNA may be greatly shortened; (c) rapid encapsidation prevents recycling of ssDNA into ss to RF DNA synthesis and in the capsid mutants, where encapsidation cannot occur, the viral DNA is quickly converted to RF DNA. Several observations make the third explanation seem most likely. Even during productive infections with wild-type virus, very little free ss viral DNA is seen (Rhode, 1976; Siegl and Gautschi, 1976; Myers and Carter, 1981). Almost immediately after its synthesis, viral DNA appears in a faster sedimenting nucleoprotein complex from which it cannot be extracted by conventional procedures for the isolation of free low molecular weight DNA (Siegl and Gautschi, 1976). Working with a crude nuclear lysate system capable of supporting DNA replication and encapsidation, Muller and Siegl (1983a,b) found nascent viral DNA to be present in virions within 15 minutes after its synthesis. By analogy, rapid encapsidation of viral DNA is thought to be used in ØX174 replication for the same reason (Fujisawa and Hayashi, 1977; Sims, 1978).

Encapsidation and Virion Maturation

Based on the above observations and on electron microscopic examination of virus maturation in infected cells (Richards et al., 1977), it is thought that the capsid proteins self-assemble into partial capsids into which the viral DNA is quickly packaged during or immediately after its synthesis as depicted in Figure 1 (p. 9). The large number of empty capsids produced during infection are probably the result of synthesis of capsid proteins in excess of what is needed for DNA packaging, or they may reflect inefficiency in the encapsidation process itself.

Once the DNA is packaged inside, the virion undergoes proteolytic processing in which about 30 amino acids are removed from the carboxyl terminus of one of the two capsid proteins, generating the third capsid protein (Clinton and Hayashi, 1975, 1976; Richards et al., 1977; Tattersall et al., 1977). This "maturation" process results in a decrease in buoyant density and an increase in infectivity of the virus particle and will be discussed in more detail in Chapter II.

3. AIMS OF THE DISSERTATION

Two major areas of research will be discussed in the following chapters. The first (Chapter II) is a study of the structure of KRV and mechanisms of stabilization of this structure. Structural studies using small angle neutron scattering were used to determine the radial distribution of protein in the capsid and the possible interactions

between capsid proteins and the viral DNA. Factors involved in the charge neutralization of the DNA as a means of stabilizing the virus structure were also examined. The viral and intracellular RF DNA were also examined for the presence of modified bases such as 5-methylcytosine and 6-methyladenine (Chapter III).

The second area of research (Chapter IV) involves the identification of proteins which are tightly bound to the intracellular RF DNA of KRV. Two proteins have been identified and partially characterized which appear to correspond to the covalently bound RF terminal proteins proposed by others (Revie et al., 1979; Astell et al., 1982). In addition, other proteins were found which are very tightly, but non-covalently bound to the RF DNA, some of which appear to originate from the nuclear lamina. The possible role of nuclear cytoskeletal structures in parvovirus replication and assembly will be discussed.

CHAPTER II

STUDIES ON THE STRUCTURE OF THE CAPSID OF KILHAM RAT VIRUS

1. INTRODUCTION

The capsid of KRV consists of three proteins--A, B, and C--with apparent masses of 80, 64, and 59 kilodaltons (kDa), respectively (Mitra et al., 1982). In MVM, these three proteins appear to share extensive sequence homology on the basis of two-dimensional peptide mapping (Tattersall et al., 1977). This is consistent with other experimental evidence indicating that: i) messages for polypeptides A and B are transcribed from overlapping regions of the viral genome in H-1 (Rhode and Paradiso, 1983), and ii) protein C is generated by proteolytic cleavage of B during the maturation of DNA-containing, full virions (Clinton and Hayashi, 1975, 1976). The cleavage of B is accompanied by a decrease in the virion's buoyant density in CsCl and an increase in infectivity.

The A protein is particularly interesting for two reasons. First, it is present in both empty and full capsids in roughly a constant proportion relative to B and C (about 1:6) (Tattersall et al., 1976). Moreover, A does not undergo maturational proteolytic cleavage, unlike B, despite the fact that the B sequence is contained within A (Tattersall et al., 1977). Second, the region of the A protein that does not overlap with B or C is known to contain highly basic peptides that give the A protein a much more basic pI than

B or C (Mitra et al., 1982; Tattersall et al., 1976). Together, these observations suggest a conformation-specific functional role for the A protein in the virus capsid, possibly in DNA binding and partial charge neutralization.

The mechanism by which KRV utilizes its capsid proteins to package its DNA and maintain its stability will be one of the major concerns of this chapter. Riemer and Bloomfield (1978) described four factors which, in order of decreasing contribution, contribute to a high positive Gibbs free energy for the packaging of viral nucleic acid: polyelectrolyte repulsion of the negatively charged nucleic acid phosphate groups, the melting of short regions of the double helix (in the case of duplex genomes) due to torsional strain or sharp turns of the polymer chain, bending of the double helix, the loss of entropy upon condensation of DNA chain. Only two of these factors are relevant to KRV, namely polyelectrolyte repulsion and condensation, since the single-stranded nature of KRV DNA precludes any necessity for melting a double helix and the much greater flexibility of such a molecule compared to a double-stranded DNA renders the bending energy term negligible.

In general, viruses appear to deal with the unfavorable energies of polyelectrolyte repulsion and condensation of the nucleic acid in four ways, summarized below and in Table 1 along with representative viruses utilizing each type of mechanism. One common way of neutralizing the DNA phosphate and condensing the DNA is through the use of polyamines such as putrescine, spermidine, and spermine (see Cohen and McCormick, 1979). It has been shown that polyamines alone can

Table 1. Nucleic acid phosphate charge neutralization mechanisms of various viruses.

Virus	Polyamines[a,b]	Histones	Arg-rich Core Protein	Capsid Protein N-terminus[d]	References
T-even	Put, Spd	-	-	?	Ames and Dubin (1960)
Cowpea mosaic	Spd, Spm	-	-	A	Nickerson and Lane (1977)
Turnip yellow mosaic	Spd, Spm	-	-	A	Virudachalam et al. (1983b)
Belladonna mottle	Spd, Spm	-	-	A	Virudachalam et al. (1983b)
Herpes simplex	Spd, Spm	-	-	?	Gibson and Roizman (1971)
Vaccinia	Spd, Spm	-	-	?	Lanzer and Holowczak (1975)
Adenovirus	Spd, Spm[c]	-	+	?	Shortridge and Stevens (1973) Prage and Pettersson (1971) Lauer (1970)
Densonucleosis	Put, Spd	-	-	?	Kelly and Elliot (1977)
SV-40	?	+	-	?	Frearson and Crawford (1972)
T-5	-	-	?	?	Bachrach et al. (1975)
ØX174	-	-	+	-	Fujisawa and Hayashi (1977)
Tomato bushy stunt	-	-	-	B	Ames and Dubin (1960) Harrison et al. (1978)
Cowpea chlorotic mottle	-	-	-	B	Virudachalam et al. (1983) Hare (1977)
Southern bean mosaic	-	-	-	B	Virudachalam et al. (1983) Hermondson et al. (1982)
Brome mosaic	-	-	-	B	Kaper (1975) Nickerson and Lane (1977)

[a] Abbreviations: Put (putrescine); Spd (spermidine); Spm (spermine).

[b] Polyamine listed if $\frac{\text{moles polyamine}}{\text{moles phosphate}} \geq 0.2$.

[c] $\frac{\text{Moles polyamine}}{\text{Moles phosphate}} = 0.1$.

[d] Amino acid content of N-terminus. Rich in acidic (A) or basic (B) amino acids.

cause the condensation of nucleic acids in solution (Mitra and Kaesberg, 1965; Gosule and Schellman, 1976) into highly compact structures. Generally, viruses that use polyamines encapsidate enough to neutralize 20-50% of the DNA phosphate (see Table 1 for references). In SV 40 and polyoma viruses, histones are packaged along with the viral DNA (Frearson and Crawford, 1972). Adenovirus, in addition to a rather small quantity of polyamines, encapsidates an arginine-rich 17 kDa polypeptide of viral origin which can neutralize about 60% of its DNA phosphate (Laver, 1970; Prage and Pettersson, 1971). The fourth mechanism involves the use of basic regions of the virus capsid proteins themselves to bind the virion DNA. Amino acid sequence analysis and preliminary crystallographic data of several viruses which use this mechanism (see Table 1 for references) have revealed that their capsid proteins have clusters of lysine, arginine, and histidine residues which project into the center of the virion and interact with the nucleic acid.

Several items in Table 1 are worthy of note. First, most of the viruses which do not encapsidate polyamines have single-stranded genomes, like KRV. Second, the viruses in which highly basic regions of the capsid proteins interact with their nucleic acids are, as a class, devoid of polyamines. In contrast, cowpea mosaic, turnip yellow mosaic, and belladonna mosaic viruses, which use polyamines, have been found to have highly acidic polypeptide chains projecting into the center of the virion. This might imply that the acid-base characteristics of the interior of the virion dictate whether polyamines will be packaged along with the nucleic acid,

although the number of cases examined is clearly very small at this time.

Because the interactions discussed above involve ionic binding between acidic (phosphate) and basic (amino) groups, exposure of viruses to pH's approaching or above the pK_a's of the amino groups would be expected to result in a disruption of these interactions and, presumably, of the virus itself. As reviewed by Kaper (1975), a number of studies have revealed pH-dependent disruption of virions in three stages, corresponding to destabilization of nucleic acid-nucleic acid, nucleic acid-protein, and protein-protein interactions with the second class being disrupted at or near the pK_a of the charge neutralizing groups.

In this chapter, the polyamine content of KRV will be examined as the basis for a possible mechanism for virion stabilization. The stability of KRV full capsids as a function of pH will also be discussed and compared to that of empty capsids, indicating the effect of the viral DNA on the stability of the virion.

As can be seen from the preceding discussion, it is difficult to discuss virion stability adequately in the absence of structural considerations. To date, little work has been done on the three dimensional structure of parvoviruses. Small-angle neutron scattering has proven to be a useful tool for the study of a number of icosahedral viruses in solution (Jacrot, 1981). An examination of the structure of empty capsids of KRV using this technique and a model for the radial distribution of protein in empty capsids at 40 Å resolution

will be presented in this chapter. We also suggest a revised triangulation number and possible roles for the capsid proteins in virion stabilization based on this model.

2. MATERIALS AND METHODS

Materials

Tris (tris[hydroxymethyl]aminomethane) (reagent grade), MES (2[N-Morpholino]ethanesulfonic acid), EDTA (Ethylaminediamine-tetraacetic acid) were purchased from Sigma. CsCl was Schwarz-Mann "ultrapure."

Cells and Virus

Normal rat kidney (NRK) cells (Doc-nguyen et al., 1966) strain N153, kindly provided by W. K. Yang of this division, were maintained in Eagle's Minimum Essential Medium plus 10% fetal calf serum (GIBCO). KRV strain 171 has been described previously (Mitra et al., 1982).

Virus Infection and Purification of Empty Capsids

Cultures of NRK cells in roller bottles were infected at about 20% confluence in serum-free medium and 1 hour later the medium was adjusted to 10% fetal calf serum. After 96 hours growth at 37° the cells were scraped, pelleted, and resuspended in 20 mM Tris-Cl, pH 8.0. The cells were then lysed and virus was obtained as previously described (Mitra et al., 1982), except that protease treatment was omitted and the extract was made to 0.5% Sarkosyl (CIBA-Geigy) and 10 mM EDTA after nuclease treatment.

Empty capsids recovered from the first round of equilibrium sedimentation in CsCl ($\rho \tilde{=} 1.32$) were layered on a step gradient of 30 and 35% CsCl (wt/wt) and rebanded at 33,000 rpm for 18 hr at 15° in the SW 41 rotor (Beckman). Complete empty capsids were separated from partially assembled capsids and adventitiously associated proteins by chromatography on Biogel A-5m (Biorad). The capsids were concentrated by pelleting at 400,000 x g for 2 hr and resuspended at the appropriate concentrations in the buffers indicated. This procedure gave homogeneous preparations of empty capsids as shown by electron microscopy (Figure 2), ultraviolet spectrum (Figure 3), and lack of DNA labeling by [^{3}H]thymidine (data not shown).

Full capsids were obtained in the same manner except that the pH was maintained at 6.0 with 10 mM MES (Sigma) throughout purification. The full virus band from the first round of equilibrium sedimentation ($\rho \tilde{=} 1.40$) was layered on a step gradient of 35 and 40% CsCl (wt/wt) and rebanded at 45,000 rpm for 16 hr in the SW 50.1 rotor (Beckman). The rebanded virus was concentrated by vacuum dialysis. The ultraviolet spectrum (Figure 4) was consistent with the presence of nucleic acid (cf. Figure 3).

Amino Acid Analysis

For amino acid analysis, a suspension of empty capsids of known A_{280} was hydrolyzed in evacuated (<50 μm Hg) sealed tubes with 6N HCl/10 mM 2-mercaptoethanol at 110° for 21 hr. After drying *in vacuo*, hydrolysates were subjected to chromatography on a Beckman

Figure 2. Electron micrographs of empty (E) and full (F) KRV capsids at various pH's. Samples were stained with uranyl acetate at the indicated pH and photographed as described in the text.

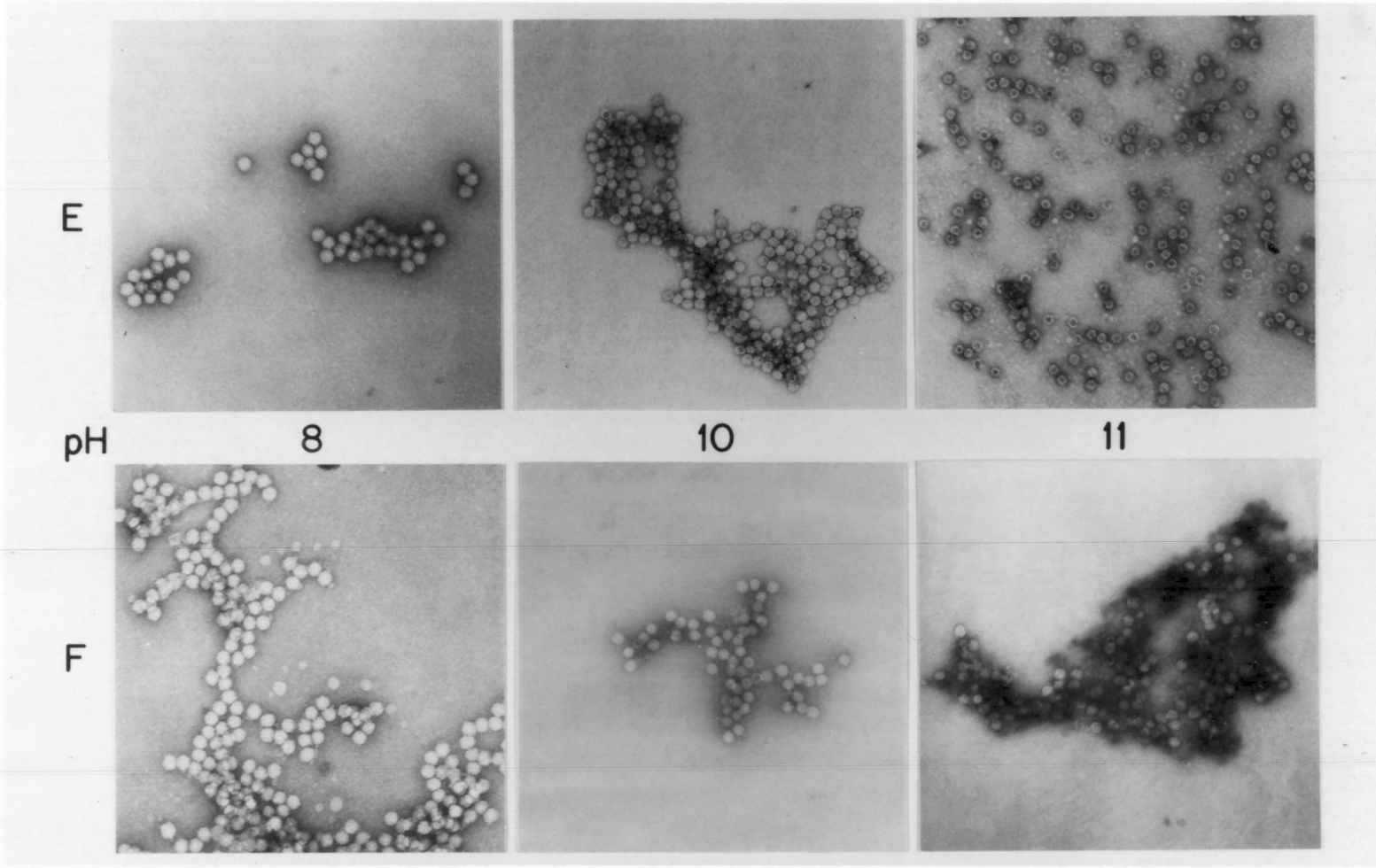
E
pH
8
10
11
F

Figure 3. Ultraviolet spectrum of KRV empty capsids. Determined by continuous scanning from 200-400 nm using a Cary Model 14PM recording spectrophotometer (Applied Physics Corp.). Capsids were suspended in 10 mM Tris-HCl, pH 8.0.

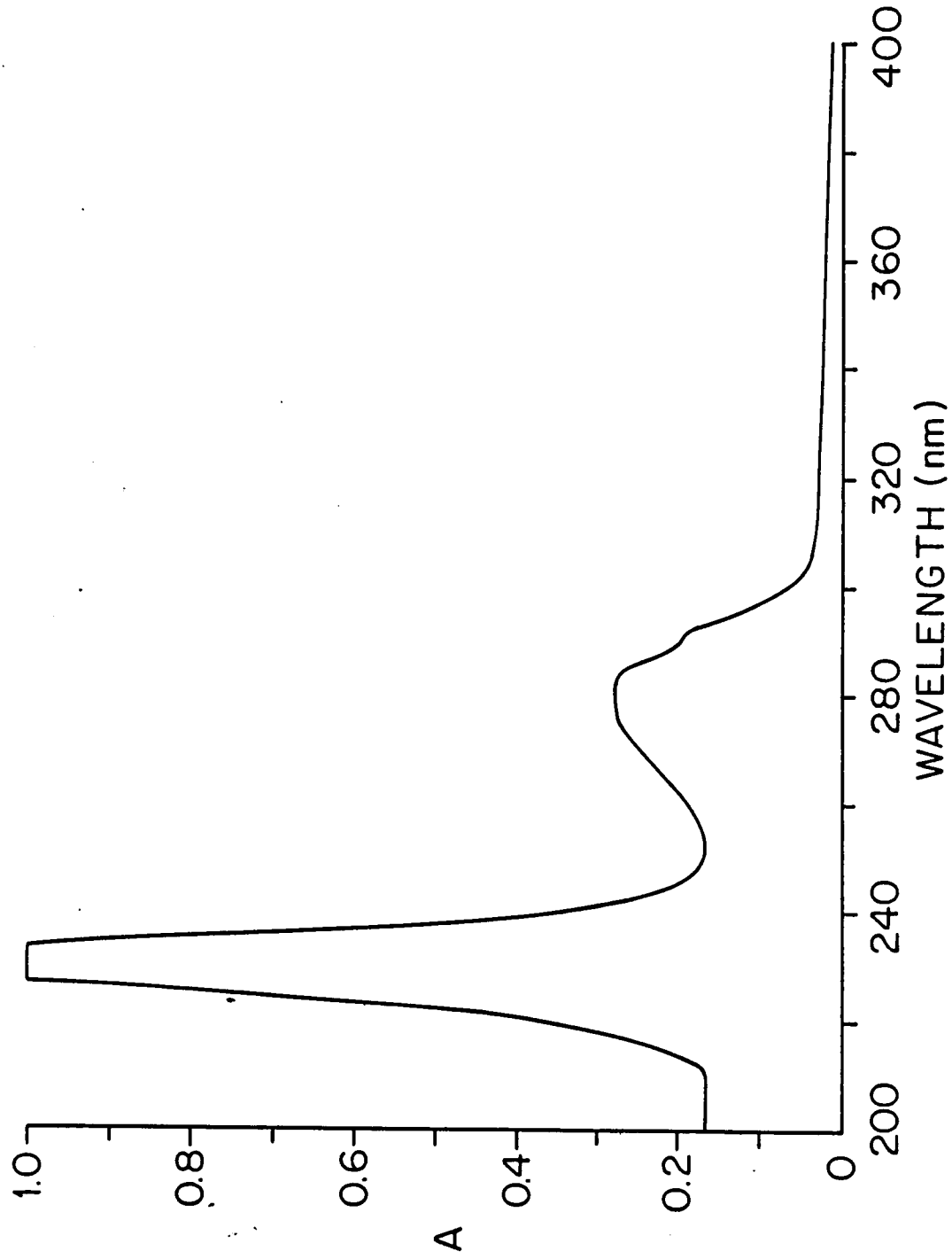

Figure 3

Figure 4. Ultraviolet spectrum of KRV full capsids. Absorbance at 4 nm intervals determined for full capsids suspended in 10 mM MES, ph 6.0 using Zeiss Model M4 QIII spectrophotometer.

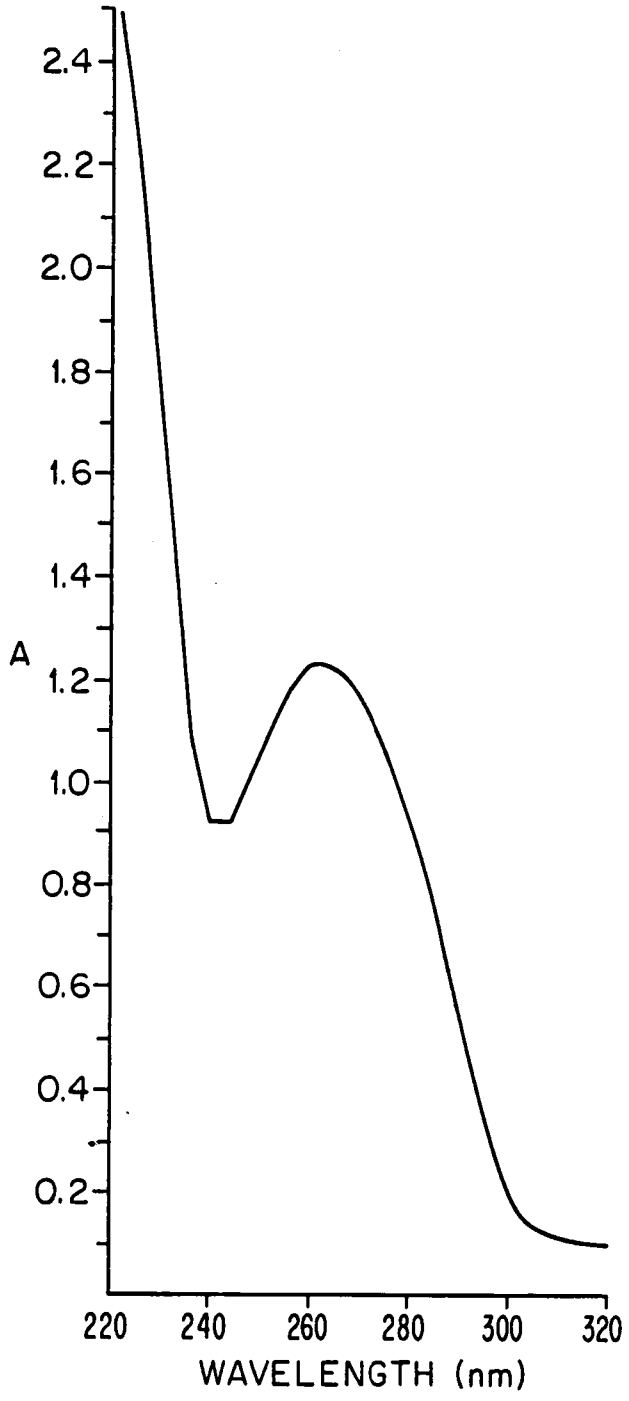
2.4
2.2
2.0
1.8
1.6
1.4
A
1.2
1.0
0.8
0.6
0.4
0.2
220
240
260
280
300
320
WAVELENGTH (nm)

Figure 4

121 M amino-acid analyzer using Beckman's "3-hour-single-column system" by Claude Stringer of this Division. The results are the average of duplicate analyses. Norleucine was used as an internal standard.

Phosphate Analysis

The total phosphate in empty and full capsids was analyzed by the procedure of Ames and Dubin (1960). Briefly, a sample of known A_{260} and A_{280} was mixed with .05 ml 10% $Mg(NO_3)_2 \cdot 6H_2O$ in ethanol and heated over a flame until all ethanol had evaporated and the sample was an ashy white. 0.3 ml 1 N HCl was added and the tube was heated in a boiling water bath for 15 minutes. 0.7 ml ascorbate-molybdate mixture (Ames and Dubin, 1960) was then added and the tube was heated at 45° for 20 minutes after which the absorbance at 820 nm was determined and compared to standard curves prepared using uridine monophosphate.

Polyamine Analysis

Five, 10, and 20 µg of full virus and 50 µg of empty capsids were lysed with 12% perchloric acid at 50° for 5 minutes. The precipitated capsid proteins and DNA were removed by centrifugation at 10,000 x g for 10 minutes and the pellet was washed with 2% perchloric acid. The supernatants were combined and neutralized with 1 N K_2CO_3. After centrifugation (10,000 x g, 5 minutes) to remove the insoluble $KClO_4$, the supernatant was reacted overnight with 0.5 ml 2 mg/ml (acetone) dansyl chloride (Pierce). The dansylated polyamines were

extracted with 5.0 ml n-heptane, which was evaporated off, collected in 200 µl methanol plus 10 µl glacial acetic acid and analyzed by high performance liquid chromatography as described by Brown et al. (1982). A Spectra-Physics model 3500 high-performance liquid chromatography with an Alltech Partasil ODS III column (25 cm x 4.6 mm) was used for the analysis. The mobile phase was a 50% acetonitrile/ 50% 0.02 M 1-heptanesulfonic acid (Whatman Pic B7 reagent) to 80% acetonitrile/20% 0.02 M 1-heptanesulfonic acid concave gradient (program 3) run at 2 ml/min at ambient temperature. Eight µl 0.2 µM 1,6-diaminohexane (Aldrich) was included as an internal standard. Standard curves were prepared using various amounts of putrescine, spermidine, and spermine (Sigma) treated with perchloric acid as described above.

Electron Microscopy

Staining was done by diluting approximately 300 µg/ml suspensions of KRV empty capsids or full virions 10-fold with 2% uranyl acetate in 0.1 M Na-glycine buffer at the pH's indicated. After allowing 5 minutes for equilibration, samples were spread onto carbon-coated nitrocellulose which had been glow discharged and photographed using a Siemens 101 electron microscope (accelerating voltage = 80 kV), by D. P. Allison of this Division. The final magnification on the photographs was 200,000x.

Neutron Scattering

Prior to scattering measurements, samples of the viral capsids were dialyzed against scattering buffer made up in H_2O or D_2O

(10 mM Tris-Cl, pH 8.0, 1 mM EDTA). The samples were then placed in cylindrical quartz cells of 1 mm path length and 2 cm diameter obtained from Precision Cells. Scattering measurements were done on the 30 meter small-angle neutron scattering instrument of the National Center for Small Angle Scattering Research at Oak Ridge National Laboratory (Koehler et al., 1981). Data were collected by a two-dimensional position-sensitive ^3He detector with 64 x 64 1 cm^2 channels. A collimation of 7.5 meters with a source slit of 3.5 cm and a sample slit of 1.74 cm was used. The sample-detector distance was varied from about 9.0 meters for the radius of gyration measurements to 3.0 meters for measurements of the extended scattering curves. The flux incident on the sample was 3.5×10^4 neutrons cm^{-2} sec^{-1} with a wavelength of 4.75 Å and a wavelength spread, $\Delta\lambda/\lambda$, of 6% (full width at half maximum). Measurements lasted between 5 and 15 hr. Sample transmissions were used to determine D_2O content. In each case, the transmissions of the sample and buffer were virtually identical, thus eliminating a possible source of systematic errors.

The raw data were normalized to 1000 monitor counts, corrected for background and sensitivity, and radially averaged to give the measured intensity, I(k), as a function of k (= $4\pi/\lambda)\sin 2\theta$) where 2θ is the scattering angle and λ is the wavelength. Statistical errors from counting were propagated throughout the data reduction procedure. The subsequent data analyses were done with the generous assistance of Dr. Venki Ramakrishnan, of Brookhaven National Laboratory.

Data Analysis--Radius of Gyration and Forward Scatter

At low angles, Guinier's law,

$$I(k) = I(0)\, e^{-k^2 \frac{R_g^2}{3}} \qquad \text{(II-1)}$$

holds (Guinier and Fournet, 1955). Guinier plots (ln I vs. k^2, Figure 5) of the data were used to determine the forward scatter, I(0), and the radius of gyration, R_g. The plots were linear in the Guinier region, and yielded the same R_g for concentrations of 3 mg/ml and 20 mg/ml, showing the absence of any concentration effects in the range studied.

Because of the geometry, which was chosen to optimize flux, a certain amount of instrumental smearing is present in the data, which tends to reduce I(0) and R_g. The effect is more severe in the 3.0 meter sample-detector distance. The data were de-smeared by the indirect Fourier transformation algorithm of Moore (1980). This procedure yielded an independent estimate of the forward scatter and radius of gyration. The values obtained from this procedure should be more reliable because the procedure not only considers all the data rather than just those from Guinier region, but also takes into account smearing effects. The values of R_g obtained by the two methods differed by a few percent.

Data Analysis--Calculation of Radial Density by Fourier Transformation

Indirect Fourier transformation of the scattering intensity data (ln I vs. k) results in a determination of the length distribution

Figure 5. Guinier plot (ln(I) vs. k^2) for KRV empty capsids in D_2O.

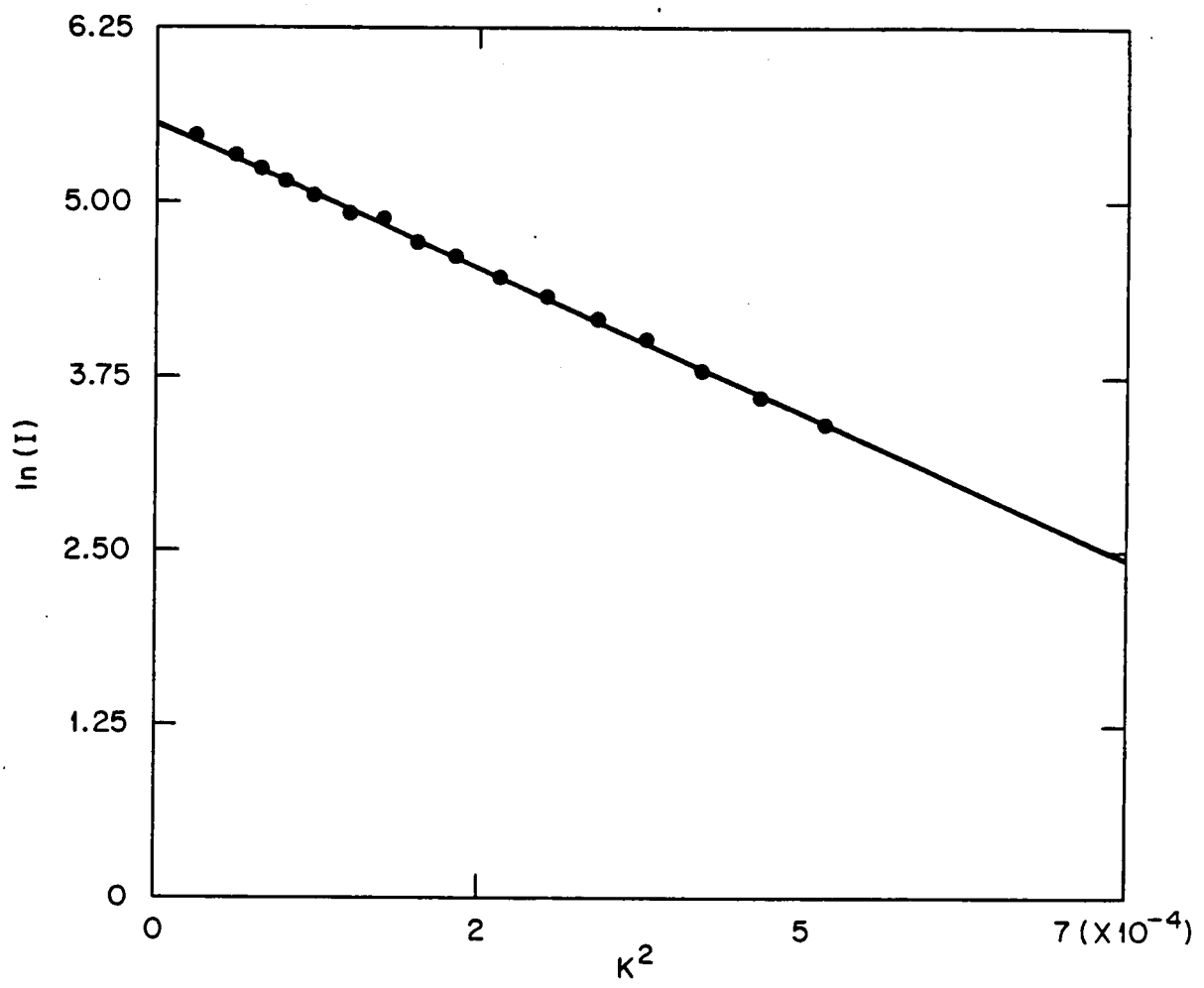

Figure 5

function P(r) (Moore, 1980), where:

$$P(r) = \frac{1}{2\pi r^2} \int_0^\infty kI(k) \sin(kr)\, dk \qquad \text{(II-2)}$$

The point at which P(r) becomes zero is an estimate of the maximum dimension of the particle.

At low resolution, icosahedral viruses can be considered as objects with spherical symmetry (Chauvin et al., 1978). In this case, the amplitude, A(k), is equal to $\pm I(k)^{1/2}$. The intensity curve for a spherically symmetric object becomes zero at different values of k, and A(k) alternates in sign between the zeros of I(k). The scattering length density of the virus is then given by

$$\rho(r) = 1/r \int_0^\infty kA(k) \sin(kr)\, dk \qquad \text{(II-3)}$$

where r is the distance from the center and $\rho(r)$ is the excess scattering length density of virus over solvent (Jacrot, 1981) as a function of r. The de-smeared I(k) was used to calculate $\rho(r)$ from the scattering data. The data were truncated around k = 0.18 Å^{-1} for the transformation.

Data Analysis--Contrast Variation for KRV Full Capsids

The R_g of KRV full capsids (2 mg/ml) in various concentrations of D_2O (see below) was determined by Guinier analysis (Equation II-1 and Figure 5). Changing the relative amounts of H_2O and D_2O in the solvent has the effect of varying the contrast ($\bar{\rho}$) between solute

and solvent ($=\rho_{solute} - \rho_{solvent}$, where ρ_{solute} and $\rho_{solvent}$ are the scattering length densities of the solute and solvent, respectively). Contrast is defined by the following equation:

$$\bar{\rho} = \frac{\Sigma(b_i)(m_i) - \rho_{solvent}\bar{V}}{M} \qquad \text{(II-4)}$$

where b_i refers to the scattering length density of the component parts of the macromolecule in question (amino acids of protein or nucleotides of DNA or RNA), m_i is the mole fraction of that component in the macromolecule, $\bar{V}$ is an approximation of the partial specific volume of the macromolecule determined from $\Sigma\bar{V}_i m_i$ and M is the molecular weight of the solute. Given that $\bar{V}_{protein}$ and $\bar{V}_{DNA}$ were determined to be 0.776 and 0.52 from the above considerations, and given $M_{protein} = 4.0 \times 10^6$ (see below) and $M_{DNA} = 1.5 \times 10^6$, the following formulas can be used to calculate the contrast for each component of the virus as a function of mole fraction D_2O (X) in the solvent:

$$\bar{\rho}_{protein} = (3.2 - 7.68\ X) \times 10^{-14}\ cm\ \text{Å}^{-3}$$

$$\bar{\rho}_{DNA} = (3.18 - 0.68\ X) \times 10^{-14}\ cm\ \text{Å}^{-3}$$

and for the virus as a whole:

$$\bar{\rho} = \frac{M_{protein}}{M_{virus}}(\bar{\rho}_{protein}) + \frac{M_{DNA}}{M_{virus}}(\bar{\rho}_{DNA})$$

$$= (3.33 - 7.04\ X) \times 10^{-14}\ cm\ \text{Å}^{-3}$$

The mole fraction D_2O at which $\bar{}$ is zero is referred to as the match point for the solute. At this point, the average scattering length density of the solute is equal to the scattering length density of the solvent and no net scattering due to solute is observed. For KRV, the match points for DNA and protein are 0.685 and 0.417, respectively.

If the center of mass of a particle is equivalent to its center of volume, then a plot of R_g^2 as a function of $1/\bar{\rho}$ will be linear and be described by the following equation (Jacrot, 1976):

$$R_g^2 = R_{gv}^2 + \frac{1}{\bar{\rho}}[1/V\int_V \rho(r)r^2 d^3r] \qquad \text{(II-5)}$$

with y-intercept R_{gv}^2 and slope $1/V\int_V \rho(r)r^2 d^3r$, where $\rho(r)$ is the scattering length density of the particle as a function of radius and R_{gv}^2 is the radius of gyration at infinite contrast (i.e., the mechanical radius of gyration of the particle as a whole). At the match point for DNA for KRV, the R_g determined from such a plot is the R_g of the protein, and at the match point for KRV protein, the R_g is primarily due to the DNA. A negative slope for this plot is indicative of the fact that the nucleic acid lies inside of the domain occupied by the protein.

Model Building

Two approaches were used to test models of the virus. In the first case, a model scattering function was compared to the de-smeared data, and the parameters of the model estimated by the non-linear least squares procedure of Marquardt (1963). In the other approach, the model function was smeared and then fit to the measured I(k). The two methods yielded essentially the same parameters. The models considered were hollow spheres consisting of a single shell or two concentric shells of different densities.

3. RESULTS

Amino Acid Analysis

The amino-acid composition for the KRV empty capsids is shown in Table 2. The value for tryptophan was calculated from the difference between the measured A_{280} and that calculated from the amino acid analysis. The analysis gives an $E_{280\ nm}^{1\%,1\ cm} = 22.7$ for the ampty capsids. The rather high extinction coefficient agrees well with the published values for another parvovirus, MVM (Tattersall et al., 1976).

Phosphate Analysis and Extinction Coefficient of KRV

An 85 µl aliquot of full virus with $A_{260} = 2.19$ at pH 6.0 contained .718 µg phosphorus. Given the atomic weight of 31 for phosphorus, assuming the average molecular weight of a monosodium nucleotide to be 330, and the molecular weights of KRV DNA (Snyder et al., 1962) and capsid (see below) to be 1.68×10^6 and

Table 2. Amino acid analysis of KRV empty capsids.

Amino Acid	Mole %
Asx	12.36
Thr	8.26
Ser	5.35
Glx	9.40
Pro	6.58
Gly	8.89
Ala	6.70
Val	6.05
Met	1.92
Ile	3.62
Leu	6.62
Tyr	3.57
Phe	3.86
His	4.52
Trp	3.86
Arg	4.24
Lys	3.76

4.00×10^6, respectively, an $E^{1\ mg/ml,1\ cm}_{260\ nm} = 7.19$ was calculated for the virus. The empty capsids were found to contain less than 0.1 phosphorus atom per protein molecule (<5 mole phosphorus/mole capsids).

Polyamine Content of KRV

An example of the separation of polyamine standards is shown in Figure 6. Ten µg of KRV was analyzed as described above and found to contain 9.93 pg spermidine and 4.84 pg spermine. Given molecular weights of 154 for spermidine and 202 for spermine, this translates into .039 mole spermidine/mole virus and .014 mole spermine/mole virus. Putrescine was not detected.

Electron Microscopy of Empty and Full Capsids

Empty and full capsids were indistinguishable under the electron microscope at near neutral pH (Figure 2, p. 26). As the pH was raised to around 10, full particles appear to be more unstable as judged by an increase in the fraction of stain-permeable and disrupted particles ("empties") as shown in Figure 2. This is expressed graphically in Figure 7, where full particles undergo a sharp transition in stability (a higher ratio of "empties" to "fulls") at pH 10-10.5, while empties do not. At higher pH's, (>11) all particles are disrupted.

Neutron Scattering--Molecular Weight and Radius of Gyration

The scattering length per unit mass, $\Sigma b_i/M$, and the partial specific volume were calculated from the amino acid-composition

Figure 6. Separation of dansylated polyamines by high-performance liquid chromatography. 160 pmole putrescine (put), 120 pmole spermidine (spd), 80 pmole spermine (spm), and 160 pmole 1,6-diaminohexane (1,6-DAH) were dansylated, extracted, and analyzed as described in Materials and Methods. Injection volume: 10 µl

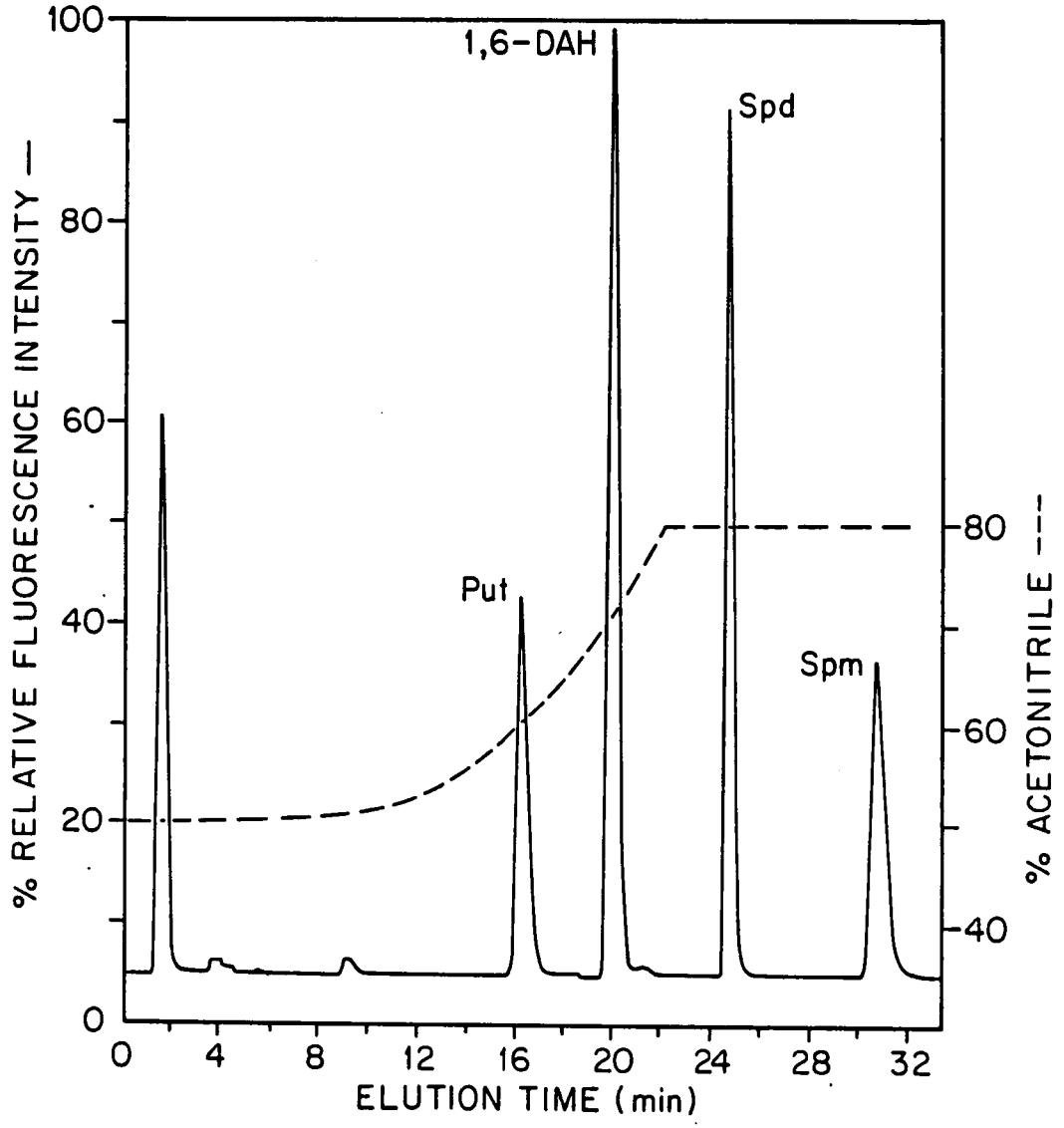
100
80
60
40
20
0
% RELATIVE FLUORESCENCE INTENSITY —
1,6-DAH
Spd
Put
Spm
80
60
40
% ACETONITRILE ---
0
4
8
12
16
20
24
28
32
ELUTION TIME (min)

Figure 6

Figure 7. Ratio of stain-permeable to stain-impermeable particles of KRV. Empty capsids (——■——) or full virions (——▲——), separated by equilibrium sedimentation in CsCl, were stained and spread at the indicated pH and examin-d under the electron microscope as described in Materials and Methods for penetration of uranyl acetate stain. For each point, at least 300 particles were scored.

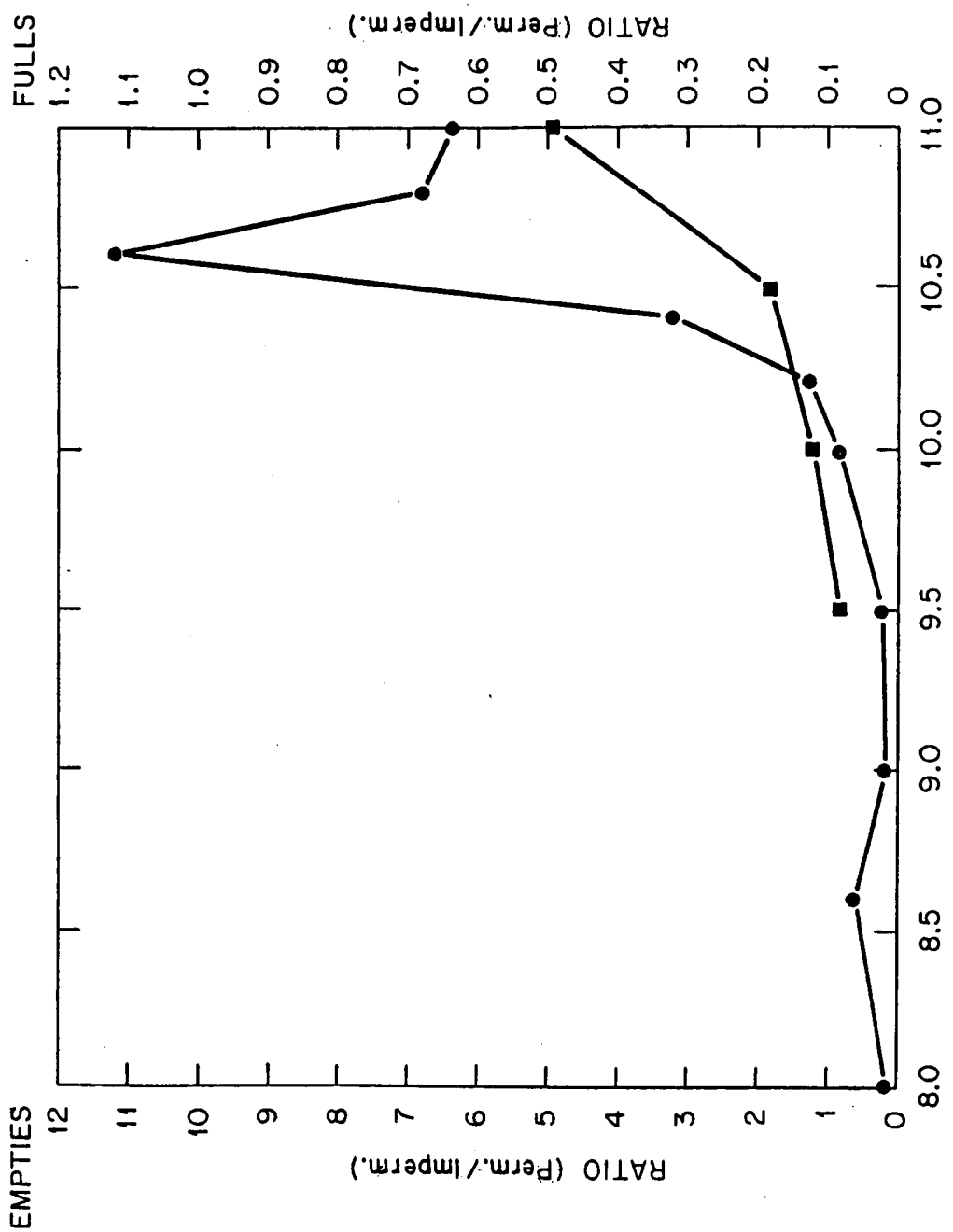
EMPTIES
FULLS
RATIO (Perm./Imperm.)
RATIO (Perm./Imperm.)
pH
8.0
8.5
9.0
9.5
10.0
10.5
11.0

Figure 7

(Jacrot, 1976). Along with a measurement of the incoherent scatter of water and the forward scatter, I(0), in H_2O of a known concentration of capsids, these values were used to determine a molecular weight (Jacrot and Zaccai, 1981) of 4.0×10^6 for the KRV empty capsids. The error in the molecular weight comes primarily from the error in the measurement of the absolute concentration, and is less than 10%.

The R_g was determined to be 105.1 ± 0.5 Å in D_2O and 103.7 ± 0.5 Å in H_2O. In both cases, the maximum dimension determined from the length distribution function was about 240 Å.

Neutron Scattering--Radial Density Function

The radial density calculated from the amplitude A(k) in H_2O and D_2O is shown in Figure 8. The Fourier transformation method has the drawback that truncation of the data at $k = 0.18$ $Å^{-1}$ has the effect of introducing spurious oscillations in $\rho(r)$, especially for values or r less than $2\pi/k$, i.e., for $r < 40$ Å.

In both H_2O and D_2O, there is a principal peak in $\rho(r)$ at about 105 Å; however, there is a shoulder indicating a non-zero $\rho(r)$ between 60 and 90 Å, with the main peak occurring between 90 and 120 Å. The relative height of the shoulder compared to the main peak height is larger in H_2O than in D_2O.

The density profiles indicate that, while the empty capsid is primarily a shell that extends between r = 90 and 120 Å, there may also be an inner shell of smaller density from 60-90Å. To test whether this inner shell is justified by the data or whether

Figure 8. Radial density function for KRV empty capsids in H_2O (a) and D_2O (b). Calculated from scattering function as described in Materials and Methods from desmeared values of I(k).

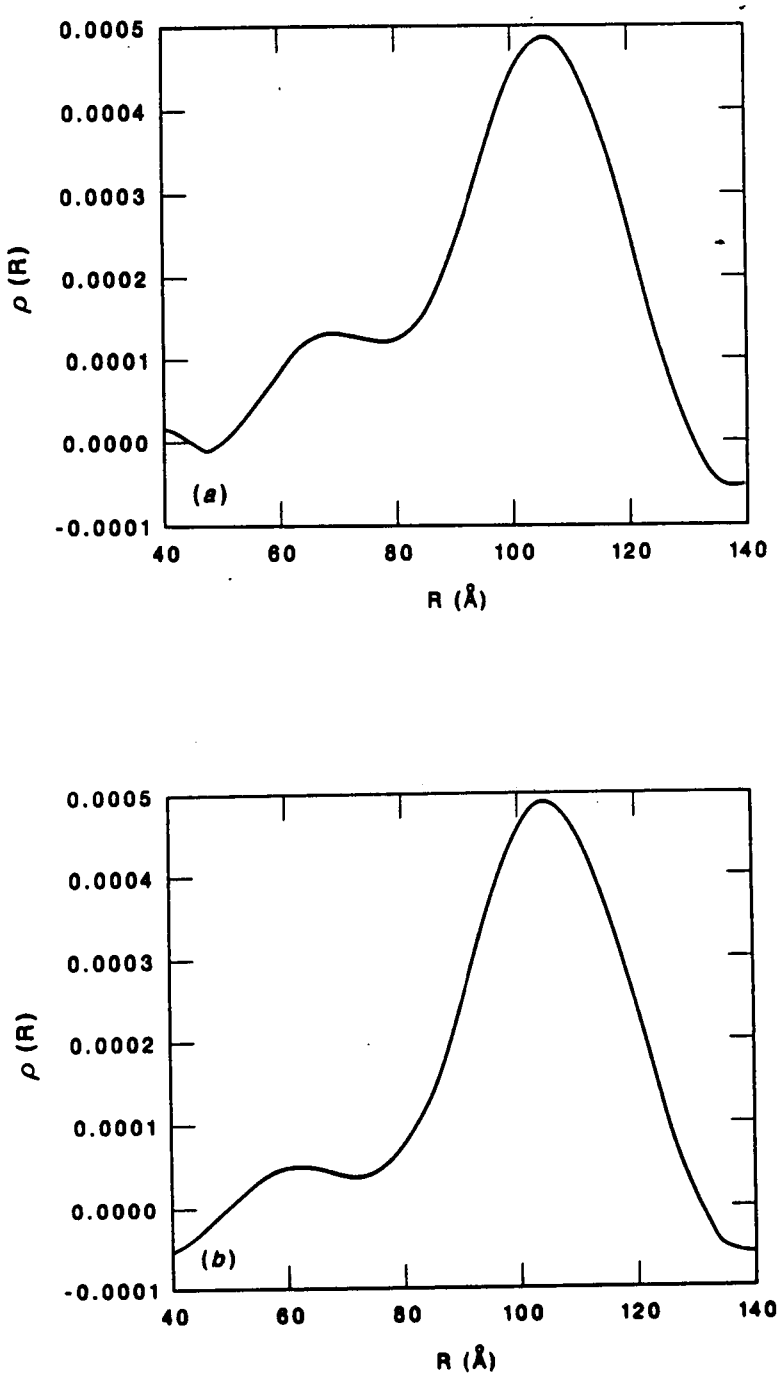
0.0005
0.0004
0.0003
0.0002
0.0001
0.0000
-0.0001
ρ (R)
(a)
40
60
80
100
120
140
R (Å)
0.0005
0.0004
0.0003
0.0002
0.0001
0.0000
-0.0001
ρ (R)
(b)
40
60
80
100
120
140
R (Å)

Figure 8

it is an artifact introduced by Fourier transformation, the model building approach was used.

Model Building

The results of fitting data to one- and two-shell spheres are shown in Table 3 and Figure 9. At low values of k, corresponding to very low resolution, both one- and two-shell models agree with the data reasonably well. However, at higher resolution, a considerably better fit is made by the two-shell model. The values of reduced χ^2 obtained for each model can be used to determine whether the addition of a second shell is significant. An F-test, with 40 degrees of freedom, shows that the second shell is extremely significant. Also striking is the fact that the parameters obtained from model building agree with the density profiles obtained from Fourier transformation.

The model indicates that the KRV empty capsid consists of a primary shell that extends from 90 to 121 Å and a second shell extending inward from 90 Å to about 58 Å as seen in D_2O and 50 Å as seen in H_2O. The difference between the inner radius in H_2O and D_2O is primarily due to the fact that the scattering intensity is relatively insensitive to moderate changes in this parameter. Relative to the outer shell, the inner shell has a scattering density of 0.19 in D_2O and 0.24 in H_2O. These results are summarized in the model of the KRV capsid structure in Figure 10.

Table 3. Structural parameters for one- and two-shell models of KRV[a]

	One-shell	Two-shell
D_2O	r_1 = 80.5 A	r_1 = 58.7 A
	r_2 = 123.2 A	r_2 = 90.9 A
	χ^2 = 101.0[c]	r_3 = 121.1 A
		ρ = 0.206[b]
		χ^2 = 4.9[c]
H_2O	r_1 = 74.0 A	r_1 = 49.2 A
	r_2 = 124.3 A	r_2 = 91.0 A
	χ^2 = 46.7[c]	r_3 = 120.6 A
		ρ = 0.241[b]
		χ = 4.3[c]

[a]See Figure 10 for definition of r_1, r_2, and r_3.

[b]Scattering density of inner shell relative to outer shell (=1).

[c]Calculated from F-test assuming 40 degrees of freedom.

Figure 9. Desmeared experimental scattering values for KRV empty capsids (16.6 mg/ml) (oooooo) in H_2O (a) and D_2O (b) compared to model theoretical scattering curves for single-(-----) and double- (———) shelled capsids with properties described in Table III.

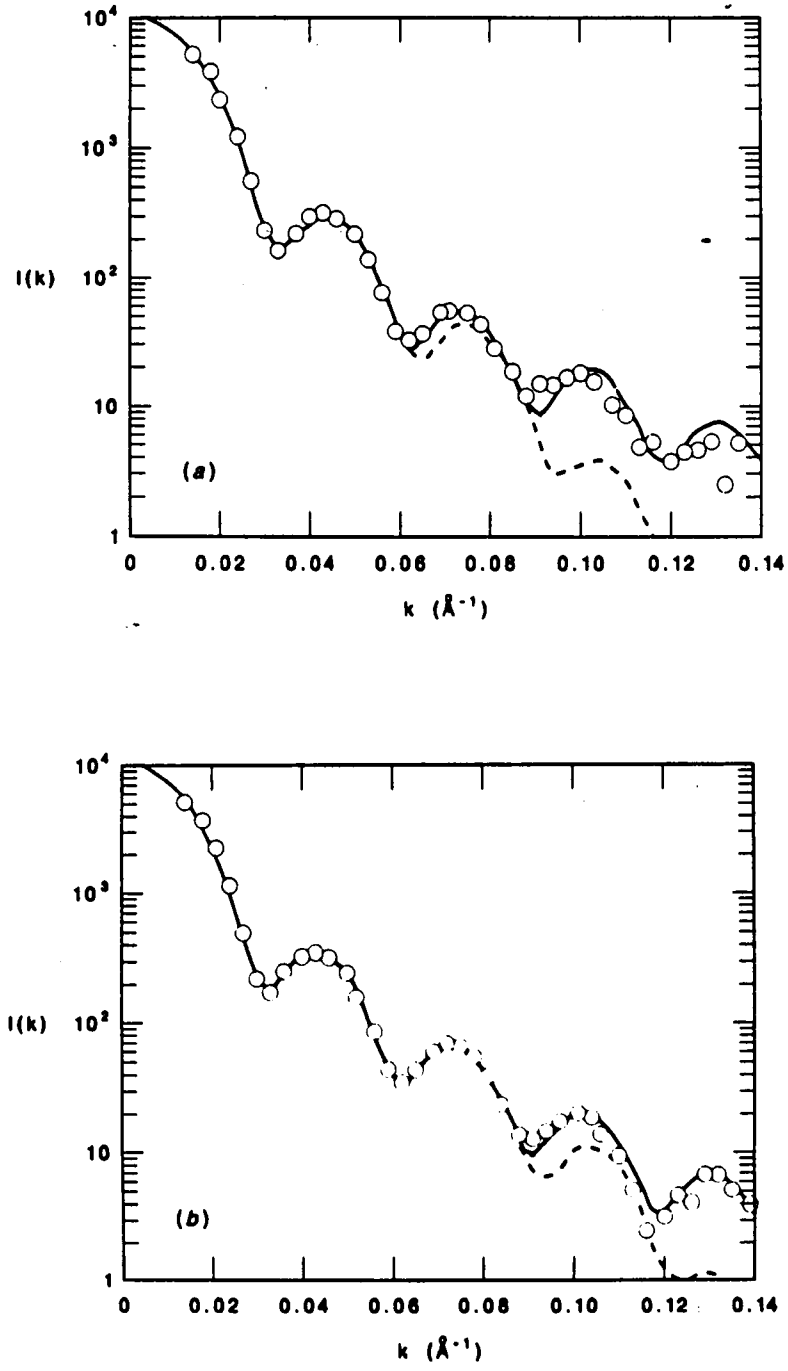
I(k)
10⁴
10³
10²
10
1
(a)
0
0.02
0.04
0.06
0.08
0.10
0.12
0.14
k (Å⁻¹)
I(k)
10⁴
10³
10²
10
1
(b)
0
0.02
0.04
0.06
0.08
0.10
0.12
0.14
k (Å⁻¹)

Figure 9

Figure 10. Cross section of model for the structure of KRV. ρ_1 and ρ_2 refer to the relative scattering densities of the inner and outer shells, respectively. At right is schematic illustration of single protein subunit.

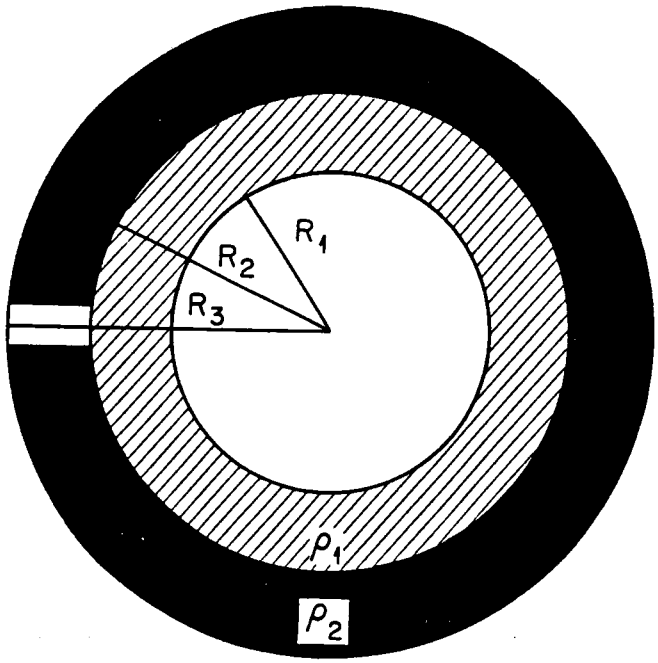

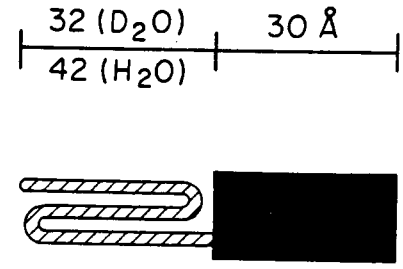

	D_2O	H_2O
R_1	= 58.7 Å	= 49.2 Å
R_2	= 90.9 Å	= 91.0 Å
R	= 121.1 Å	= 120.6 Å
ρ_1/ρ_2	= 0.206	= 0.241

Figure 10

Contrast Variation and Radius of Gyration of DNA

R_g, R_g^2, $\bar{\rho}$, and $1/\bar{\rho}$, determined for KRV full capsids at various mole fractions of D_2O (X), are shown in Table 4. From a least squares fit of R_g^2 vs. $1/\bar{\rho}$ (Figure 11), the R_g of the virus was determined to be 110 Å and the R_g of the DNA (at the match point for protein) was determined to be 66 Å. The minimum outer radius of the DNA (R), calculated from the relation $R_g^2 = 0.6\ R^2$ (assuming the DNA forms a solid sphere), is 85 Å. It is immediately apparent from a comparison of these data with the structural model for the capsid of KRV presented in Figure 10 that there is a good deal of overlap between the inner shell of protein and the DNA. It is also important to note that the minimum outer radius for the DNA lies within the inner radius of the dense outer protein shell at 91 Å.

4. DISCUSSION

The observation of 32 capsomeres by electron microscopy led to the conclusion that the virus has a symmetry of T=3 (Vasquez and Brailovsky, 1965; Karasaki, 1966), for which a minimum of 180 protein molecules per virus capsid would be required (Caspar and Klug, 1962), inconsistent with the observed molecular weight. However, if each protein has two domains on the surface, one of which was close to the vertex (5-fold axis) and the other close to the center of the icosahedral face (3-fold axis), then it would be possible to observe 32 capsomeres, since one would see 20 face clusters and 12 vertex clusters of domains. Multidomained

Table 4. Parameters for contrast variation of KRV full capsids.

X	$\bar{\rho}$ (cm^{-2})	$1/\bar{\rho}$	R_g (Å)	R_g^2
.745	-1.64×10^{10}	$-.61 \times 10^{-10}$	104.8 ± .5	10983 ± 105
.968	-2.98×10^{10}	$-.34 \times 10^{-10}$	105.9 ± .14	11215 ± 30
0	2.84×10^{10}	$.35 \times 10^{-10}$	98.0 ± .4	9604 ± 78
.174	1.79×10^{10}	$.56 \times 10^{-10}$	95.1 ± 1.7	9044 ± 323
.685[a]	-1.28×10^{10}	$-.78 \times 10^{-10}$	110	12100
.417[b]	$.33 \times 10^{10}$	2.99×10^{-10}	58	3364

[a]Match point for KRV DNA. $\bar{\rho}$ calculated as described in text. R_g^2 calculated from least squares equation:

$$R_g^2 = 10419 - 2342 \times 10^{10}\ 1/\bar{\rho}$$

[b]Match point for KRV capsid protein. $\bar{\rho}$ and R_g^2 calculated as in a.

Figure 11. R_g^2 vs. reciprocal contrast ($1/\bar{\rho}$) for KRV full capsids (2 mg/ml) in 10 mM Tris-HCl, pH 8.0.

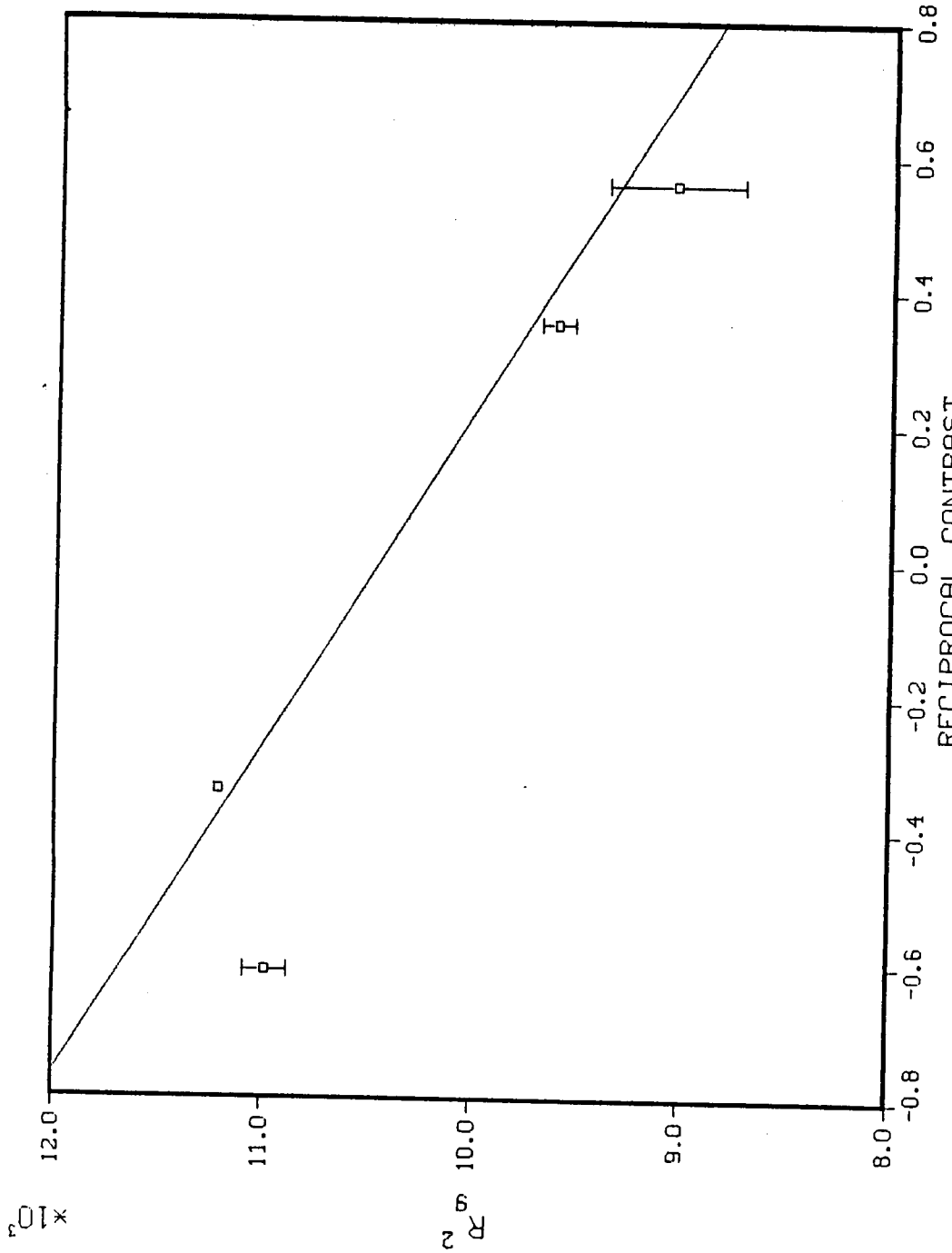
12.0
11.0
10.0
9.0
8.0
R_g^2
$\times 10^3$
-0.8
-0.6
-0.4
-0.2
0.0
0.2
0.4
0.6
0.8
RECIPROCAL CONTRAST

Figure 11

coat proteins have been observed in tomato bushy stunt virus (Olson et al., 1983; Harrison et al., 1978).

The molecular weight of the empty capsid is calculated to be 4.0×10^6 from the forward scatter. Given that the empty capsid consists primarily of B protein (M_B = 64 kDa) and a small amount of protein A (M_A = 80 kDa), we calculate that it has 60 subunits suggesting a triangulation number of 1. Assuming 60 subunits, the number of copies of A protein can be estimated to be 10 from the molecular weight by:

$$nA\ MA + (60 - nA)M_B = 4.0 \times 10^6$$

in agreement with earlier estimates of the A protein content of parvovirus capsids (Tattersall et al., 1976).

From the neuron scattering data obtained in H_2O and D_2O, we can make predictions about the composition of two shells of protein in the capsid. Generally, the R_g for a soluble protein or complex of proteins is smaller in D_2O than in H_2O due to the presence of hydrophilic groups on the exterior. These groups have a higher scattering length density and lower contrast in D_2O than do other amino acids (Jacrot, 1976). In the case of KRV empty capsids, the radius of gyration is slightly smaller in H_2O, suggesting the presence of hydrophilic amino acids on the inside.

The scattering mass of the virus that contributes to the overall scattering is defined by:

$$\Sigma b_i - \rho_s V \qquad \text{(II-6)}$$

where Σb_i is the sum of the scattering lengths of the amino acids, ρ_s is the scattering length density of the solvent and V is the excluded volume. The fraction of this scattering mass in the interior shell (f_{inner}) can be calculated from the parameters of the model as follows:

$$f_{inner} = \frac{\rho_1 V_{inner}}{\rho_1 V_{inner} + \rho_2 V_{outer}} = \frac{(\rho_1/\rho_2)(r_2^3 - r_1^3)}{(\rho_1/\rho_2)(r_2^3 - r_1^3) + (r_3^3 - r_2^3)}$$

where ρ_1 and ρ_2 are the scattering densities of the inner and outer shells, respectively, and r_1, r_2 and r_3 are radii depicted in Figure 10. The value of f_{inner} was calculated from the data to be 0.13 in H_2O and 0.09 in D_2O. The lower value in D_2O is consistent with the fact that basic amino acids have a higher contrast in H_2O than D_2O relative to the bulk of amino acids and suggests that the inner shell, which may interact with DNA, consists of peptide chains containing large numbers of basic amino acids.

The contribution of the basic amino acids, lys, arg, and his, to the total scattering mass (f_{basic}) can also be calculated from the amino-acid analysis data by the following formula:

$$f_{basic} = \frac{(\Sigma b - \rho V)_{basic\ residues}}{(\Sigma b - \rho V)_{total\ residues}}$$

Assuming that the protons of basic residues fully exchange and, for the virus as a whole, 80% of the labile protons exchange (Jacrot, 1976), this ratio turns out to be 0.12 in H_2O and 0.10 in D_2O in good agreement with the observed values for f_{inner}. This also suggests that most of the basic amino acids are in the interior shell.

The fact that the DNA appears to overlap extensively with the inner shell of protein supports the argument that this shell serves a DNA-binding and charge neutralization function. As mentioned in the introduction and as will be discussed shortly, this type of interaction is observed in the architecture of a number of viruses.

Based on the data obtained and on a knowledge of the protein composition of empty capsids of KRV, it is possible to speculate on the contributions of the capsid proteins to the inner shell. From an average of the scattering density of the inner shell in H_2O and D_2O, we estimate that 11% of the scattering mass of the capsid is in this shell. While it is possible, as proposed earlier (Tattersall et al., 1977), that the basic regions of protein A may serve a DNA binding function and thus be oriented on the inside of the capsid, it is clear that this cannot solely constitute the inner shell because it only accounts for 4% of the capsid mass. Thus, we feel that a significant contribution to the inner shell of protein is made by B (and/or C) as well.

Eleven percent of the capsid mass would correspond to 440 kDa of protein or, assuming 60 protein molecules per capsid, side chains

of about 70 amino acids per protein if each protein contributes equally to the inner shell. Since the inner shell is only 40 Å thick, a distance equivalent to 27 residues of α-helix or 11 residues of fully extended chain, it is probable that this chain is highly folded as depicted in Figure 10.

If the region of A that is non-homologous with B is entirely in the inner shell together with a common region of A and B (and/or C in full capsids), 2000 of the 4400 inner shell amino acids would be contributed by A in 200 amino acid chains with the remainder supplied by chains approximately 40 residues long from regions common to A and B. We favor this type of model as it is consistent with a possible DNA binding role for the basic A-specific region (Tattersall et al., 1977) as well as other considerations described below.

The nucleotide sequence of parvovirus H-1 has been determined and the open reading frames for the capsid proteins located, allowing prediction of the primary sequence of the capsid proteins. Figure 12 shows the predicted positions of the basic amino acids in this sequence, clearly indicating a 200 amino acid region found only in the A protein that is enriched for basic residues. There are other clusters of basic amino acids common to all three capsid proteins, shown in brackets in Figure 12. Together, these regions add up to about 11% of the capsid mass. Assuming that all of these residues are positively charged at neutral pH, they are sufficient to neutralize about 30% of the virus' DNA phosphate.

Figure 12. Schematic illustration of KRV capsid proteins A, B, and C showing location of basic amino acids predicted from nucleotide sequence of H-1 capsid protein genes of Rhode and Paradiso (1983). Brackets enclose regions of especially high basic amino acid content which may contribute to inner shell of capsid depicted in Figure 10.

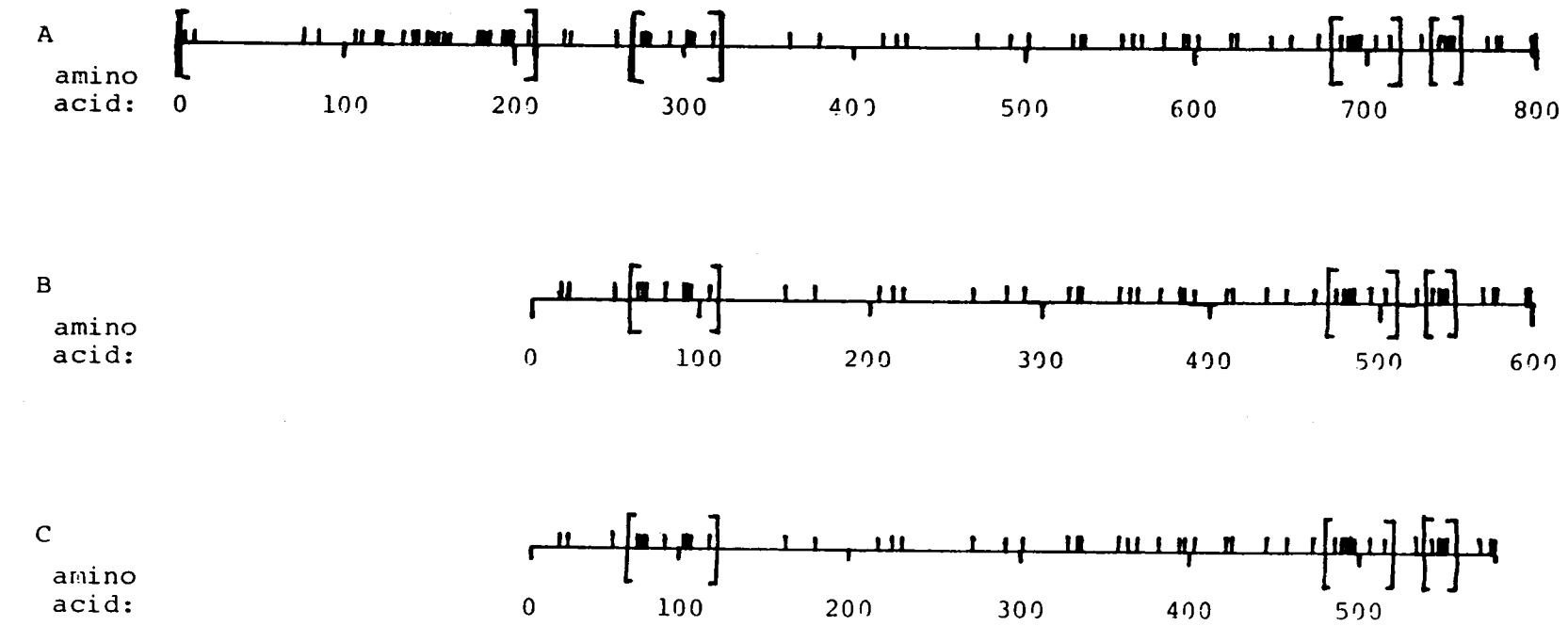
Protein
A
amino
acid:
0
100
200
300
400
500
600
700
800
B
amino
acid:
0
100
200
300
400
500
600
C
amino
acid:
0
100
200
300
400
500

Figure 12

Not shown in Figure 12 is the fact that, in some regions, the basic residues alternate with uncharged amino acids and there is a relatively high content of proline in these peptide chains, compatible with the formation of a "beta barrel" structure with the basic R-groups on the outside, such as that seen with southern bean mosaic virus (Hermondson et al., 1982). This structure would allow maximum interaction of basic R-groups with the viral nucleic acid. Also not shown in Figure 12 is the highly hydrophobic nature of the inner 2/3 of the capsid proteins of KRV, a property also seen with southern bean mosaic virus (Hermondson et al., 1982), which may form the basis for protein-protein interactions in the outer shell of the capsid. Interactions between these hydrophobic regions may form the stable outer shell of these capsids. Sequence analysis of minute virus of mice also reveals this clustering of basic and hydrophobic amino acids (Astell et al., 1982), suggesting that this overall organizational pattern is conserved in the rodent parvovirus capsids.

KRV has a number of properties in common with a group of closely related plant viruses, including southern bean mosaic virus, tomato bushy stunt, cowpea chlorotic mottle, and brome mosaic viruses (see Table 1, p. 21). They all have icosahedral capsids of the same symmetry group and approximately the same size, package a single-stranded nucleic acid in a virion with a total mass of 5.5 - 6.5 x 10^6 daltons, lack polyamines, and can readily form empty capsids. In addition, these viruses all have highly

basic interior regions which can neutralize approximately 30-40% of thenegative charge of the nucleic acid. These similarities suggest that they utilize a common mechanism for packaging the viral nucleic acid and maintaining stability, namely the use of multidomained capsid proteins; one domain binds and neutralizes the nucleic acid primarily through electrostatic interactions and the other associates with surrounding proteins via hydrophobic interactions, stabilizing the outer shell.

In view of these observations, it is interesting that full capsids undergo a transition to a highly unstable form at a pH of about 10, close to the pK_a of the ε-amino group of lysine. Since empty capsids do not undergo this transition, we propose that the destabilization of fulls is due to the repulsion of phosphae charges which are no longer neutralized. This phenomenon has been seen with a number of other viruses (Kaper, 1975).

The distribution of protein A in the capsid of KRV cannot be determined by studies of the type done here. Paradiso (1983) has recently suggested that the A protein molecules in the empty capsid of H-1 are situated in close proximity if not in contact with each other. This would eliminate the problem of symmetrically placing 10 points on an icosahedron, and would be consistent with the model presented here. Crystallographic studies would be necessary to investigate this possibility more closely; however, if protein A does serve a DNA binding role and if it is clustered in one region of the capsid, the distribution of DNA in full capsids should be similarly asymmetrically clustered.

The importance of first studying empty capsids of KRV is that the distribution of protein can be examined without the interfering effects of scattering due to nucleic acid present in full virions. It is possible to largely eliminate the contribution of nucleic acids by the use of contrast variation (Jacrot, 1976), but the scattering signal from protein is reduced by at least an order of magnitude at the match point for DNA, making structural studies in this detail impractical. Furthermore, several features of empty capsids distinguish them from full virions and suggest possible differences in organization. First, empty capsids are much less susceptible to proteolytic degradation (Tattersall et al., 1977) and alkaline destabilization (Figures 2 and 7, pp. 26 and 46) than full capsids while the latter are refractile to chemical cross-linking agents compared to empty capsids (Paradiso, 1983). Second, full capsids appear to undergo a proteolytic modification process (Clinton and Hayashi, 1975, 1976) which has not been reported to occur in empty capsids. On the other hand, empty capsids and mature full virions are similar in their hemagglutinating capacities (Tattersall et al., 1976), implying some structural similarity. The differences implied by susceptibility to proteolysis and crosslinking may, in fact, be limited to structural features of the outer surface and would not necessarily imply a different internal organization. Such differences can be explored by a complementary study on full virions.

CHAPTER III

METHYLATION OF KRV VIRAL AND REPLICATIVE FORM DNA

1. INTRODUCTION

In many eukaryotic systems, the 5-methylcytosine (m^5C) content of a gene appears to be inversely correlated with its level of expression. An excellent review of the evidence for and against the role of DNA methylation in gene expression has been given by Doerfler (1983). With two exceptions, the DNA from all mature viruses examined thus far appears to lack m^5C. One exception is frog virus 3 where 20% of the cytosines in the viral DNA are methylated and the virus causes a change in the host RNA polymerase allowing expression of methylated viral genes (Willis and Granoff, 1980). In herpes simplex virus, the viral DNA is unmethylated, but the intracellular DNA in latently infected cells is extensively methylated (Hammer et al., 1981). The addition of phytogemagglutinin to these cells results in a disappearance of m^5C from the DNA, a reversal of latency and production of infectious virus.

It is known that AAV can establish latent infections in tissue culture (Handa et al., 1977); many of the autonomous provoviruses were first isolated from animal tissues or tissue culture cells which did not produce virus but could be caused to do so by a number of stimuli (see Siegl, 1976), suggesting that these viruses have also established latent infections, analogous to HSV-1. Because of

the involvement of DNA methylation in viral latency and gene expression in the HSV-1 system, and the possibility of a similar mechanism acting in parvovirus gene expression and latency, we investigated the methylation of KRV virion DNA and intracellular RF DNA.

2. MATERIALS AND METHODS

Virus Growth and Labeling

Normal rat kidney cells were cultivated, infected, and harvested as described in Chapter II. For the m^5C determinations, virions were labeled in one of two ways. In one case, infected cells were labeled from 24 hr post-infection until harvest with 10 μCi/ml [methyl-^{3}H]methionine (0.2 Ci/mmol, New England Nuclear) in methionine-free EMEM plus 10% fetal bovine serum. Alternatively, infected cells were labeled over the same interval with 10 μCi/ml [6-^{3}H]uridine (22.4 Ci/mmol, New England Nuclear). The virus was then purified through one round of equilibrium sedimentation as described in Chapter II (see Figure 13).

Isolation of Viral and Cellular DNAs

Viral DNA was extracted by lysing labeled virions with 0.3 M NaOH, 2 mM EDTA, 0.1% Sarkosyl. The DNA was then purified by band sedimentation on a 5-20% alkaline sucrose gradient (0.3 M NaOH, 2 mM EDTA, 0.7 M NaCl, 0.1% Sarkosyl). For RF DNA preparation, the cells were labeled from 9 to 17 hr post-infection with 10 μCi/ml [6-^{3}H]uridine. At 17 hr post-infection, the cells were lysed and

Figure 13. Equilibrium sedimentation in neutral CsCl of KRV full virions from cells labeled with [methyl-^{3}H]methionine (a), or [6-^{3}H]uridine (b). Gradients were prepared and centrifuged as described in Materials and Methods. Fractions were collected from the bottom and aliquots were counted for ^{3}H.

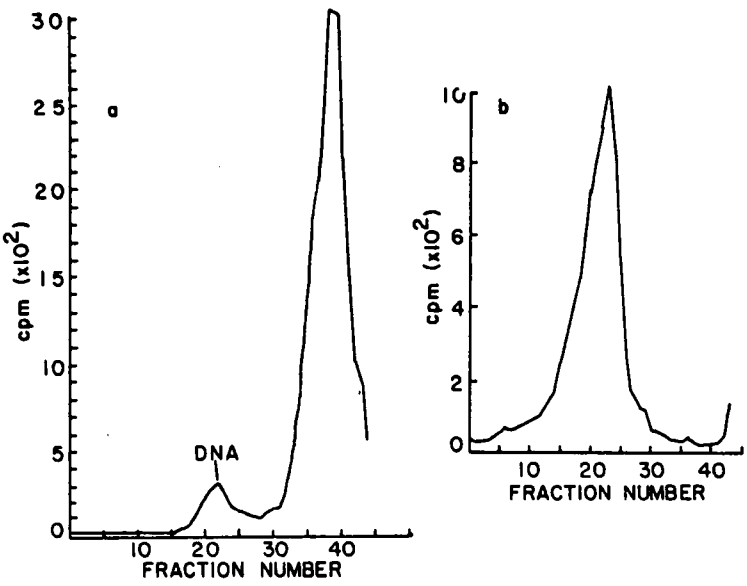
30
25
20
15
10
5
0
cpm (x10²)
a
DNA
10 20 30 40
FRACTION NUMBER
10
8
6
4
2
0
cpm (x10²)
b
10 20 30 40
FRACTION NUMBER

Figure 13

the RF was purified as described in Chapter IV through the guanidine-HCl/sucrose gradient step.

Cellular DNA was prepared by labeling uninfected cells at 50% confluence with 2 μCi/ml [6-^{3}H]uridine for 24 hr. The cells were then lysed with 0.1 M NaCl, 0.5% SDS at 37° for 5 minutes and then digested with 300 μg/ml pronase (Worthington) for 2 hr at 37°. After phenol extraction and ethanol precipitation, the DNA was further purified by gel filtration chromatography on Biogel A-5m (Bio-Rad) in 10 mM Tris-Cl, pH 8.0, 1 mM EDTA, 0.1 mM NaCl.

Hydrolysis of DNA to Bases or Nucleosides

[methyl-^{3}H]methionine labeled viral DNA was collected in 90% formic acid containing 2 μg each adenine (A), cytosine (C), guanine (G), thymine (T), m^5C and 6-methyladenine (m^6A) standards and hydrolyzed to bases by heating to 175° for 90 minutes. The formic acid was evaporated *in vacuo* and the samples were resuspended in 15 μl 1 N HCl for thin layer chromatography.

For high-pressure liquid chromatographic analysis of nucleosides, [^{3}H]uridine-labeled DNA was hydrolyzed to nucleosides with 0.5 mg/ml pancreatic DNase, 0.5 mg/ml venom phosphodiesterase and 0.70 mg/ml bacterial alkaline phosphatase (Worthington) at 37° for 5 hr. Ten μg unlabeled deocycytidine (dCyd) and 5-methyldeoxycytidine (m^5dCyd) were added as markers prior to hydrolysis.

Thin Layer Chromatography

A 2 μl aliquot of the resuspended formic acid hydrolyzed DNA was spotted near one corner of a cellulose Eastman chromogram sheet

(number 6065) and developed in two dimensions by the procedure of Nass (1973). The solvents were methanol:HCl:H_2O (7:2:1) in the first dimension and n-butanol:methanol:H_2O:NH_4OH (60:20:20:1) in the second. The spots were visualized with a short-wave ultraviolet light (see Figure 14 for sample separation), scraped from the plate and the bases were eluted from the resin with 200 µl 0.1 N HCl. The eluate of each spot was counted for ^3H in aqueous counting scintillant (Amersham). The efficiency of recovery of spotted [^3H]thymidine was 95%.

Separation of Methylated Nucleosides by High-performance Liquid Chromatography

Nucleosides were analyzed by anion exclusion chromatography on 7.6 ml bed volume Aminex A-6 column (Bio-Rad) by a modification of the procedure of Singhal (1974). Separation was accomplished by elution with 0.1 M ammonium borate, pH 7.0, at a flow rate of 0.96 ml/min, a temperature of 50°, and a pressure of 150 psi. The eluate was monitored with a Beckman DB spectrophotometer set at 260 nm. One ml fractions were collected and counted for ^3H as above. The m^5dCyd content of the DNA was determined by comparing the radioactivity in the m^5dCyd region with that in the dCyd region.

Purification of Regenerating Rat Liver DNA Methyltransferase and In Vitro Methylation of DNA

DNA methyltransferase was purified from 2/3 hepatectomized rat liver by the procedure of Simon et al., (1972). For in vitro

Figure 14. Schematic diagram of thin layer chromatogram of bases A, C, T, G, m^5C, and m^6A. Solvents, procedures, and abbreviations are described in text. R_f: migration relative to solvent front.

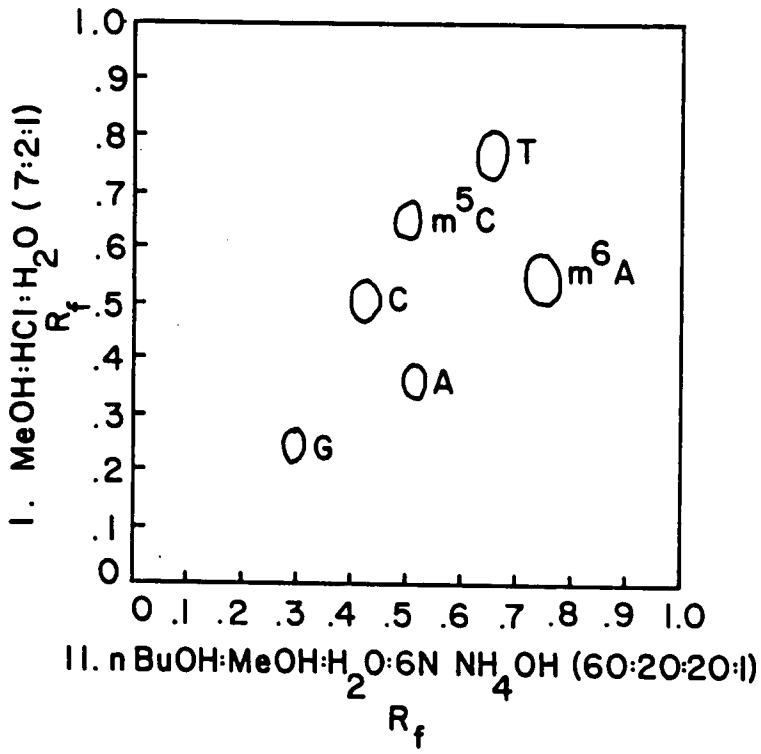
1.0
.9
.8
.7
.6
.5
.4
.3
.2
.1
0
I. MeOH:HCl:H2O (7:2:1)
Rf
T
m5C
m6A
C
A
G
0 .1 .2 .3 .4 .5 .6 .7 .8 .9 1.0
II. n BuOH:MeOH:H2O:6N NH4OH (60:20:20:1)
Rf

Figure 14

methylation, 3 μg of the DNA indicated in Table 5 was incubated with 2 units of DNA methylase (1 unit = 1 pmol [^{3}H] -CH_3 transferred/hr) and 2 μCi [methyl-^{3}H]S-adenosylmethionine (2.2 Ci/mmol, New England Nuclear) for either 1 or 20 hr under conditions described previously (Simon et al., 1972). The DNA was then precipitated with cold 10% trichloroacetic acid and collected on GF/C filters (Whatman) which were counted for bound ^{3}H. For the 20 hr samples, a second addition of 2 units DNA methyltransferase and 2 μCi [methyl-^{3}H]S-adenosylmethionine was made 12 hr after the start of the reaction.

3. RESULTS

5-methylcytosine Content of KRV Viral and RF DNA and NRK Cell DNA

As indicated in Table 6, no radioactive m^5C and m^6A were seen in KRV DNA from virions labeled with [methyl-^{3}H]methionine, which is converted to S-adenosylmethionine, the methyl group donor for DNA methylation. Given a specific activity of 0.2 Ci/mmole, one methyl group per genome equivalent should give 120 counts per minute per microgram of input DNA. This indicates that the virus contains less than 0.03 mole of m^5C per mole DNA.

To confirm these results, infected cells were labeled with [6-^{3}H]uridine, which is converted to deoxycytidine, incorporated into DNA and methylated at the 5 carbon by the host DNA methyltransferase, giving m^5dCyd. Comparison of the radioactivity present in m^5dCyd to that in dCyd separated by HPLC will indicate the extent

Table 5. *In vitro* methylation of KRV mature viral and RF DNA.[a]

DNA	CPM Incorporated 1 Hr	20 Hr[b]
Denatured Micrococcus Lysodeikticus		
Native *E. coli*	1017	22,838
KRV ss Viral	1161	2342
KRV ds RF	616	2475

[a]DNA methylase was prepared from regenerating rat liver by the method of Simon et al. (1978). Three µg of the indicated DNA was incubated with 3 units DNA methylase (1 unit incorporates 1 pmole methyl groups/hour) and 2 µCi [methyl-^{3}H]S-adenosylmethionine (2.2 Ci/mmole) for either 1 or 20 hours. DNA was TCA-precipitated and collected on GFC filters for counting radioactivity.

[b]Two units DNA methylase and 2 µCi [methyl-^{3}H]S-adenosylmethionine added after 12 hours incubation.

Table 6. Transfer of methyl-^{3}H from [methyl-^{3}H]methionine to DNA bases.[a]

	Exp. I[b]	Exp. II[b]
µg DNA hydrolyzed:	5.0	30.0
Base	CPM	CPM
A	119	1280
C	44	47
T	N.D.	N.D.
G	54	279
m^5C	31	31
m^6A	40	90

[a]Indicated amounts of KRV DNA, isolated as described in Materials and Methods from purified virions, were hydrolyzed to bases in 100 µl 90% formic acid at 175° for 90 minutes. After drying, the hydrolysate was collected in 10 µl 1M HCl containing 6 µg each m^5C, m^6A, and T and chromatographed as in Figure 14. U.V.-absorbing materials were scraped from the plate and eluted with 200 µl .1 M HCl for radioactivity measurement. Based on the specific activity of methyl-^{3}H (.2 Ci/mmole), one m^5C or m^6A per genome equivalent corresponds to 120 cpm per µg of DNA hydrolyzed.

[b][^{3}H]thymidine labeled KRV RF DNA added as marker.

N.D. = not determined.

of methylation at this nucleotide. NRK cell DNA appears to have about 3% of its cytidines methylated (Figure 15). On the other hand, KRV viral and RF DNAs lack m^5dCyd (Figures 16 and 17). Since the genome of KRV is about 20% dC (Fraenkel-Conrat, 1974), the sensitivity of this procedure is roughly 0.5 m^5dCyd per genome equivalent of KRV DNA.

Methylation of KRV DNA In Vitro

From Table 5 it is clear that both KRV viral and RF DNAs can serve as substrates of homologous DNA methyltransferase. From the specific activity of the [methyl^{3}H]S-adenosylmethionine, it is calculated that one methyl group per genome equivalent of DNA was transferred to KRV DNA. Agarose gel electrophoresis confirmed that the methylated product was KRV DNA (Figures 18 and 19).

4. DISCUSSION

The lack of m^5C in the viral and intracellular RF DNAs is not surprising in view of the fact that the DNA of most highly cytopathic viruses is not methylated (Doerfler, 1983). This lack of methylation does not appear to be due to the unsuitability of these DNAs as templates for the cellular DNA methyltransferase (Table 5 and Figures 18 and 19). These observations suggest that the intracellular forms of the viral DNA are in some manner sequestered from this enzyme or that such a small population of this DNA is methylated that it cannot be detected by the methods used here. Since the sensitivity of detection of the assays performed

Figure 15. High-pressure liquid chromatogram of nucleosides from [6-^{3}H]uridine labeled NRK cell DNA. Unlabeled dThd, dCyd, and m^{5}dCyd were added as markers. Inset: expansion of elution region of m^{5}dCyd. Mobile phase: 0.1 M ammonium borate, pH 7.0. Flow rate: .96 ml/min.

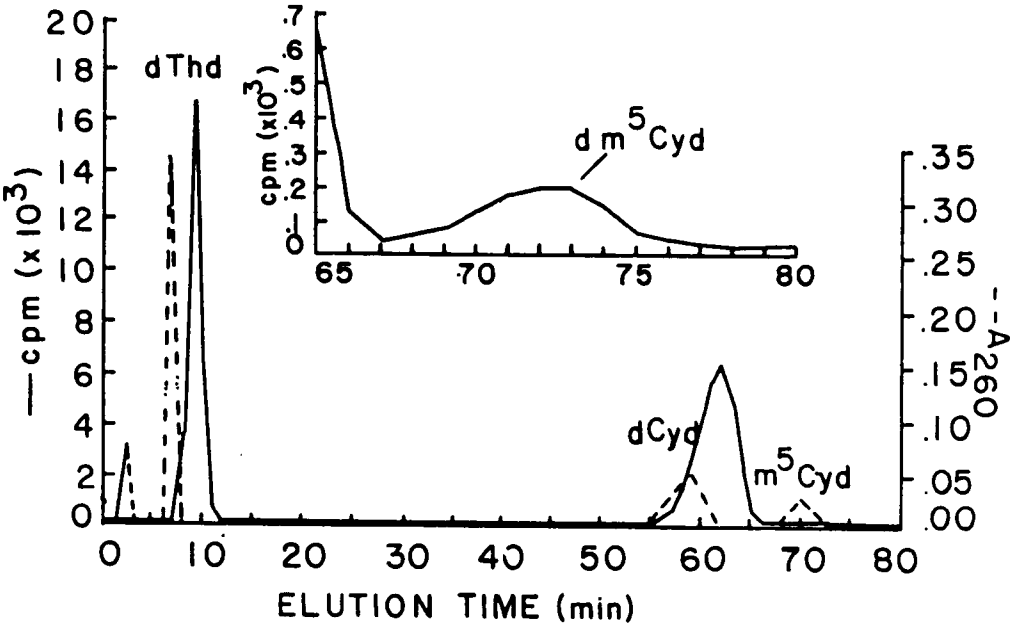
dThd
dCyd
m5Cyd
d m5Cyd
—cpm (x 10^3)
cpm (x10^3)
--A260
ELUTION TIME (min)
0 10 20 30 40 50 60 70 80
0 2 4 6 8 10 12 14 16 18 20
0 .2 .3 .4 .5 .6 .7
65 70 75 80
.00 .05 .10 .15 .20 .25 .30 .35

Figure 15

Figure 16. High-pressure liquid chromatogram of nucleosides from [6-^{3}H]uridine-labeled KRV virion DNA. Inset: expansion of elution region of m^{5}dCyd. Mobile phase and flow rate described in Figure 15.

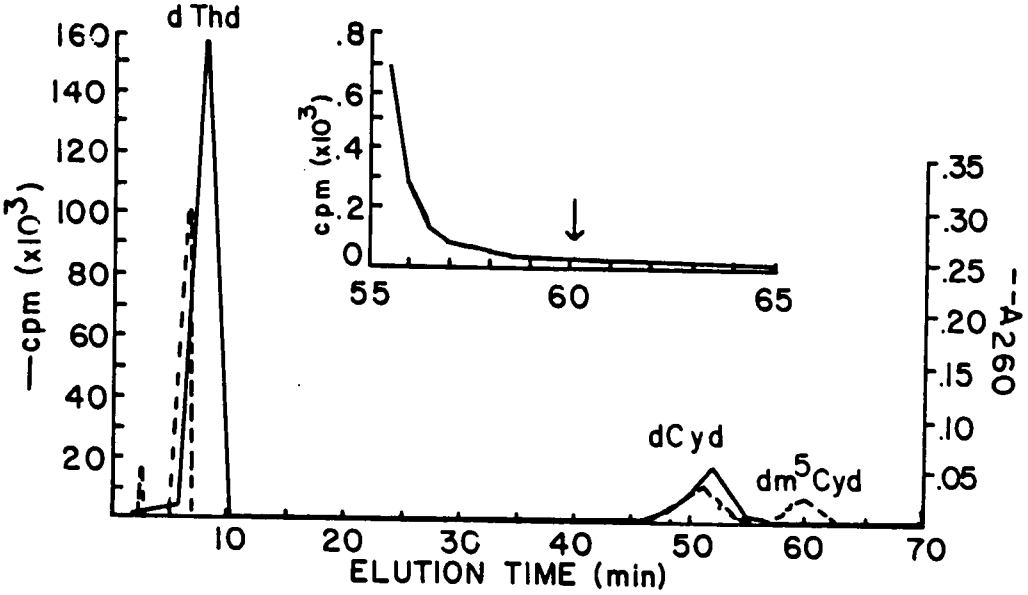
d Thd
dCyd
dm5Cyd
—cpm (x10^3)
--A260
ELUTION TIME (min)
cpm (x10^3)
160
140
120
100
80
60
40
20
.8
.6
.4
.2
0
55
60
65
.35
.30
.25
.20
.15
.10
.05
10
20
30
40
50
60
70

Figure 16

Figure 17. High-pressure liquid chromatogram of nucleosides from [6-^{3}H]uridine-labeled KRV RF DNA. Inset: expansion of elution region of m^{5}dCyd. Mobile phase and flow rate described in Figure 15.

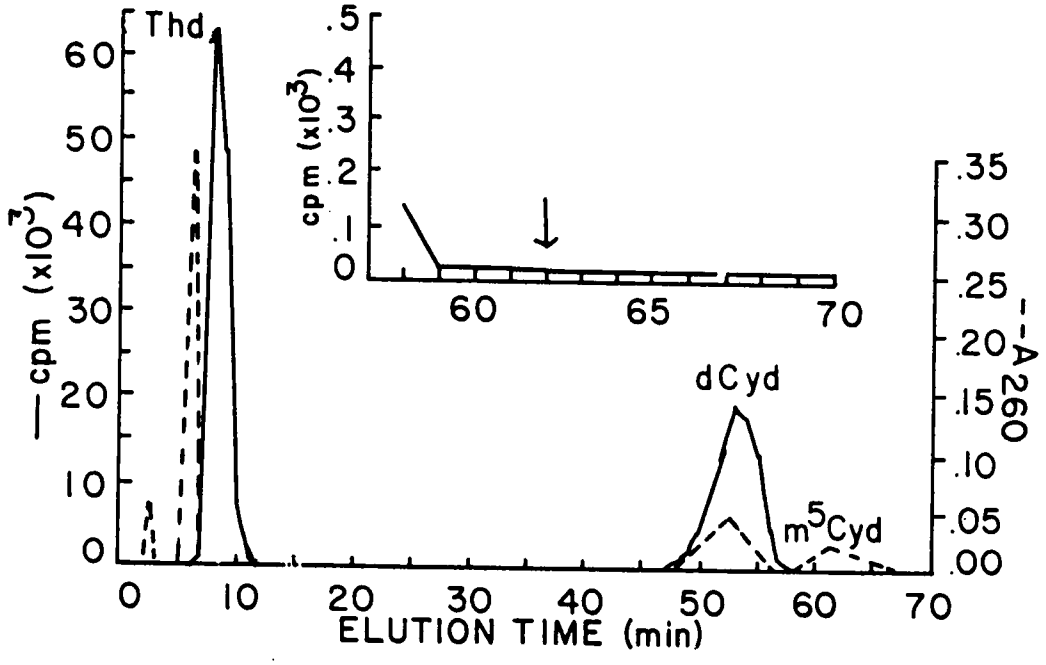
Thd
dCyd
m5Cyd
—cpm (x10³)
cpm (x10³)
--A260
ELUTION TIME (min)
0
10
20
30
40
50
60
70
65

Figure 17

Figure 18. One percent agarose gel electrophoresis of [^{3}H]thymidine-labeled RF DNA (a) and RF DNA methylated *in vitro* by regenerating rat liver DNA methyltransferase and [methyl-^{3}H]S-adenosylmethionine (b). 0.5 cm gel slices were melted in H_2O and counted for ^{3}H. Arrow indicates position of ehtidium bromide-stained KRV RF DNA standard.

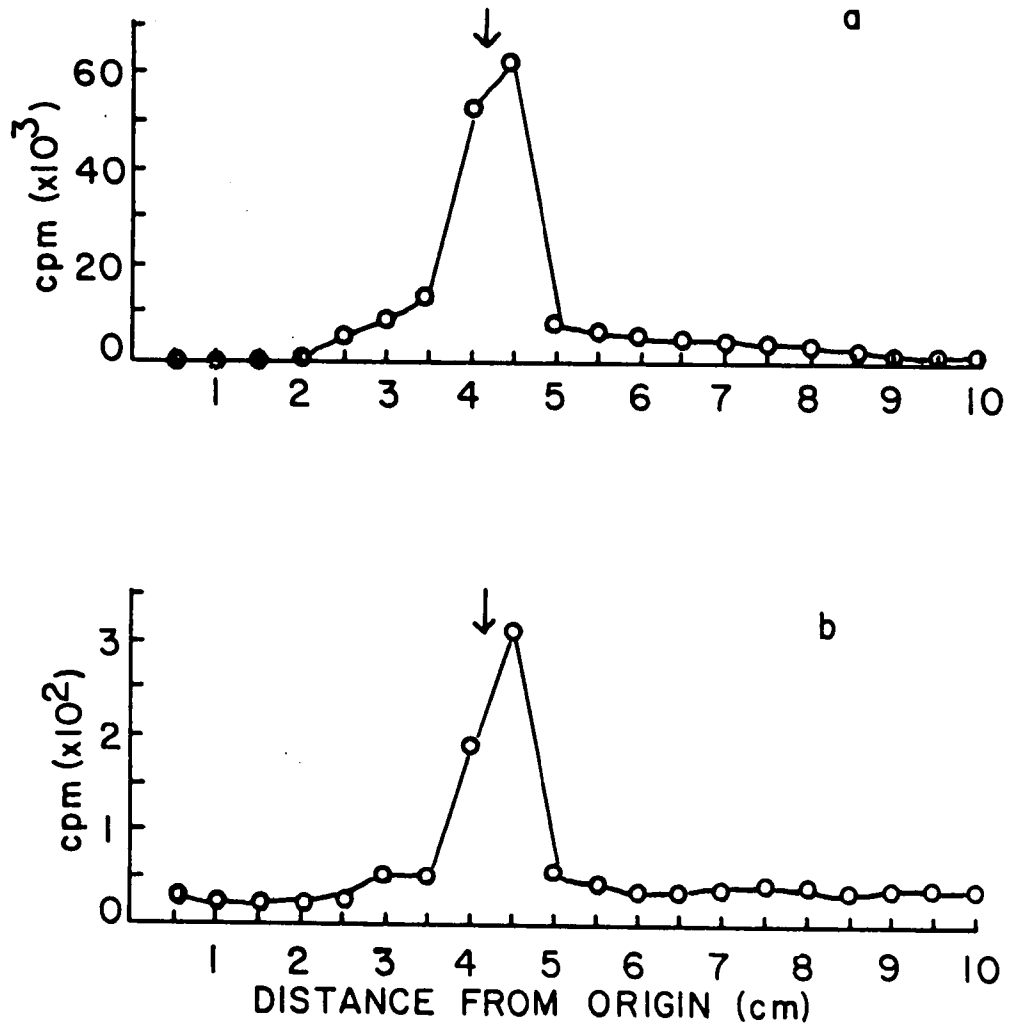
a
cpm (x10³)
60
40
20
0
1 2 3 4 5 6 7 8 9 10
b
cpm (x10²)
3
2
1
0
1 2 3 4 5 6 7 8 9 10
DISTANCE FROM ORIGIN (cm)

Figure 18

Figure 19. One percent agarose gel electrophoresis of KRV viral DNA labeled *in vitro* with regenerating rat liver DNA methyltransferase and [methyl-^{3}H]S-adenosylmethionine. 0.5 cm gel slices counted for ^{3}H as described in Figure 18. Arrow indicates position of ethidium bromide-stained KRV ss viral DNA standard.

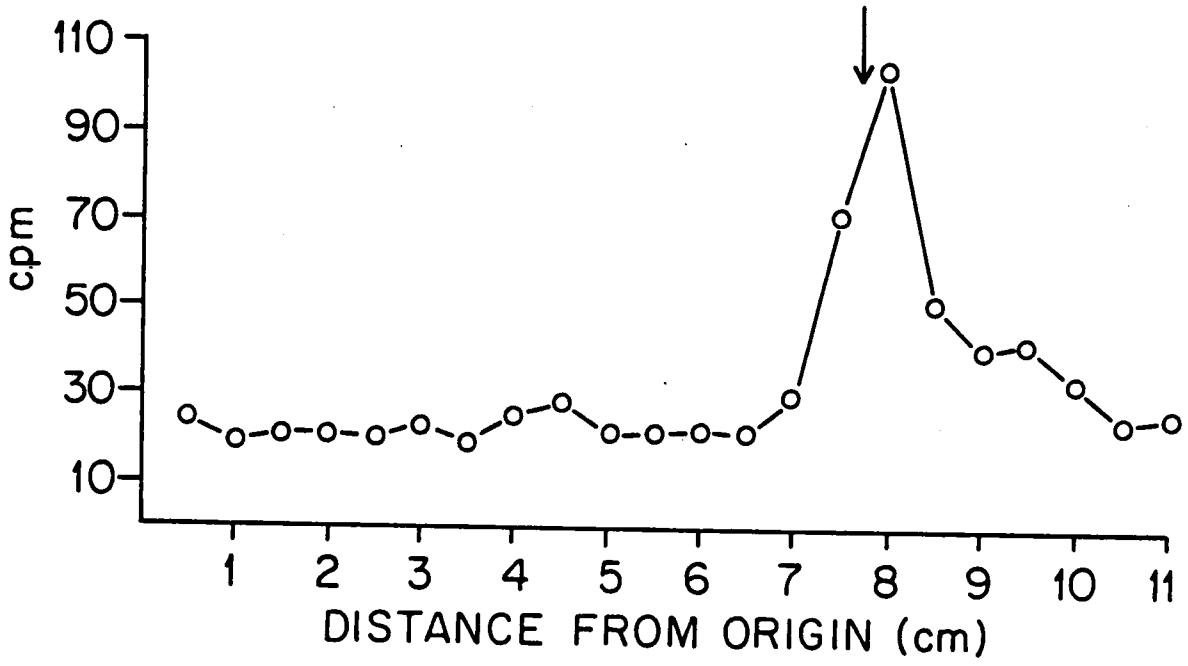

Figure 19

here was on the order of 0.1 m^5C per genome, the population of methylated DNA would have to be very small to escape detection.

CHAPTER IV

ISOLATION AND CHARACTERIZATION OF PROTEINS TIGHTLY BOUND TO THE REPLICATIVE FORM DNA OF KRV

1. INTRODUCTION

The commonly studied autonomous rodent parvoviruses (H-1, MVM, and KRV) have a number of properties in common. They have single-stranded genomes of similar sizes (approximately 5000 nucleotides) with short terminal hairpins (Snyder et al., 1982) and an icosahedral capsid about 240 Å in diameter (Vasquez and Brailovsky, 1965, and Chapter II). These viruses replicate only in host cells undergoing DNA synthesis (Tennant and Hand, 1970) and are presumed to rely largely, if not entirely, on host factors for DNA synthesis, although no reconstituted replication system using purified proteins has been developed to demonstrate this. Because of their dependence on host S phase, autonomous parvoviruses provide a model system for cellular DNA replication.

Following infection, the ss viral DNA is converted to a linear ds replicative form (RF) DNA molecule (Tattersall, 1972; Dobson and Helleiner, 1973; Salzman and White, 1973; Rhode, 1974a,b) presumably using the 3' terminal hairpin as a primer for the host replicative machinery (Figure 1, p. 9). This duplex RF DNA is then utilized for the production of the viral DNA strand from a proposed unique replication origin at the 3'-end of the complementary

strand (Singer and Rhode, 1977a,b). These observations have led to the proposal of a "hairpin transfer" model for parvovirus replication (Cavalier-Smith, 1974; Berns and Hauswirth, 1979; Mitra, 1980; Astell et al., 1982).

Based on its aberrant electrophoretic mobility in agarose and an increase in its buoyant density in CsCl following protease treatment, most of the intracellular RF DNA of H-1 appears to have a protein of approximately 60 kDa covalently bound at its termini (Revie et al., 1979). Although these workers did localize the probable binding site of the protein to the terminal restriction fragments, no evidence was presented regarding which terminus, 5' or 3', was involved. Later, Astell et al. (1982) claimed to have isolated a protein of 60 kDa that was covalently bound to the RF DNA of MVM. However, to date, no protein has been isolated which can be identified as the parvovirus RF DNA terminal protein (RF-TP) based on: a) covalent binding to RF DNA and b) location at the termini of RF DNA. In this chapter, evidence will be presented that KRV RF DNA also has covalently bound protein at its termini. The isolation of proteins which display behavior consistent with covalent linkage to the RF DNA termini will also be described. The isolation of other proteins, which appear to be tightly, but non-covalently, bound to the RF will also be described along with a discussion of their possible origin.

2. MATERIALS AND METHODS

Materials

Guanidine-HCl (Grade I), Tris [tris(hydroxymethyl)aminomethane] (reagent grade), 2-mercaptoethanol (type I), and phenylmethylsulfonyl fluoride (PMSF) were purchased from Sigma. Sucrose and CsCl were Schwarz-Mann "ultrapure." HpaII and electrophoresis grade agarose were from Bethesda Research Laboratories. Materials for polyacrylamide gels were Bio-Rad electrophoresis grade. Na[^{125}I] (Amersham) and TAGIT (Calbiochem) were used for the preparation of Bolton and Hunter reagent by the procedure of Feitelson et al. (1981). [^{3}H]thymidine labeled phage T-5 DNA was the generous gift of Dr. R. K. Fujimura of the Biology Division.

Cells and Virus

Normal rat kidney (NRK) cells (Doc-nguyen et al., 1966), strain N153, kindly provided by W. K. Yang of this Division, were maintained in Eagle's Minimum Essential Medium (EMEM) plus 10% fetal bovine serum (GIBCO). KRV strain 171 (Tennant et al., 1969) was used for all infections.

Infection of Cells and Purification of RF DNA

Parasynchronous cultures of NRK cells, grown at 37°, were obtained by trypsinization of confluent cultures and replating at 20% confluence. One hour after seeding, cells were infected with KRV in serum-free medium (multiplicity of infection = 10). One hour later, the medium was adjusted to 10% serum and cell growth

was continued at 37°. In some cases L-[^{35}S]methionine (New England Nuclear, 15 μCi/ml, 1244 Ci/mmol) was added at this time in methionine-free EMEM plus 10% dialyzed fetal bovine serum containing 10 μM unlabeled methionine, and the cells were incubated until 16 hr post-infection. For the preparation of [^{3}H]thymidine labeled RF, infected cells were allowed to grow at 37° until 16 hr after infection when [methyl-^{3}H]thymidine (New England Nuclear, 50 μCi/ml, 200 Ci/mmol) was added to the cells for an additional 30 minutes.

Following the indicated labeling periods, RF DNA was purified from infected cells by a modification of the procedure of Lavelle and Li (1977). Briefly, cells were lysed in buffer containing 20 mM Tris-HCl (pH 8.0), 10 mM EDTA, 0.5% Sarkosyl (Ciba Geigy), 4 M guanidine-HCl, 1 mM PMSF and, where indicated, 250 mM 2-mercaptoethanol. After incubation at 37° for 60 minutes, the lysate was layered onto a 10-30% sucrose gradient in buffer containing 20 mM Tris-HCl (pH 8.0), 2 mM EDTA, 0.1 mM PMSF, 4 M guanidine-HCl and, in some cases, 15 mM 2-mercaptoethanol. Gradients were centrifuged at 26,000 rpm in the SW 28 rotor (Beckman) at 10° for 38 hr giving three peaks of ^{3}H-labeled material (Figure 20), corresponding to RF, dimer-length RF and a mixed population of tetramer-length RF and a species migrating much faster than RF (Figure 21 and Li, 1977). Most of the multimer length molecules are formed as a result of hydrogen bonding of the hairpin termini of two molecules, although a small population results from DNA synthesis initiating from the complementary strand 3' hydroxyl group in the absence of the

Figure 20. Guanidine-HCl/sucrose gradient of intracellular replicative form DNA's of KRV. One 100 mm plate of [^{3}H]thymidine-labeled KRV-infected cells was lysed and centrifuged on a 10-30% guanidine-HCl/sucrose gradient as described in the text. One ml fractions were collected from bottom and aliquots were counted for ^{3}H.

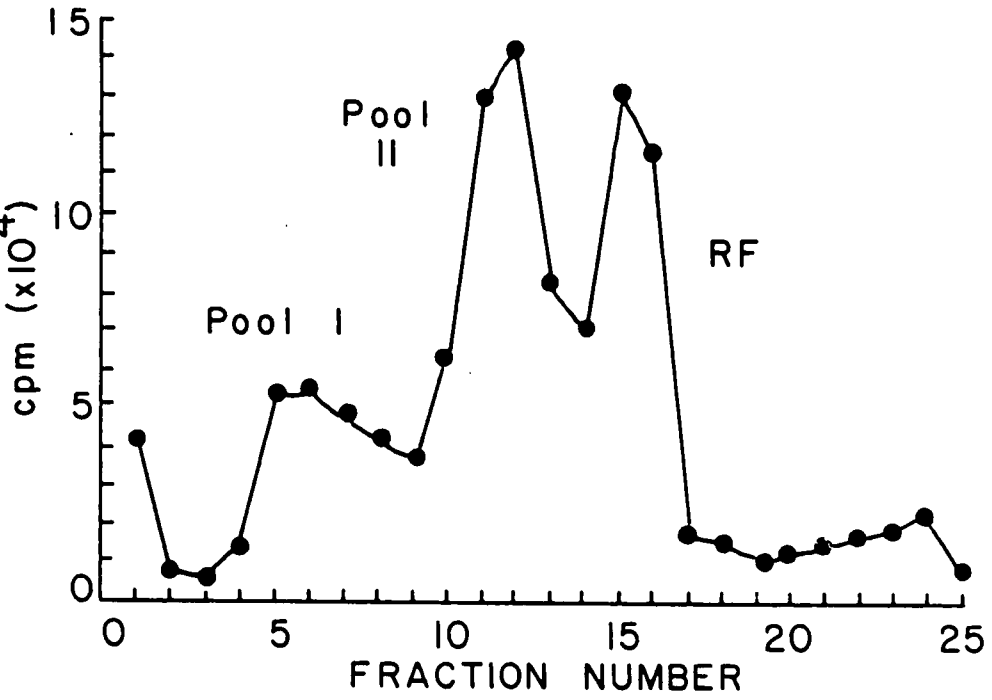
15
10
5
0
cpm (x10^4)
Pool II
Pool I
RF
0
5
10
15
20
25
FRACTION NUMBER

Figure 20

Figure 21. One percent gel electrophoresis of guanidine-HCl/sucrose gradient-purified KRV intracellular RF DNA's. Lane 1, RF pool after proteinase K digestion as described in Materials and Methods; Lane 2, RF pool before protease digestion; Lane 3, HindIII cleaved phage λ DNA; Lane 4, EcoRI cleaved phage λ DNA; Lane 5, Pool I material (see Figure 20) after protease digestion; Lane 6, Pool II material (see Figure 20) after protease digestion.

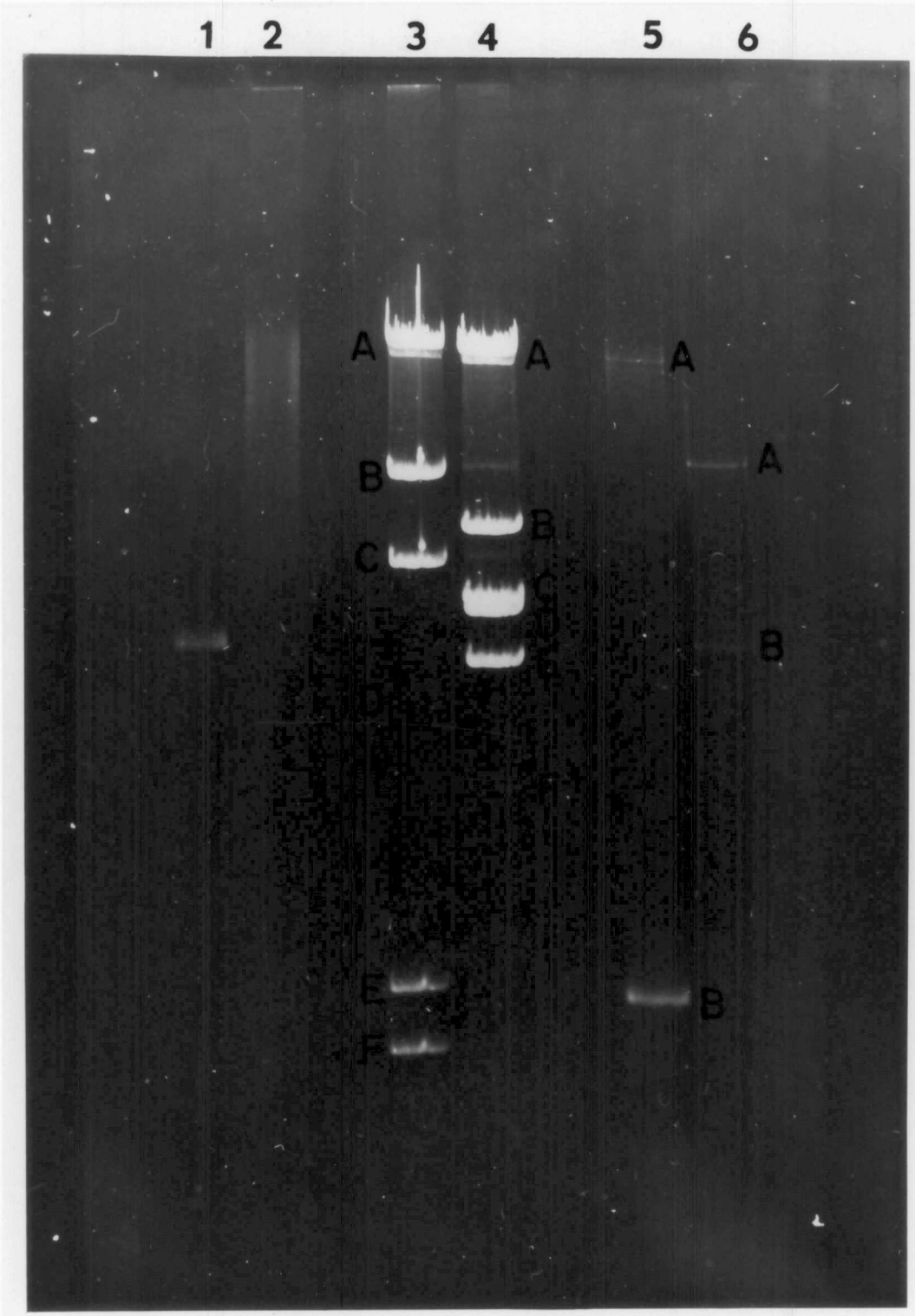
1
2
3
4
5
6
A
A
A
A
B
B
C
C
B
E
F
B

site-specific nick at the viral 3' end, giving rise to covalently linked RF DNA multimers (Ward and Dadachanji, 1978).

Peak fractions from the guanidine-HCl/sucrose gradients containing the RF DNA were dialyzed against buffer containing 20 mM Tris-HCl (pH 8.0), 2 mM EDTA, 0.1 M NaCl, 0.1% Sarkosyl and 0.1 mM PMSF. Following ethanol precipitation, RF was isopycnicaly banded in 53% neutral CsCl (in 20 mM Tris-HCl (pH 8.0), 2 mM EDTA, 0.1 mM PMSF, 0.1% Sarkosyl, plus or minus 15 mM 2-mercaptoethanol) at 40,000 rpm for 48 hr in a Beckman type 50 rotor at 10°. These preparations of RF were free of cellular DNA as judged by SDS/agarose gel electrophoresis (see below).

Alkaline CsCl Sedimentation

Neutral CsCl-purified RF DNA was suspended in 6.0 ml 57% (w/w) CsCl in 50 mM Na_3PO_4, ph. 12.8, 25 mM EDTA, 0.2% Sarkosyl, 25 µg/ml calf thymus DNA, 25 µg/ml bovine serum albumin. After centrifugation at 40,000 rpm in a Beckman type 50 rotor for 48 hr at 4°, fractions were collected from the bottom.

Labeling and Isolation of NRK Cell DNA

Uninfected cultures, seeded as described above, were labeled with 100 µCi/ml [^{3}H]thymidine for 1 hr. The cells were lysed with 0.2 M NaOH at 100° for 10 minutes. The DNA was then precipitated onto GFC filters (Whatman) with ice cold 10% trichloroacetic acid (TCA). After washing extensively with 5% TCA and 70% ethanol, the filters were dried and counted for ^{3}H.

Nuclease Digestions

For λ exonuclease digestions, 30,000 cpm (~1 μg) RF DNA or 50,000 cpm phase T5 DNA (~1 μg) were suspended in buffer containing 67 mM potassium glycinate, pH 9.4, 2 mM $MgCl_2$, 20 μg/ml salmon sperm DNA and 22 units of λ exonuclease (prepared by C. Snyder) and incubated at 37°. At various times after start of the reaction, aliquots were removed, the DNA precipitated with cold 10% TCA, and the supernatant counted for soluble ^3H.

E. coli exonuclease III digestions were performed with the same quantities of RF or T5 DNA in buffer containing 67 mM Tris-HCl, pH 8.0, 2 mM $MgCl_2$, 10 mM 2-mercaptoethanol, 20 μg/ml salmon sperm DNA and 25 units exonuclease III (prepared by C. Snyder). Incubation was at 37° and acid-soluble ^3H was determined as described above.

For total digestion of RF DNA, samples were suspended in 20 mM Tris-HCl, pH 8.6, 10 mM $MgCl_2$, 2 mM $CaCl_2$, 0.5% Triton X-100, and 1 mM PMSF. After 200 μg/ml micrococcal nuclease, 200 μg/ml venom phosphodiesterase and 100 μg/ml bacterial alkaline phosphatase (Worthington) were added, the mixture was incubated at 37° for 30 minutes. Under these conditions, the RF DNA was rendered completely acid-soluble.

Radioiodination of Proteins

Purified RF was treated with 50-150 μCi of ^{125}I Bolton and Hunter reagent as described elsewhere (Feitelson et al., 1981) and separated from the unreacted reagent by gel filration on Sephadex

G-25 (Pharmacia) of Jahn et al. (1984). Antisera were diluted 1:100 for use and included porcine parvovirus-infected pig and H-1 and KRV-infected hamster antisera generously donated by T. Molitor (University of Minnesota) and P. Paradiso (Praxis Biologicals), respectively. Rabbit anti-KRV capsid protein antiserum was prepared by S. Mitra. Anti-lamin C antibody from guinea pig was obtained from L. Gerace (Johns Hopkins University). S. aureus protein A (Accurate Biochemicals) was radioiodinated as described above (specific activity = 20-50 μCi/μg).

Peptide Analysis

Acetone/NH_4OH precipitates of electrophoretically purified proteins were resuspended in 10 μl 0.125 M Tris-HCl, pH 6.8, 1 mM EDTA, 0.1% SDS and digested with either S. aureus V-8 protease or α-chymotrypsin (PL Biochemicals) at the concentrations indicated below for 30 min at 37°. Peptides were then separated and identified by SDS/polyacrylamide gel electrophoresis and autoradiography as described above except that 15% acrylamide resolving gels were used.

3. RESULTS

Rate of Synthesis of KRV RF DNA and NRK Cell DNA

The first detectable synthesis of cellular DNA in mock-infected NRK cells occurs at 6 hr post-(mock)infection or 7 hr post-seeding (Figure 22). There is a sharp rise in the rate of cell DNA synthesis over the next 4 hr, detected as an increase in the amount of

Figure 22. Rate of synthesis of NRK cell DNA and KRV RF DNA infection time. Uninfected and KRV-infected NRK cells were pulse-labeled with [^{3}H]thymidine for 30 min. at the times indicated and the respective DNA's purified and analyzed for ^{3}H as described in the text.

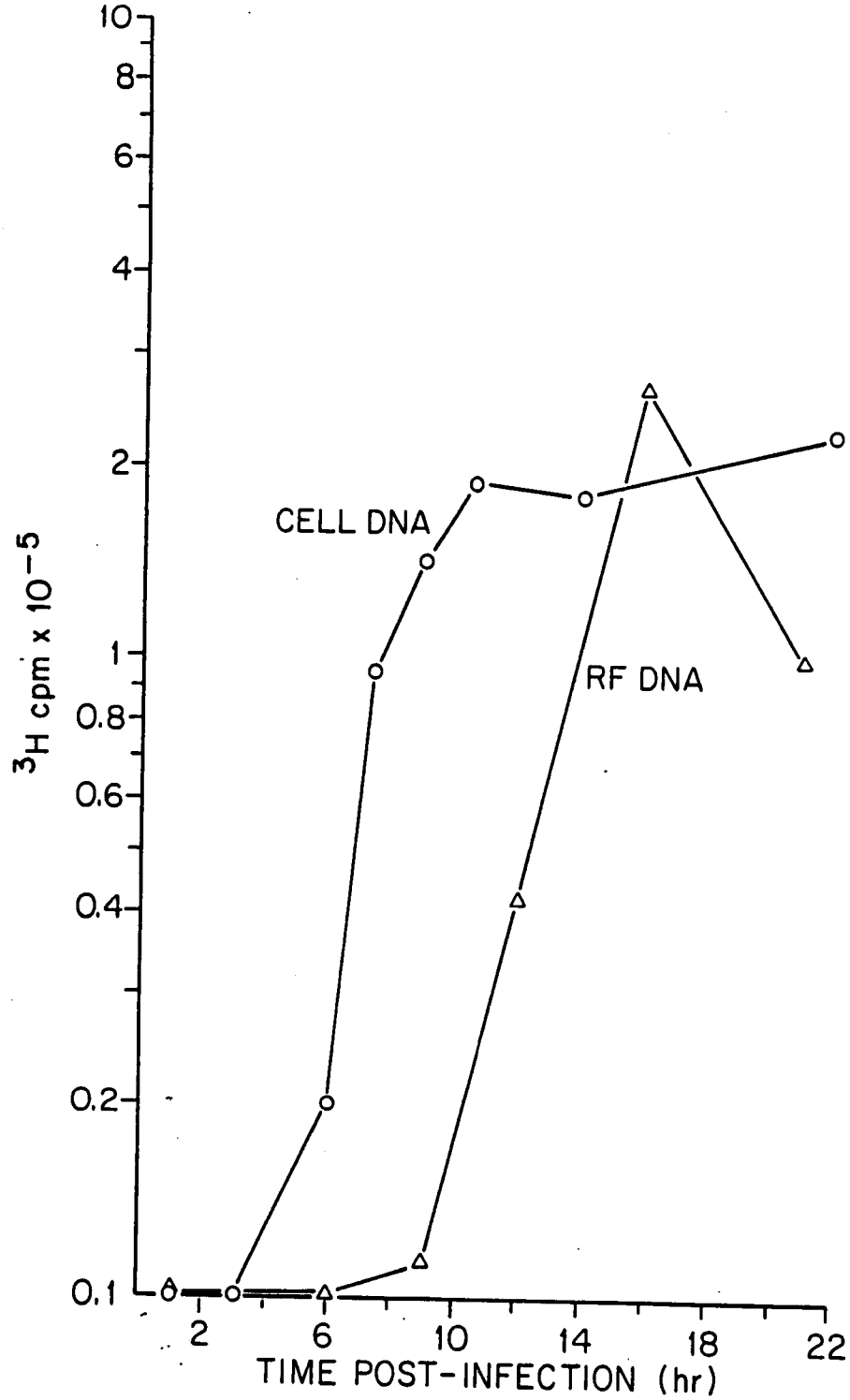
10
8
6
4
2
1
0.8
0.6
0.4
0.2
0.1
^{3}H cpm x 10^{-5}
CELL DNA
RF DNA
2
6
10
14
18
22
TIME POST-INFECTION (hr)

Figure 22

[^{3}H]thymidine incorporated during a 1 hr pulse, followed by a plateau, consistent with the parasynchronous growth of these cultures.

When infected cells are labeled for 1 hr intervals at various times post-infection, no RF synthesis is detected by guanidine-HCl/sucrose sedimentation until 9 hr post-infection (Figure 22). This is followed by an increase in the rate of RF synthesis to a peak at 15-17 hr post-infection, followed by a decline at 22 hr post-infection. Consequently, for all subsequent experiments, RF DNA was purified at 16 hr post-infection, since this appeared to be the time of peak RF DNA synthesis.

The observation of the onset of RF DNA synthesis within 3 hr after host S-phase has begun, as opposed to 8-10 hr reported previously (Rhode 1974a,b; Siegl, 1976), suggests that there is no requirement for some undefined "late" S-phase factor in parvovirus replication. Recently, Rhode has been able to detect H-1 RF DNA synthesis much closer to, and sometimes coincident with, the commencement of host S-phase simply by increasing the multiplicity of infection (personal communication). Therefore, the apparent delay in the onset of RF DNA synthesis may be merely a kinetic phenomenon, where the effective concentration of viral DNA template is initially very low compared to host cellular DNA replication origins. Earlier studies used a modified Hirt in 50 mM NH_4HCO_3 (pH 7.5), 0.1% SDS. Iodinated RF was stored at -80° in 70% ethanol and pelleted immediately prior to use. Labeled

preparations were routinely analyzed within 2 days to minimize radiochemical damage to proteins.

Restriction Digestion

1-5 μg of KRV RF DNA was digested with 4 units of HpaII or 5 units PstI in 50 mM Tris-HCl (pH 8.0), 10 mM $MgCl_2$, 1 mM dithiothreitol, 100 μg/ml bovine serum albumin, 1 mM PMSF at 37° for 2 hours. The restriction fragments were then separated on neutral SDS/agarose gels as described below.

Gel Electrophoresis

RF DNA or its restriction fragments were electrophoresed in neutral agarose gels in Tris/acetate/EDTA buffer (Maniatis et al., 1982) plus 0.1% SDS. Prior to loading, samples were heated to 37° for 20 minutes in 10 mM EDTA, 20% glycerol, 1.0% SDS, 0.1% bromophenol blue. When the separated fragments were to be further analyzed, a trough was cut in the gel just ahead of the ethidium bromide-stained band, lined with dialysis tubing and filled with electrophoresis buffer. The DNA, which could be followed under ultraviolet light, was then electrophoresed into the trough, collection, and concentrated by ethanol precipitation.

Alkaline SDS/agarose gels were prepared by dissolving agarose at the indicated concentration in 50 mM NaCl, 2 mM EDTA. After the gel had solidified, it was equilibrated with alkaline running buffer (30 mM NaOH, 2 mM EDTA, 0.1% SDS) for at least 60 minutes prior to use. Samples were heated to 50° for 5 minutes in 30 mM NaOH,

2 mM EDTA, 1.0% SDS, 10% glycerol, 0.1% bromophenol blue before loading.

Proteins were separated on SDS/polyacrylamide gels by the procedure of Laemmli (1970) using a 4.5% polyacrylamide stacking gel with a 12% polyacrylamide resolving gel (acrylamide:bis-acrylamide = 37.5:1). Iodinated proteins were detected by autoradiography with XAR-5 film (Kodak). For peptide analysis, protein bands identified by autoradiography were excised and briefly rehydrated with electrophoresis running buffer (Laemmli, 1970). The gel slice was then macerated and incubated at 37° for 3 hr in running buffer after which the polyacrylamide was removed by centrifugation. The eluted proteins were precipitated with 5 volumes acetone:conc. NH_4OH (18:1) and pelleted by centrifugation at 10,000 x g for 15 min.

Electrophoretic Transfer and Immunoblotting

Proteins separated on SDS/polyacrylamide gels as described above were transferred to nitrocellulose sheets (Schliecher and Schuell BA 85) according to the procedure of Burnette (1981). The gel was placed in a sandwich next to the nitrocellulose and submerged in 20 mM Tris base, 150 mM glycine, 20% methanol, and a current of 300 mA was applied (nitrocellulose toward the anode) for 24 hr. The nitrocellulose, containing the proteins, was then washed in buffer containing 50 mM Tris-HCl, pH 7.4, 0.9% NaCl and 5% bovine serum albumin, incubated with antibodies and probed with 1×10^6 cpm ^{125}I labeled S. aureus protein A according to the procedure for the isolation of RF DNA (Rhode, 1974a,b; Siegl, 1976), which results

in high background levels of contaminating cellular DNA, making detection of small quantities of RF DNA, such as those present early in infection, difficult. The guanidine-HCl/sucrose procedure described here gives much lower cellular DNA contamination and reduces the "noise" level for RF DNA detection (see Figures 19 and 20, pp. 90 and 97).

Evidence for Proteins Covalently Bound to KRV RF DNA--
Electrophoretic Mobility

When RF DNA purified as described above is electrophoresed in non-denaturing agarose gels, most of it remains bound at the origin or migrates as a broad smear of high apparent molecular weight (Figure 21, lane 2, p. 99). When the RF is treated with protease, it then displays normal electrophoretic mobility (Figure 21, lane 1). This abnormal electrophoretic mobility is consistent with the tight binding of protein to the DNA. Since phenol extraction in the presence of high concentrations of SDS and 2-mercaptoethanol (Figure 23) and treatment with 0.1 M NaOH for as long as 18 hr (Figure 24) did not result in normal electrophoretic mobility of the RF DNA, it was concluded that the putative protein may be covalently bound by an alkali-resistant protein-nucleotide linkage.

In order to localize the binding site for the protein, the RF DNA was digested with the restriction endonuclease PstI prior to electrophoresis. PstI generates four fragments of the RF, in order from (viral) 3' to 5' end: A (2140 bp), B (1320 bp), C (1070 bp), and D (560 bp) (Banerjee et al., 1981). Without protese digestion

Figure 23. One percent agarose gel electrophoresis of KRV RF DNA after: (A) no treatment; (B) phenol extraction in the presence of 2% 2-mercaptoethanol; and (C) proteinase K digestion. Extractions and digestions were done as described in the text; 0.2 cm gel slices were analyzed for ^{3}H as in Figure 18.

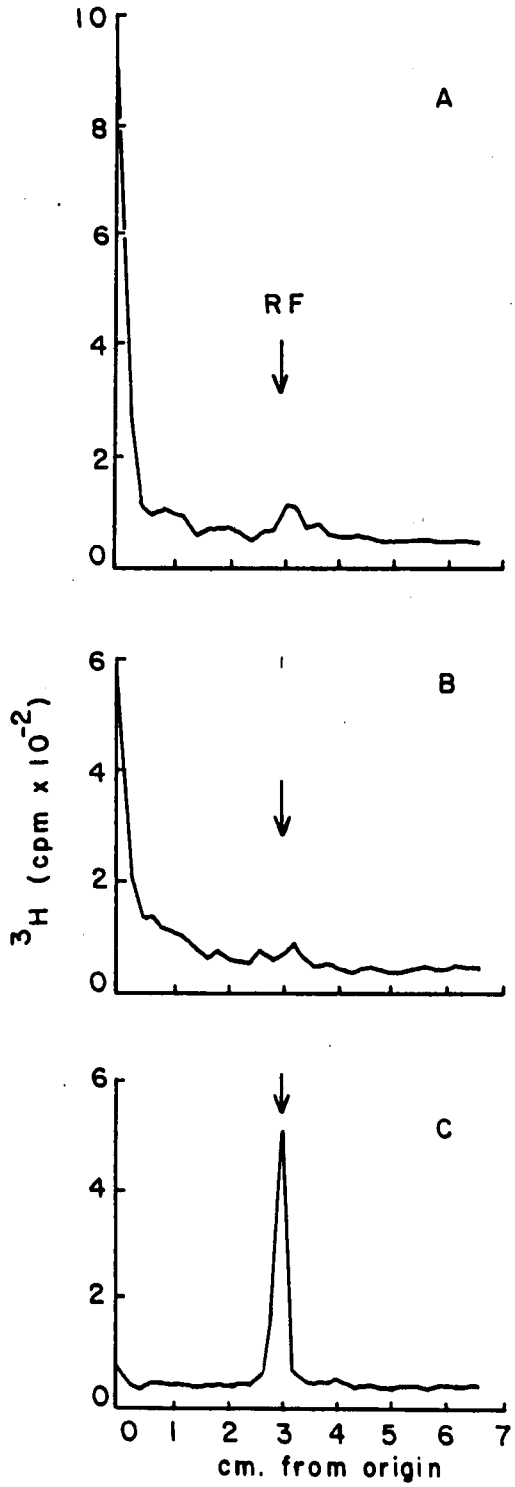

Figure 23

Figure 24. One percent agarose gel electrophoresis of KRV RF DNA after exposure to alkali. Lane 1, RF DNA incubated with 0.1 M NaOH at 37° for 18 hours followed by renaturation by dialysis against 20 mM Tris-Cl (pH 8.0), 200 mM NaCl; Lane 2, proteinase K digested RF DNA. Gel was stained with 1 µg/ml ethidium bromide and photographed under ultraviolet light.

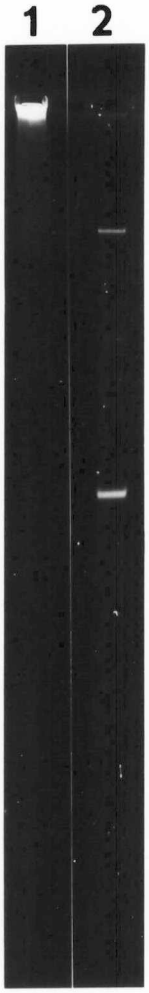
1
2

prior to electrophoresis, only the internal (B and C) fragments entered the gel, while after protease treatment all fragments entered the gel (Figure 25). This suggests that the protein is associated only with the termini of the RF DNA, a fact noted earlier by Revie et al., (1979) using H-1 RF DNA and HaeIII, which generates seven fragments.

Evidence for Proteins Covalently Bound to KRV RF DNA--
Isopycnic Sedimentation

If a protein is covalently bound to the RF DNA, then one would expect to see an increase in the apparent byoyant density of the DNA after digestion with proteases. Using the formula of Davidson and Szybalski (1971):

$$\frac{M_n}{M_p} = \frac{(\theta_c - \theta_p)\ \theta_n}{\theta_n - \theta_c\ \theta_p} \qquad \text{(IV-1)}$$

where M_p and M_n are the molecular weights of the protein and nucleic acid, respectively, and θ_c, θ_n, and θ_p are the densities of the complex, the nucleic acid and the protein, respectively, it would be possible to estimat the molecular weight of the protein based on this buoyant density shift.

As shown in Figure 26, the buoyant density of RF DNA does increase after protease digestion. Assuming a partial specific volume of 0.75 for protein and a molecular weight of 3.36×10^6 for KRV RF DNA (Snyder et al., 1982), this density shift would be

Figure 25. One percent agarose gel electrophoresis of PstI digested RF DNA before (——●——) and (——▲——) proteinase K digestion. 0.2 slices were cut and counted for ^{3}H as before.

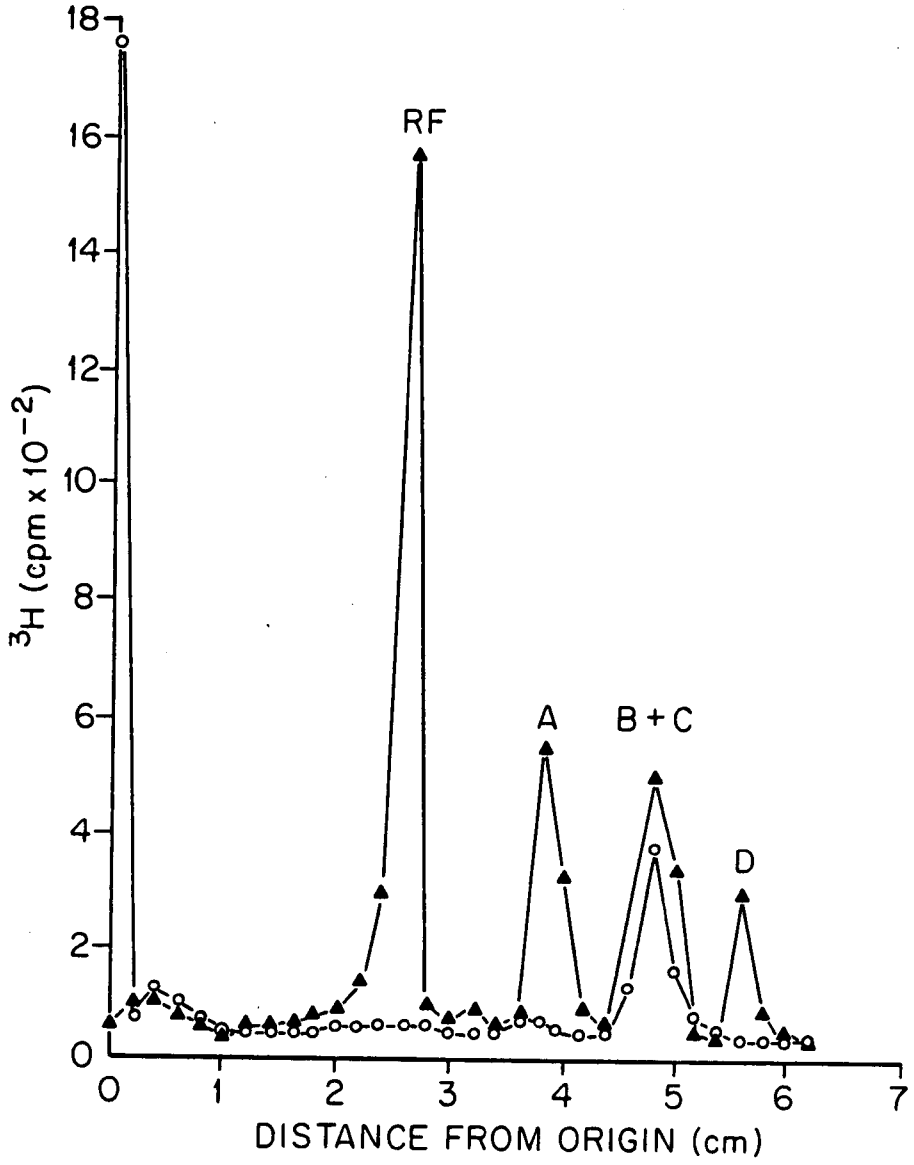
18
16
14
12
10
8
6
4
2
0
^3H (cpm x 10^{-2})
RF
A
B+C
D
0
1
2
3
4
5
6
7
DISTANCE FROM ORIGIN (cm)

Figure 25

Figure 26. Neutral CsCl gradient sedimentation of KRV RF DNA before (A) and after (B) digestion with proteinase K. (-----) Density of CsCl determined by refractometry.

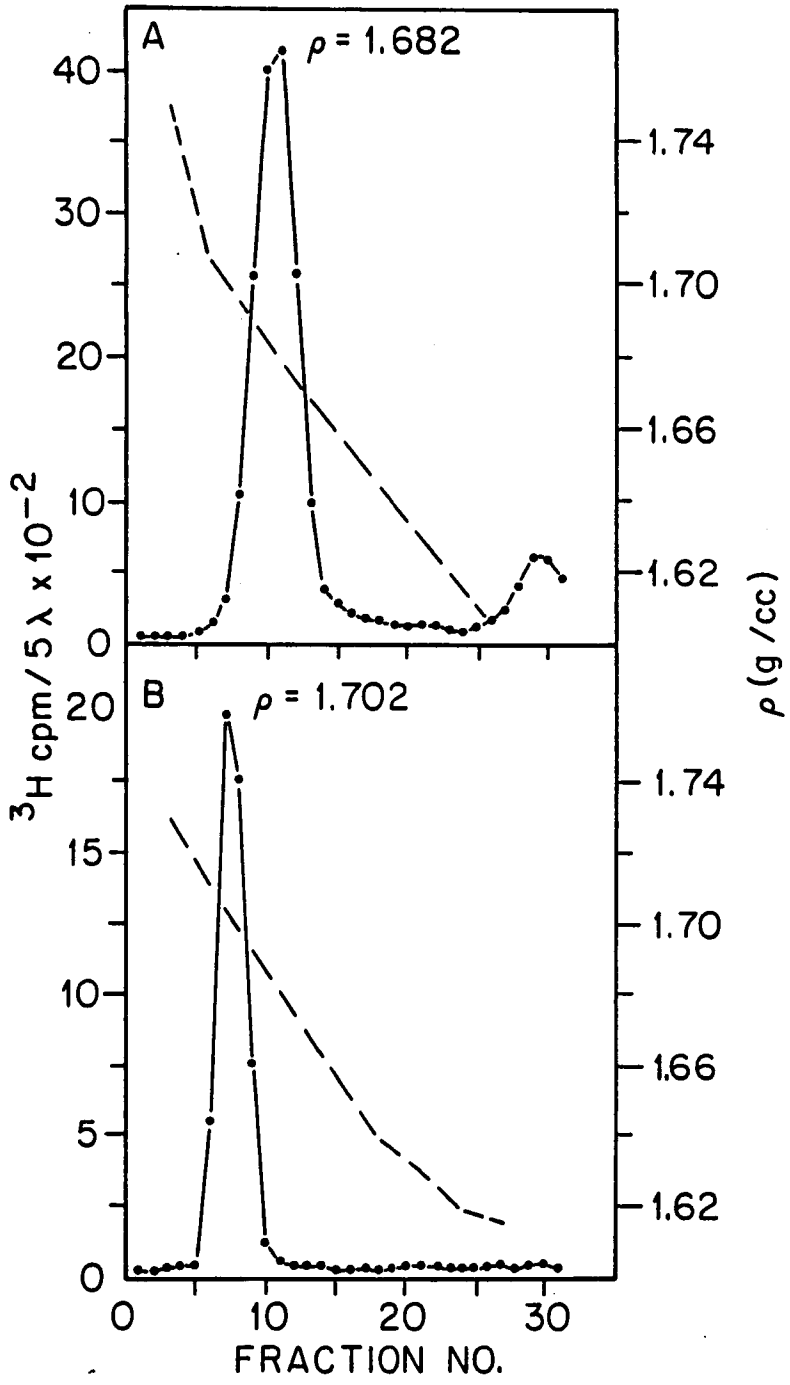
A
ρ = 1.682
B
ρ = 1.702
40
30
20
10
0
20
15
10
5
0
1.74
1.70
1.66
1.62
1.74
1.70
1.66
1.62
0
10
20
30
FRACTION NO.
^{3}H cpm/5λ x 10^{-2}
ρ (g/cc)

Figure 26

consistent with the loss of about 75 kDa of protein from each end of the DNA. This observation is similar to that made by Revie et al. (1979) for the H-1 RF DNA terminal protein.

Evidence for Proteins Covalently Bound to KRV RF DNA--
Copurification of ^{35}S and ^{3}H Label

When infected cells were labeled with L-[^{35}S]methionine as described above and purified in parallel with [^{3}H]thymidine labeled RF through guanidine-HCl/sucrose (Figure 27), neutral CsCl (Figure 28), or alkaline CsCl (Figure 29) gradients, ^{35}S and ^{3}H labeled material cosedimented. Cosedimentation in alkaline CsCl is strongly suggestive of a covalent linkage between protein and DNA. The observation that ^{35}S and ^{3}H comigrated suggested that the protein was bound to a molecule the size (in addition to density) of the RF DNA (Figure 30).

Exonuclease Sensitivity of RF DNA

As shown in Figure 31b, KRV RF DNA purified through neutral CsCl is completely sensitive to exonuclease III, which digests double-stranded DNA from the 3' end provided that end has an unblocked 3' OH. On the other hand, λ exonuclease, which digests double-stranded DNA in a 5' to 3' direction only if there is a free 5' terminal phosphate, did not digest RF DNA under conditions where an identical amount of phage T5 DNA was digested to completion (Figure 31a). These results suggest that 5' terminus of the RF DNA is blocked, presumably by a terminal protein. Assuming that a maximum of 25,000 cpm of radioactive nucleotides would have been

Figure 27. Guanidine-HCl/sucrose gradient of [^{35}S]methionine (——▲——) and [^{3}H]thymidine (——●——) labeled KRV RF DNA. Centrifugation as described in Materials and Methods. One ml fractions were collected from the top and aliquots counted for ^{3}H or ^{35}S.

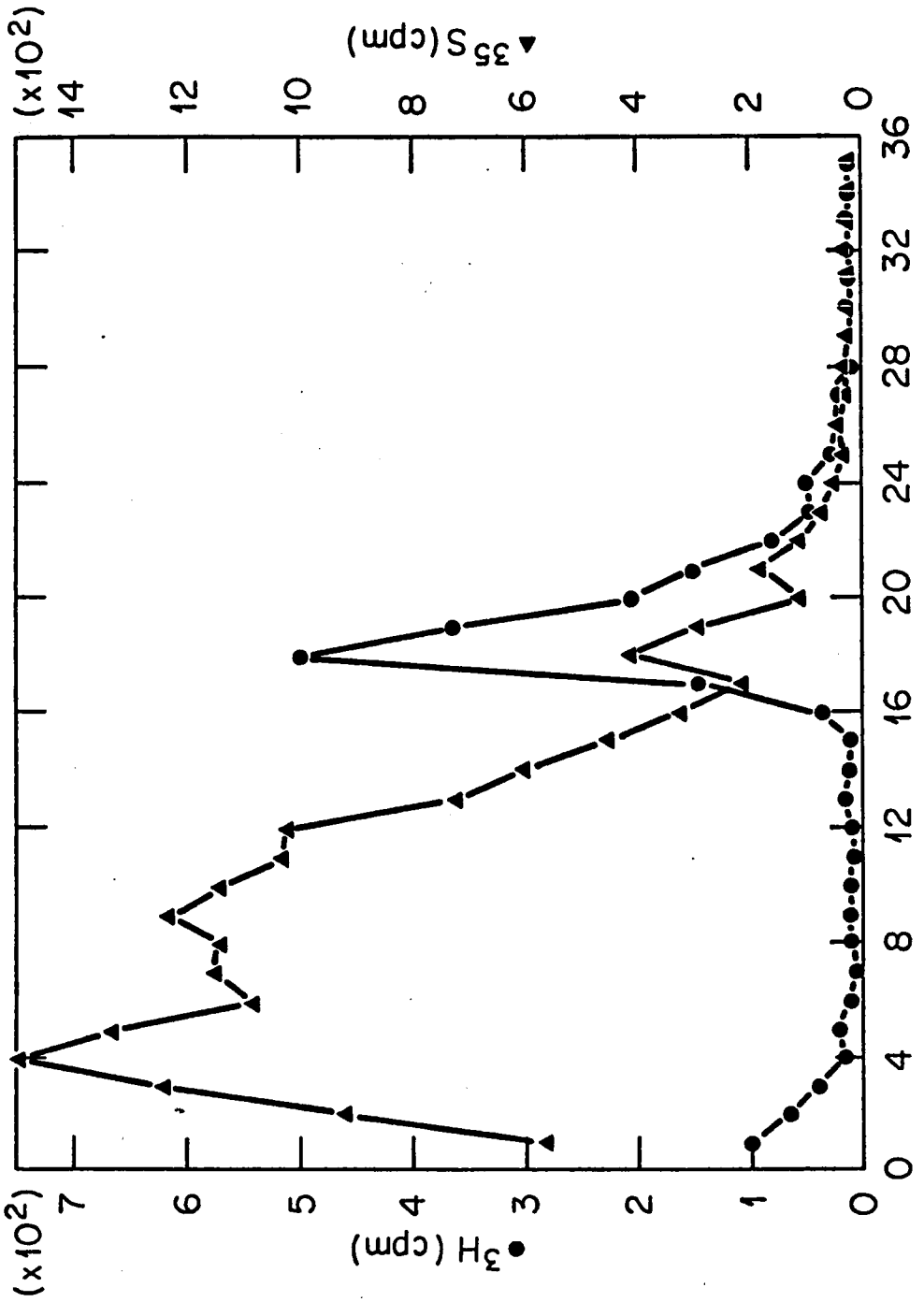
(x10²)
14
12
10
8
6
4
2
0
▲ ³⁵S (cpm)
(x10²)
7
6
5
4
3
2
1
0
● ³H (cpm)
0
4
8
12
16
20
24
28
32
36
FRACTION NO.

Figure 27

Figure 28. Neutral CsCl gradient sedimentation of [^{35}S]methionine (——▲——) and [^{3}H]thymidine (——●——) labeled KRV RF DNA (see Materials and Methods). Starting material was RF peak from Figure 27; 10 drop fractions collected from bottom and aliquots counted for ^{3}H or ^{35}S.

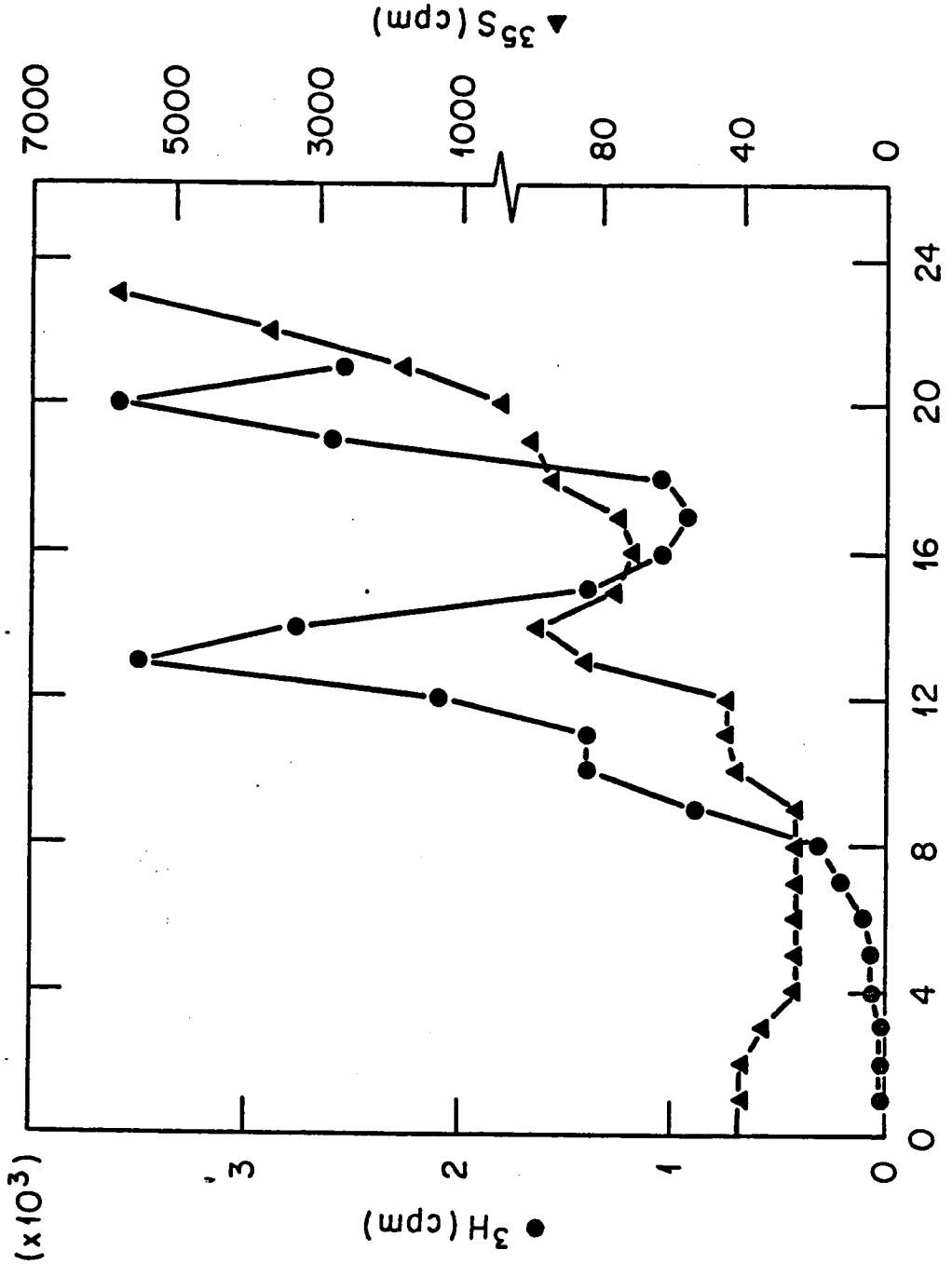
▲ 35S (cpm)
7000
5000
3000
1000
80
40
0
● 3H (cpm)
(x10³)
3
2
1
0
0
4
8
12
16
20
24
FRACTION NO.

Figure 28

Figure 29. Alkaline CsCl gradient sedimentation of KRV RF DNA from [^{35}S]methionine (——▲——) and [^{3}H]thymidine (——●——) labeled cells. Starting material was RF peak from Figure 28; 10 drop fractions collected from bottom and counted for ^{3}H or ^{35}S.

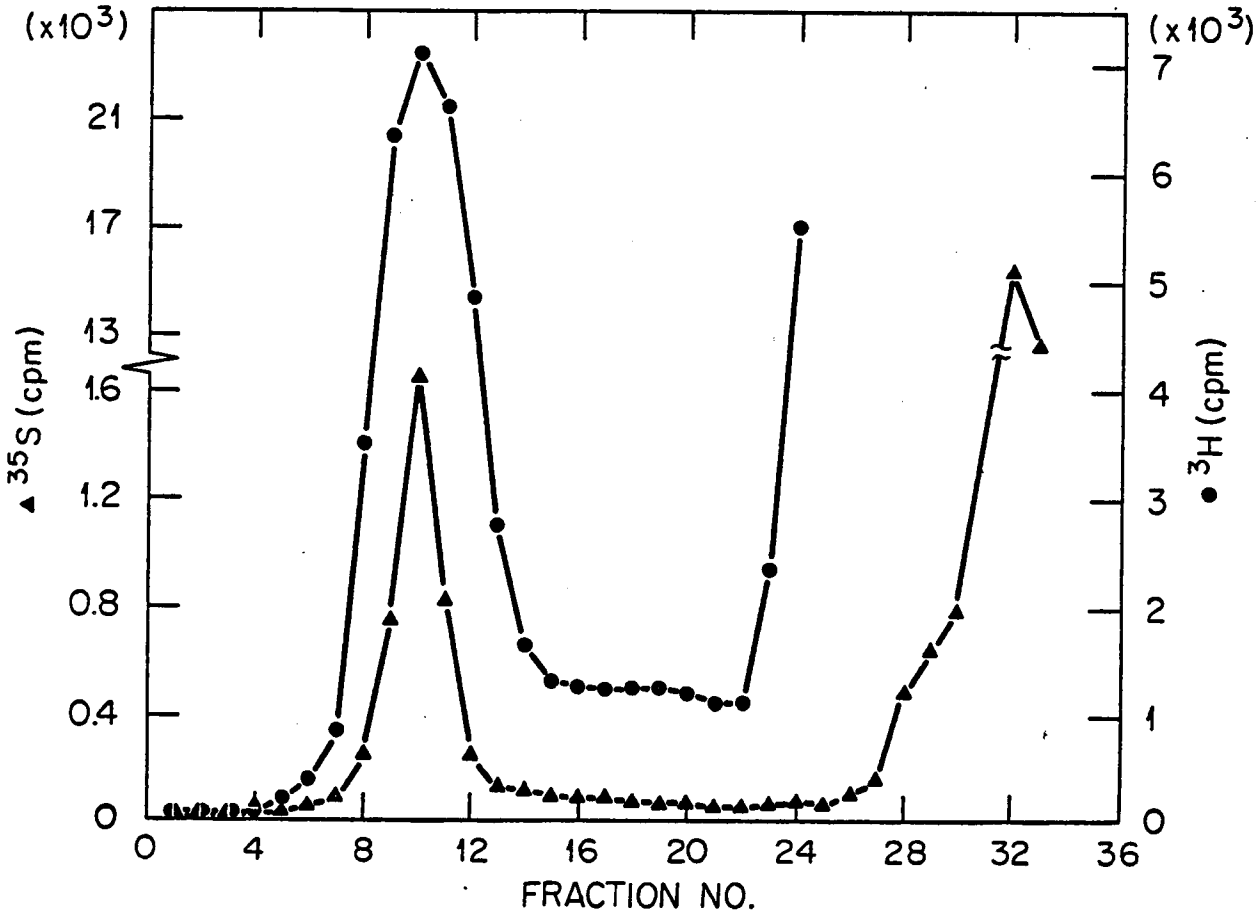
(x10³)
21
17
13
1.6
1.2
0.8
0.4
0
▲ ³⁵S (cpm)
(x10³)
7
6
5
4
3
2
1
0
● ³H (cpm)
0
4
8
12
16
20
24
28
32
36
FRACTION NO.

Figure 29

Figure 30. SDS/agarose gel electrophoresis of KRV RF DNA from cells labeled with [^{35}S]methionine (——▲——) and [^{3}H]thymidine (——●——). One percent agarose/0.1% SDS gel (described in text) of neutral CsCl purified KRV RF DNA (see Figure 27); 0.5 cm slices were counted for ^{3}H.

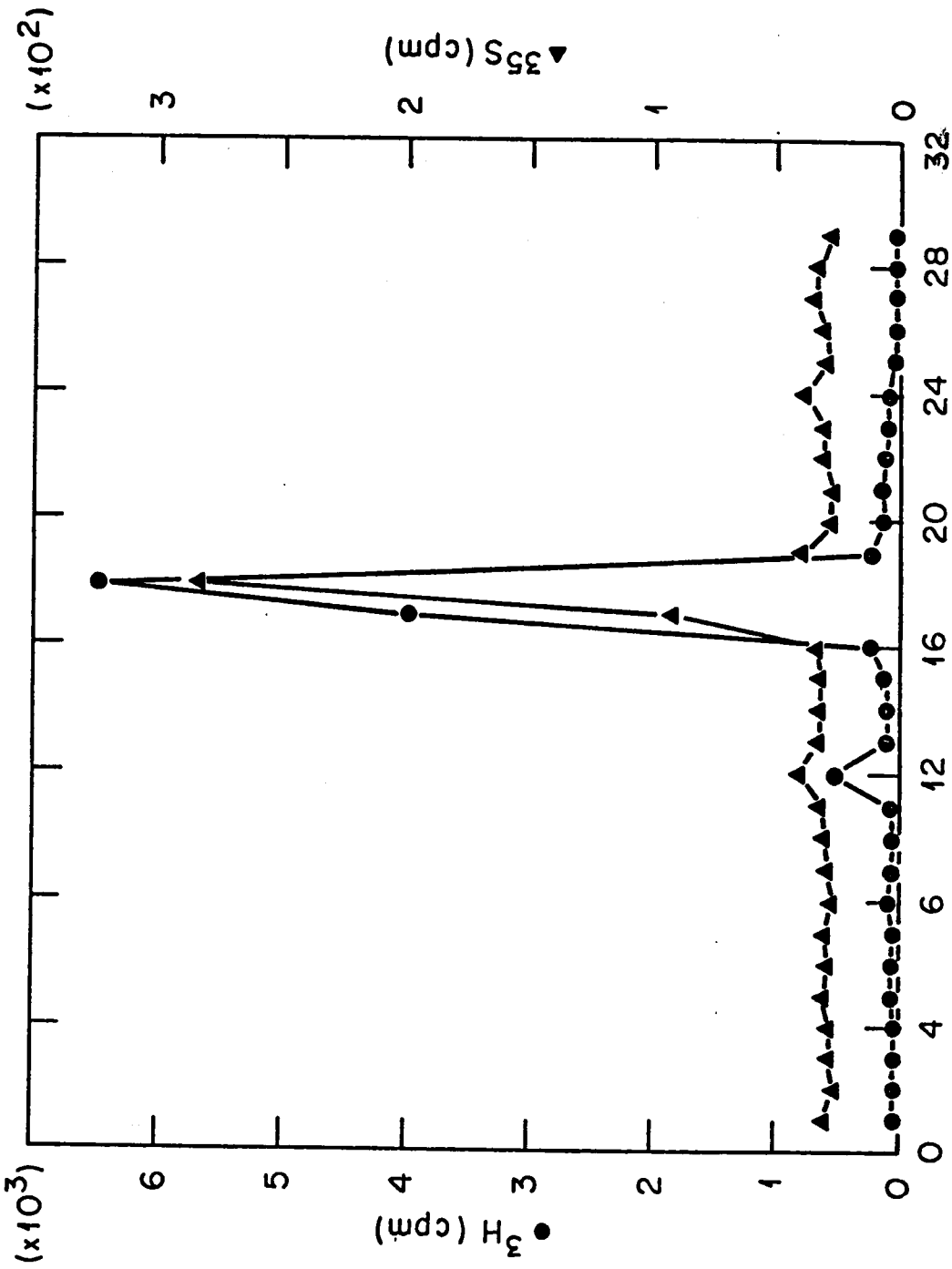
(x10²)
▲ ³⁵S (cpm)
3
2
1
0
(x10³)
● ³H (cpm)
9
6
5
4
3
2
1
0
0
4
6
12
16
20
24
28
32
FRACTION NO.

Figure 30

Figure 31. Sensitivity of KRV RF DNA (——Δ——) and bacteriophage T5 DNA (——o——) to λ exonuclease (A) and E. coli exonuclease III (B).

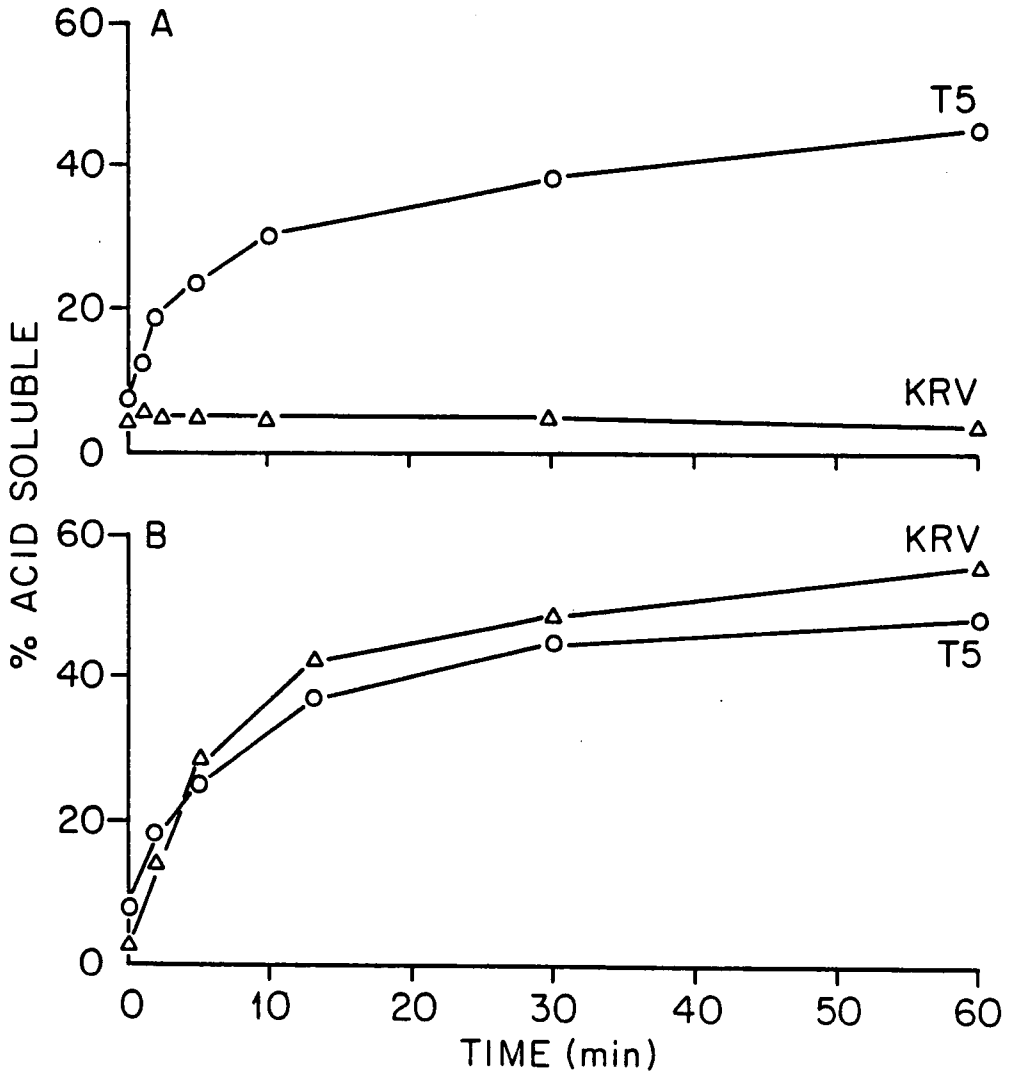
60
A
T5
40
20
KRV
0
% ACID SOLUBLE
60
B
KRV
40
T5
20
0
0
10
20
30
40
50
60
TIME (min)

Figure 31

released by a limit digest, it appears that >99% of the 5' ends are blocked or that >99% of the RF DNA has terminal protein.

Proteins Associated with CsCl-purified RF DNA

Incorporation of ^{35}S label into RF DNA-associated protein was very limited, and highly purified preparations (Figure 30) had too little radioactivity for further detailed analysis. As a result, ^{125}I Bolton and Hunter reagent was chosen to label proteins. This reagent is highly specific for labeling primary amino groups of proteins; in our hands 500-1000 times more iodine was incorporated into bovine serum albumin than into an equal mass of *E. coli* DNA or tRNA (unpublished observation). Iodinated RF DNA gave a protease-sensitive band on SDS/agarose gels which comigrated with ethidium bromide-stained RF DNA (Figure 31) plus a large amount of much faster migrating material.

When CsCl-purified ^{125}I labeled RF was electrophoresed in SDS/polyacrylamide gels, several radioactive proteins, of approximately 300, 68-72 and 55 kDa, were seen (Figure 33a, lane 1). The fact that these bands were observed without digestion of RF DNA and that micrococcal nuclease treatment did not alter their intensity (Figure 33a, lane 2) suggests that they are not covalently bound to RF DNA. Nuclease digestion of the RF resulted in the appearance of a new protein at about 40 kDa (Figure 33a, lane 2) which may have been covalently associated prior to digestion. All of these bands were eliminated by protease treatment prior to electrophoresis (data not shown).

Figure 32. Autoradiogram of 1% SDS/agarose gel of ^{125}I-labeled KRV RF DNA before (lane 1) and after (lane 2) digestion with proteinase K. Abbreviations: kbp, kilobase pairs (HindIII-digested λ DNA markers); RF, position of ethidium bromide-stained KRV RF DNA marker.

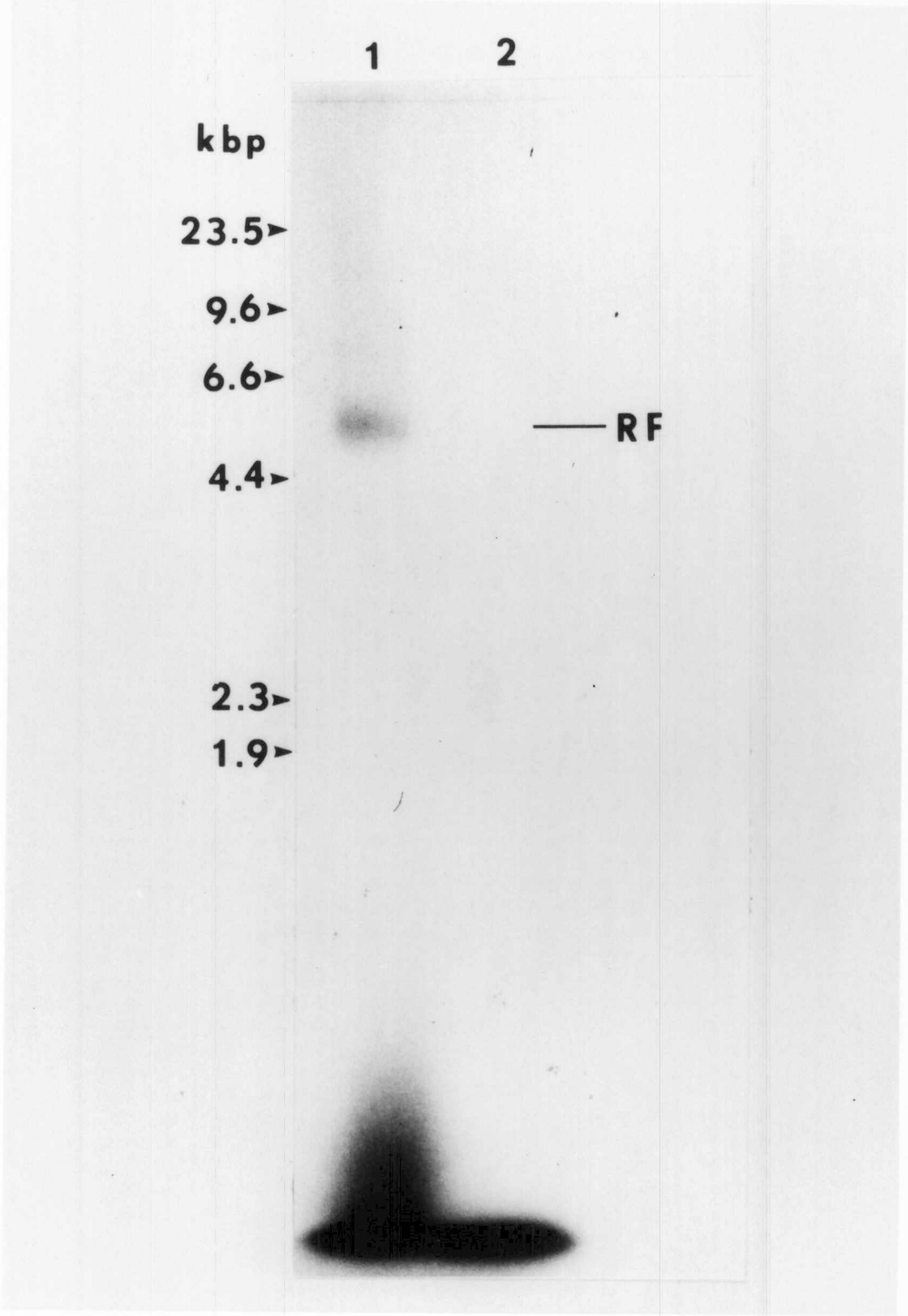
1
2
kbp
23.5
9.6
6.6
RF
4.4
2.3
1.9

Figure 33. Autoradiograms of SDS/polyacrylamide gels of ^{125}I-labeled proteins associated with KRV RF DNA. (A) Proteins associated with neutral CsCl-purified RF DNA. Lane 1, undigested RF DNA; Lane 2, RF DNA digested with nucleases as described in Materials and Methods prior to electrophoresis. (B) Proteins associated with RF DNA following phenol extraction in the presence of 1% Sarkosyl (lanes 1 and 2) or 1% Sarkosyl, 2% 2-mercaptoethanol (lanes 3 and 4). Material in lanes 1 and 3 was loaded onto gels without prior nuclease or protease digestion, and material in lanes 2 and 4 was digested with proteinase K before loading. (C) Uninfected host cell proteins reassociating with protease treated RF DNA. Lane 1, undigested RF DNA; Lane 2, RF DNA digested with nucleases before loading. kDA, molecular weights of protein standards.

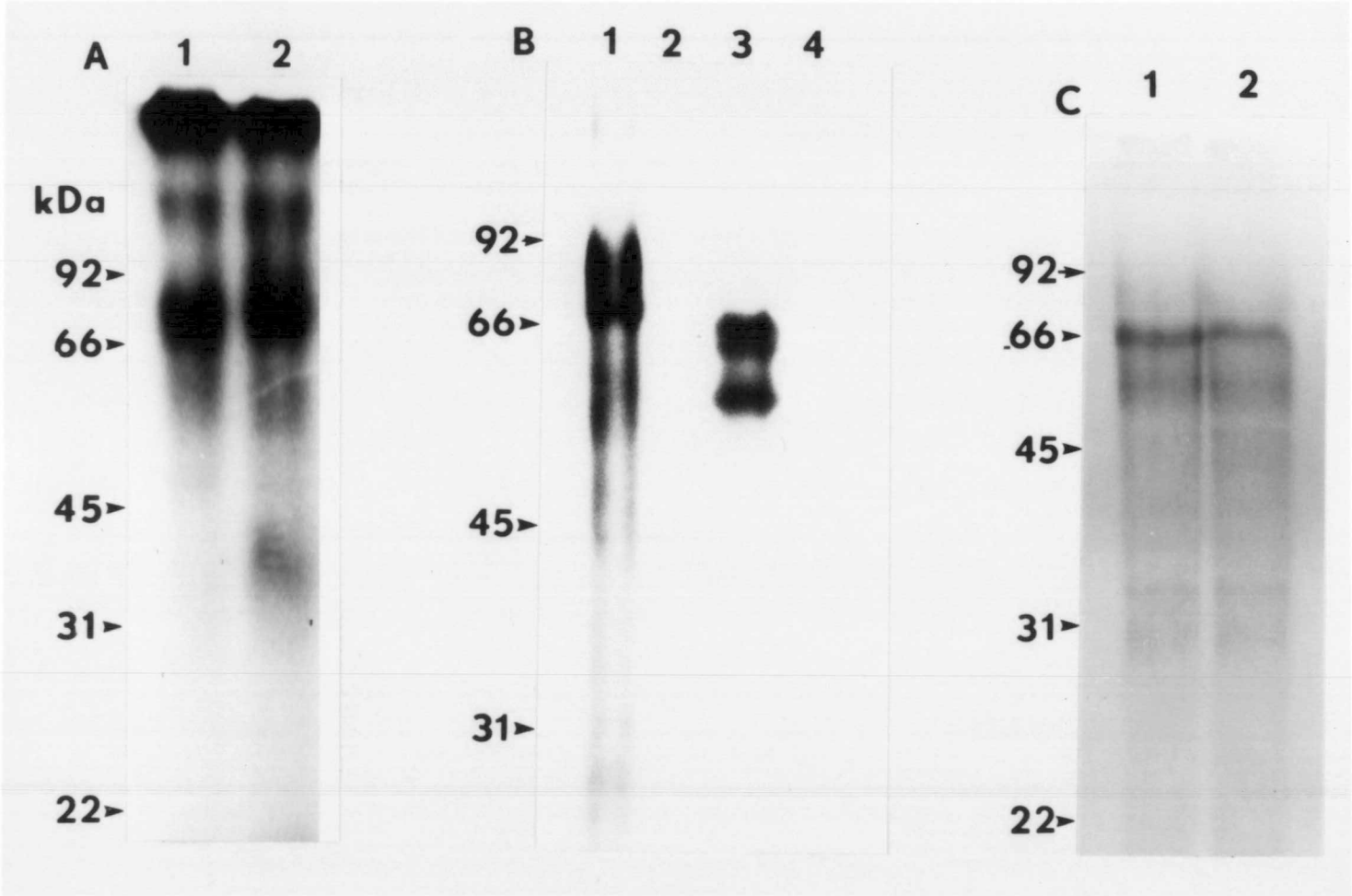
A
1
2
kDa
92
66
45
31
22
B
1
2
3
4
92
66
45
31
C
1
2
92
66
45
31
22

Attempts to remove the non-covalently associated proteins by phenol extraction in the presence of detergent (Figure 33b, lane 1) were unsuccessful. However, phenol extraction in 2% 2-mercapto-ethanol removed the 68-72 kDa material while proteins of 64, 62, and 55 kDa became more prominent (Figure 33b, lane 3). As above, release of this material from non-nuclease treated RF and its protease sensitivity (Figure 32b, lanes 2 and 4) indicated its non-covalent association and proteinaceous nature, respectively. These proteins probably correspond to the faster migrating material seen on SDS/agarose gels (Figure 30). The removal of some of these proteins by 2-mercaptoethanol led to the inclusion of this reagent during subsequent purifications of the RF DNA (see Materials and Methods). Iodination by Bolton-Hunter reagent does result in small changes in the apparent molecular weight of some proteins (Feitelson, 1981) so the true molecular weights of these proteins may be somewhat different from those observed here by a few percent.

Binding of Uninfected Cellular Proteins to Deproteinized RF

Some of the proteins associated with RF DNA may have arisen from aggregation of cellular proteins onto the DNA induced by guanidine-HCl treatment or from virus capsid assembly intermediates. [Two of the capsid proteins have molecular weights of 64 and 59 kDa (Mitra et al., 1982).] To test this possibility, RF DNA purified by centrifugation in guanidine-HCl/sucrose was digested with proteinase K, phenol-extracted, and mixed with uninfected cells lysed by the procedure used for RF DNA preparation. After rebanding in

guanidine-HCl/sucrose followed by CsCl banding, this RF DNA was radioiodinated and electrophoresed in SDS/polyacrylamide gels with and without nuclease digestion. Major proteins of 62-64 and 55 kDa were found to be non-covalently associated with this RF (Figure 33c), suggesting that the non-covalent proteins mentioned above (Figure 32a,b) are not of viral origin. Nuclease treatment resulted in no new proteins being released from the RF DNA (Figure 33c, lane 2) indicating that no covalent DNA-protein linkages are induced by this procedure.

Proteins Associated with Electrophoretically Purified RF

Because SDS/agarose gels appeared to remove a great deal of labeled material from the RF DNA, we chose to use electrophoresis as a purification step following CsCl banding. RF DNA purified in this manner appeared to be free of non-covalently associated proteins (Figure 34, lane 1), while nuclease digestion resulted in the appearnace of two protease-sensitive bands at 90 and 40 kDa (Figure 34, lanes 2 and 3).

Association of Protein with Terminal Restriction Fragments

If either the 40 or 90 kDa protein is covalently attached to the termini of RF DNA, it should be released exclusively from terminal restruction fragments of the RF DNA by nuclease digestion. CsCl-purified ^{125}I-labeled RF DNA was digested with HpaII and the fragments were separated by SDS/agarose gel electrophoresis, electroeluted and analyzed by SDS/polyacrylamide gel electrophoresis

Figure 34. Autoradiogram of SDS/polyacrylamide gel of ^{125}I-labeled proteins associated with electrophoretically purified RF DNA. Electroeluted RD DNA was loaded onto SDS/polyacrylamide gel before (lane 1) or after (lane 2) digestion with nucleases or after digestion with nucleases and proteinase K (lane 3). kDA, molecular weights of protein standards.

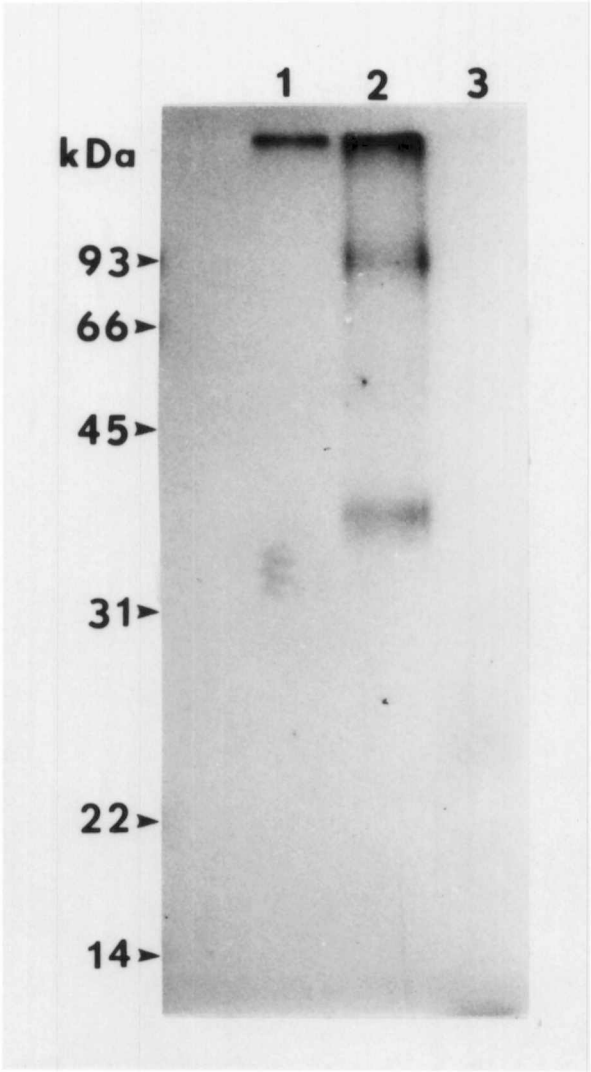
1
2
3
kDa
93
66
45
31
22
14

before and after nuclease treatment. The results (Figure 35) indicate that both the 40 and 90 kDa proteins are associated only with the terminal restriction fragments, A and B, and not with the internal (C) fragment (see Banerjee et al., 1981 for KRV restriction map). Similar results were obtained with PstI which generates four fragments of the RF DNA (data not shown). Because of their association with the RF DNA termini, these two proteins will be designated RF TP-90 and RF TP-40, for RF DNA terminal protein, 90 and 40 kilodaltons, respectively.

Immunoblot Analysis of Covalently and Non-covalently Bound Proteins

The "Western" immunoblotting procedure described above has been successfully used for the identification of nanogram quantities of a number of proteins. It has the advantage of giving molecular weight information as well as an indication of immunologic cross-reactivity of proteins.

When nitrocellulose sheets containing electrophoretically separated, unlabeled proteins from nuclease-digested RF DNA were probed with rabbit anti-KRV capsid protein antiserum and ^{125}I protein A, no cross-reacting bands were detected (Figure 36, lane 3). In contrast, as little as 20 ng of capsid protein was easily detected (Figure 36, lane 2). Since 1 µg of RF DNA ($M_r = 3.2 \times 10^6$) was loaded, one molecule of a 60 kDa protein per RF DNA molecule would have been within the detection limits of the assay as performed here.

Figure 35. Autoradiogram of SDS/polyacrylamide gel of ^{125}I-labeled proteins associated with electrophoretically purified HpaII restriction fragments of RF DNA. A (lanes 1-3), B (lanes 4-6), and C (lanes 7-9) fragments were either digested with nucleases (lanes 2, 5, 8) or with nucleases and proteinase K (lanes 3, 6, 9) prior to loading. Lanes 1, 4, and 7 are undigested controls. kDA, molecular weights of protein standards.

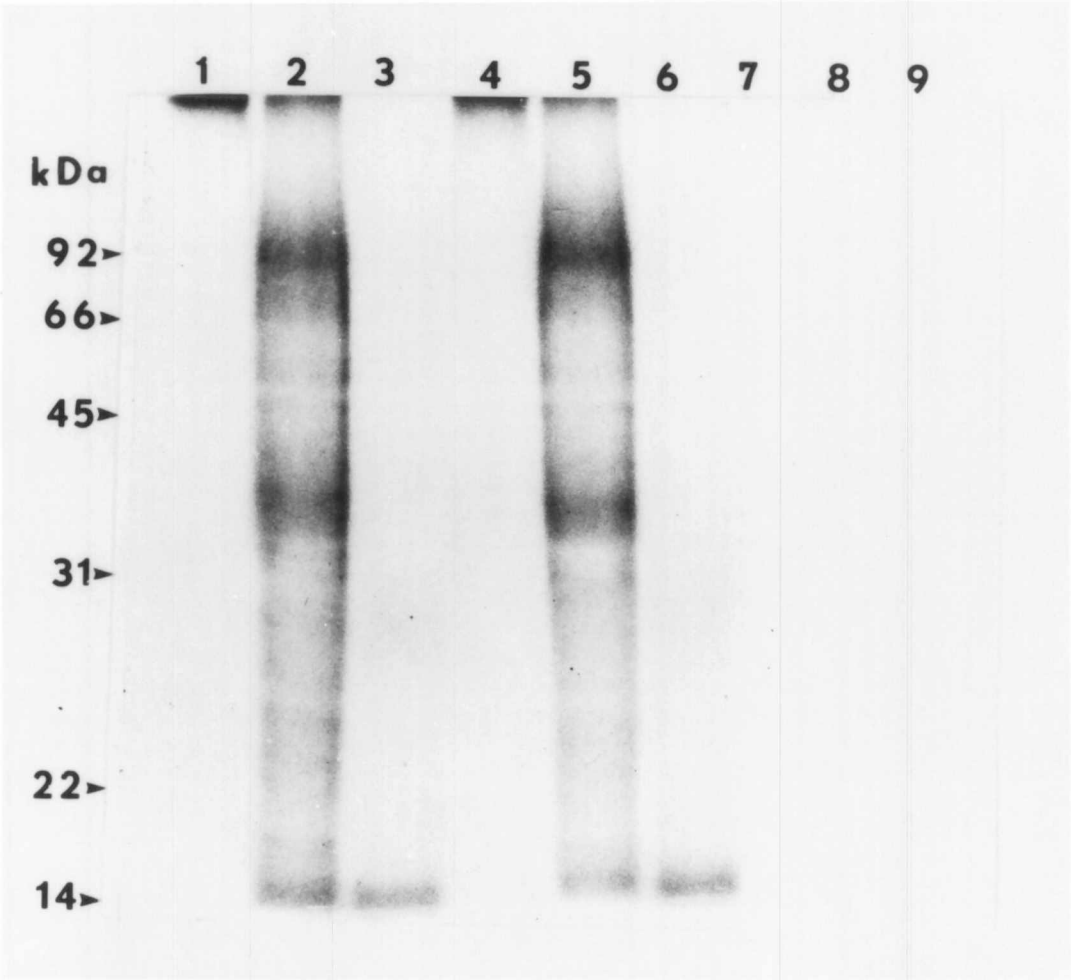
1
2
3
4
5
6
7
8
9
kDa
92
66
45
31
22
14

Figure 36. Autoradiogram of "Western" immunoblot of KRV capsid proteins and nuclease-treated CsCl-purified KRV RF DNA incubated with rabbit anti-KRV capsid antiserum and ^{125}I protein A. Lanes 1 and 2, 400 and 20 ng, respectively, of KRV capsids; Lane 3, 1 µg nuclease-digested CsCl-purified RF DNA. Electrophoresis and transfer were as described in Materials and Methods. A, B, and C indicate positions of capsid proteins A, B, and C.


1
2
3
A
B
C

Because the non-structural proteins of many of the autonomous parvoviruses are encoded by highly conserved DNA sequences (Banerjee et al., 1983), these proteins display a high degree of immunologic cross-reactivity (Cottmore et al., 1983; Rhode and Paradiso, 1983). Therefore, antiserum to one parvovirus' non-structural protein can be used to probe for the non-structural proteins of another parvovirus without interference from reactivity with capsid proteins since capsid proteins appear to be immunologically unrelated among the parvoviruses (see Chapter I). As shown in Figure 37, none of the proteins bound to the RF DNA reacted with antibodies to the non-structural proteins of KRV, H-1, or porcine parvovirus. This is interesting in view of the similarity in molecular weight of RF TP-90 and these non-structural proteins (See Chapter I).

The nuclear lamina is a highly stable, proteinaceous cytoskeletal structure underlying the nuclear membrane consisting largely of three proteins: lamins A, B, and C (Gerace et al., 1978; Boutielle et al., 1983). Since it has been shown that these proteins are also DNA-binding proteins (Lebkowski and Laemmli, 1982a,b) and have molecular weights close to those of two proteins non-covalently bound to RF DNA, nitrocellulose sheets with the non-covalently bound proteins on them were probed with antiserum to lamin C (M_r = 60,000), which will also cross-react with lamin A (M_r = 67,000) (L. Gerace, personal communication). As shown in Figure 38, the proteins from the RF with molecular weights close to those of lamins A and C do react with this antiserum. This observation, along with Figure 33c (page 133), suggests that these proteins originate from the host nuclear lamina.

Figure 37. Autoradiogram of "Western" immunoblot of KRV infected NRK cell lysate and nuclease-digested CsCl-purified KRV RF DNA incubated with PPV-infected pig (A) or H-1-infected hamster (B) antiserum and ^{125}I protein A. Lanes 1, µl of KRV-infected NRK cell lysate prepared by procedure of Paradiso (1984) loaded onto gel; Lane 2, µg nuclease-digested CsCl-purified KRV RF DNA loaded onto gel. kDa, molecular weights of protein standards.

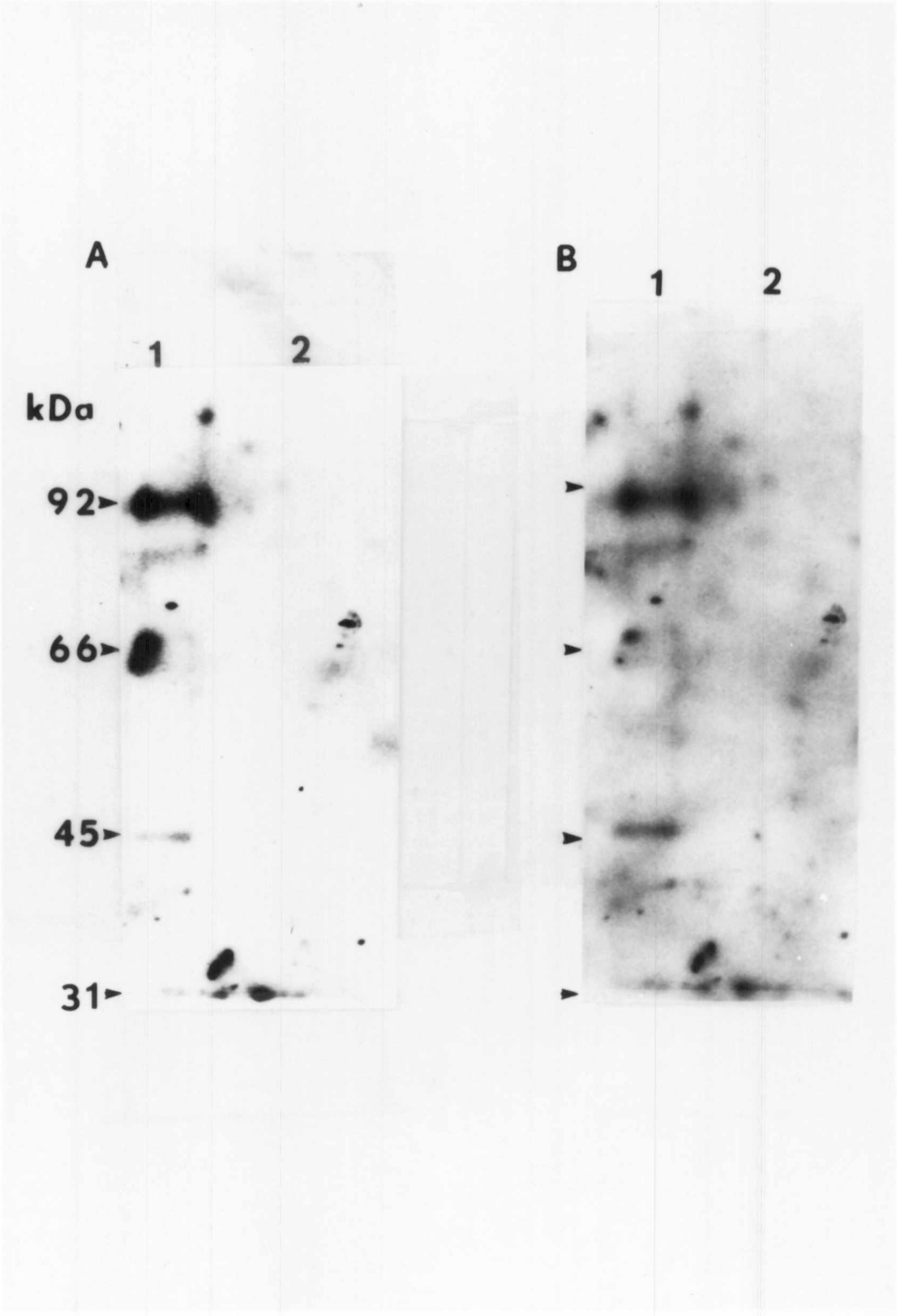
A
1
2
kDa
92
66
45
31
B
1
2

Figure 38. Autoradiogram of "Western" immunoblot of uninfected NRK cell lysate and CsCl-purified KRV RF DNA incubated with guinea pig anti-rat lamin C and ^{125}I protein A. (A) lane 1, uninfected NRK cell lysate prepared by procedure of Paradiso (1984); lane 2, 1 µg CsCl-purified undigested KRV RF DNA; lane 3, molecular weight markers; lane 4, 1 µg CsCl-purified undigested KRV RF DNA electrophoresed, transferred, and incubated with pre-immune guinea pig serum. At left are molecular weights (kDa) of protein standards.

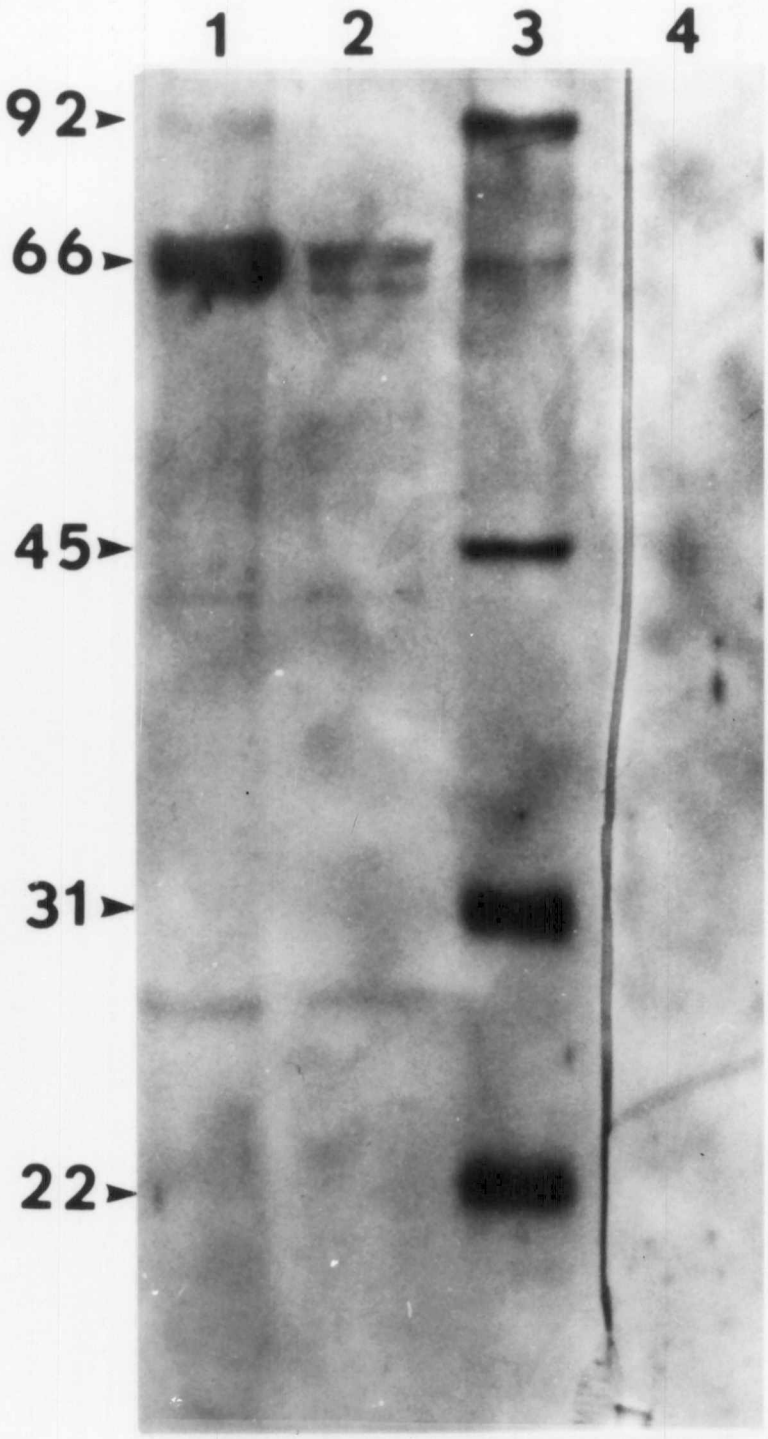
1
2
3
4
92
66
45
31
22

Peptide Analysis

The peptide analysis procedure used here is a variation of the procedure of Cleveland et al. (1977) for the comparison of proteins separated by SDS/polyacrylamide gel electrophoresis. The proteolytic fragments generated are separated on the basis of size alone and homologous regions of proteins should give peptides with identical mobilities. As shown in Figure 39, the peptides generated by V-8 or α-chymotrypsin cleavage of RF TP-40 also appear to be present in digests of RF TP-90.

Alkaline Agarose Gel Electrophoresis of PstI-digested RF DNA

To determine whether both RF TP-40 and 90 bind to the same end (simultaneous binding) or some ends have RF TP-90 while others have RF TP-40 (mutually exclusive binding), PstI-digested RF DNA was subjected to alkaline SDS/agarose gel electrophoresis. In the case of simultaneous binding, two populations of the terminal (A and D) fragments should be seen: a faster migrating band corresponding to the strand with no protein bound and a slower band from the strand with both proteins bound. If these proteins show mutually exclusive binding, three sub-populations should be seen corresponding to (in order of decreasing mobility): the strand with no protein, the strand with RF TP-40, the strand with RF TP-90. Three sub-species of the A fragment (A, A_1, A_2) can be seen in Figure 40 (lane 1), consistent with a mutually exclusive binding model. The fact that the two slower migrating bands (A_1 and A_2) are eliminated and the faster migrating band (A) becomes more intense after

Figure 39. Autoradiogram of 15% SDS/polyacrylamide gel of partial proteolytic digests of ^{125}I RF TP-90 (lanes 1, 3, 5) and RF TP-40 (lanes 2, 4, 6). Samples were treated as follows prior to electrophoresis: Lanes 1 and 2, undigested control; lanes 3 and 4, digestion with 400 µgα-chymotrypsin; lanes 5 and 6, digestion with 10 ng S. aureus V-8 protease. Purification and digestion of RF TP-90 and 40 were as described in Materials and Methods.

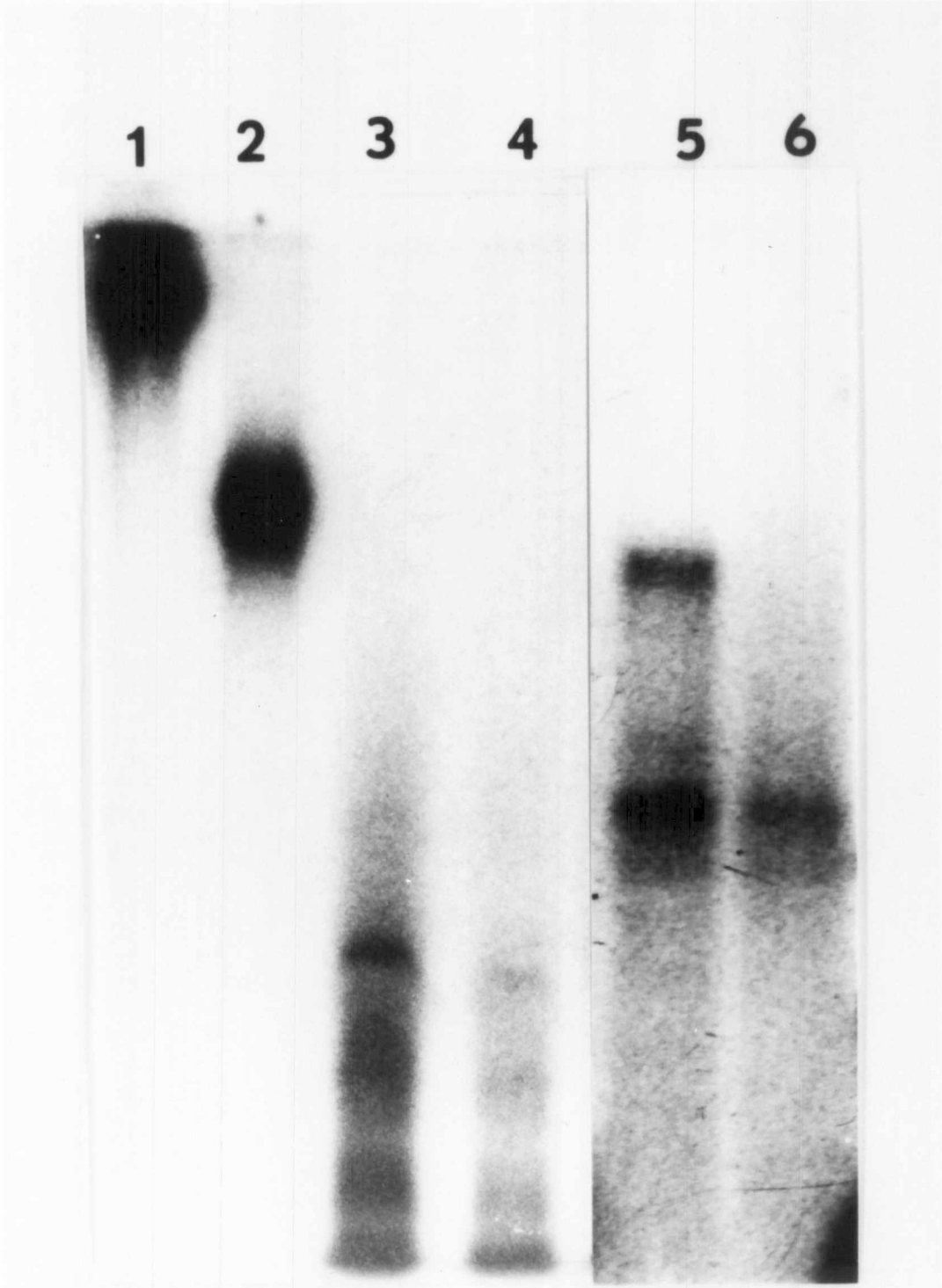
1
2
3
4
5
6

Figure 40. Alkaline SDS/agarose gel (1.5%) electrophoresis of PstI-digested KRV RF DNA before (lane 1) and after (lane 2) digestion with proteinase K. Labels are explained in text. Gel was neutralized with 1.0 M Tris-Cl, pH 8.0, washed with water before staining as described in Figure 23 (p. 110).

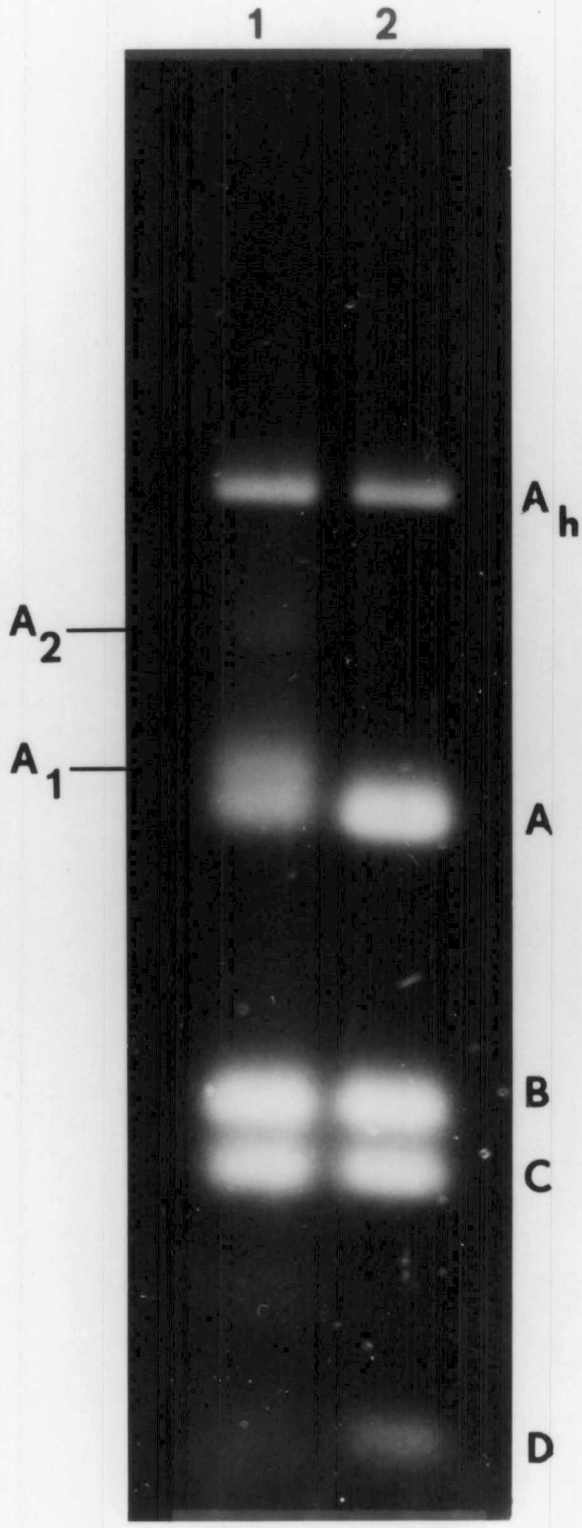
1
2
A h
A 2
A 1
A
B
C
D

protease treatment (Figure 40, lane 2) indicates that this altered mobility is indeed due to the presence of protein. The band designated A_h corresponds to the A fragment from RF molecules with covalently linked viral and complementary strands (see Figure 1, structure II, p. 9). The observation that the mobility of this band is unaffected by proteolysis (Figure 40, lanes 1 and 2) is expected since this molecule has no free 5' end to which the protein can bind. Unfortunately, only two sub-species of the D fragment can be seen, the third being obscured by the B and C bands.

4. DISCUSSION

This chapter describes the first isolation of two proteins, RF TP-40 and RF TP-90, which appear to be covalently bound to the termini of KRV RF DNA. Previous studies (Revie et al., 1979) provided evidence suggesting that a protein of 60-70 kDa was covalently linked to the RF DNA of parvovirus H-1. Subsequently, Astell et al. (1982) claimed to have isolated a 60 kDa RF TP for MVM, consistent with the predicted result (Revie et al., 1979), but did not demonstrate an exclusive association with RF DNA termini. Polypeptides in the 60 kDa range were also detected here, but results clearly indicate that they are non-covalently bound. This difference may be due to the virus and cell systems used or to differences in sample preparation. The difference between the observed molecular weights of the KRV RF TP's and the value predicted by buoyant density shift experiments could be explained by considering the RF DNA to be a

mixed population of molecules with either RF TP-40 or 90 at either end. Thus, the predicted "molecular weight" would be the average of the two, with 30% of the ends bearing RF TP-40 and 70% bearing RF TP-90, assuming that the density shift is due entirely to the loss of these two proteins.

The copurification of RF TP-40 and 90 with RF DNA through a number of harsh conditions expected to eliminate non-covalent association (Figures 26, 27, 29; pp. 117, 120, 124) and the fact that they are released only after digestion of the RF DNA (Figures 32-34; pp. 131, 133, 137) strongly suggest that they are covalently bound to the DNA. The specific association of these proteins with terminal restriction fragments of the RF DNA (Figure 35, p. 140) suggests that they are covalently bound to the termini of the DNA. The sensitivity of the RF DNA to exonuclease III and resistance to λ exonuclease (Figure 31, p. 128) suggests that the covalent linkage is to the 5' termini. Alkaline SDS/agarose gel electrophoresis results (Figure 40) are consistent with mutually exclusive binding of these two proteins to the RF DNA termini and also with their binding to the 5' terminal phosphate, since molecules with no free 5' ends also appear to lack protein.

The origin of these proteins remains to be determined. They do not appear to be related to the virus capsid proteins (Figure 36, p. 142). Antisera to the virus-encoded non-structural proteins of KRV, H-1, MVM, and porcine parvovirus (Rhode and Paradiso, 1983; Cottmore et al., 1983), which have molecular weights close to RF TP-90,

do not cross-react with either terminal protein (Figure 37, p. 145). A 90 kDa protein covalently bound to H-1 RF DNA has recently been isolated that displays the same antigenic behavior (P. Paradiso, personal communication) as KRV RF TP-90. These observations suggest that RF TP-90 and RF TP-40 are not encoded by any of the virus' open reading frames (Rhode and Paradiso, 1983) and, by elimination, are of host origin. A caveat to this conclusion is that RF TP-90 or 40 may be highly-modified, and consequently, non-cross-reactive, forms of the non-structural protein.

An interesting parallel can be drawn between the structure and replication of KRV RF and the genes for the ribosomal RNA of lower eukaryotes (rDNA). Physarum polycephalum rDNA exists as an autonomously replicating episome with about 150-200 copies per nucleus (Vogt and Braun, 1977). The termini of these linear molecules have palindromic regions which are thought to be used in a hairpin transfer-type mechanism of replication (Bergold et al., 1983). This DNA also appears to have protein covalently bound at its 5' termini as well (Cheung et al., 1981). Tetrahymena rDNA has a similar structure and, in addition, has been shown to be acted upon by a site-specific nicking endonuclease in situ that becomes covalently bound to the DNA (Gocke et al., 1983). These and other observations suggest that KRV may in fact take advantage of an already-extant mechanism within the host cell for the amplification of linear episomal DNAs.

One hypothesis for the origin of RF TP-40 is that it is generated from RF TP-90 by site-specific proteolysis analogous to the processing of the adenovirus terminal protein (Challberg and Kelly, 1981). If this were the case, then the two proteins should have sequence homology which could be detected by common proteolytic peptides. The results shown in Figure 39 are consistent with such homology and suggest that this hypothesis may be correct.

Covalent nucleic acid-protein complexes have been observed in a number of viral systems (Rekosh et al., 1977; Harding et al., 1978; Flanagan et al., 1977; Brown et al., 1982) and have been suggested to occur in the chromosomal DNA of a number of higher organisms (Werner and Petzelt, 1981; Werner et al., 1981). The viral covalently bound proteins have usually been implicated in the initiation of the replication of the DNA to which they are bound (Brown et al., 1982; Licky et al., 1982; Penalva and Salas, 1982; Nomoto et al., 1977). As yet, there has been no direct demonstration for such a role for the parvovirus terminal protein, although RF DNA synthesized de novo in the cell-free system of Siegl and co-workers (Muller and Siegl, 1983a,b) behaved as if it had covalently bound protein.

Several authors have proposed that the terminal protein is the site-specific endonuclease in the "hairpin transfer" replication model for parvoviruses (Revie et al., 1979; Astell et al., 1982; Rhode and Klaassen, 1982). A possible precedent for this would be the case of Tetrahymena rDNA (Cheung et al., 1981), discussed above. This role would be, at least superficially, analogous to that of the

gene A protein in ØX174 DNA replication (Brown et al., 1982), namely, generation of a site-specific nick with a 3' OH, that is elongated by host replicative enzymes, and a 5' phosphate to which the protein is covalently bound. This similarity continues in that, in both systems, the covalent DNA-protein complex is not observed in the mature virion, but is cleaved during encapsidation of the DNA (see Muller and Siegl, 1983a,b and above). This implies that newly-synthesized viral DNA initially has covalently bound terminal protein that is removed by some activity within the cell that is capable of cleaving alkali-stable nucleic acid-protein linkages, since the DNA of mature virions appears to be devoid of covalently bound protein (Snyder et al., 1982; Mitra et al., 1982). In fact, an activity has been found in HeLa cells which can cleave the phosphotyrosine linkage between poliovirus RNA and 5' terminal protein (Ambros et al., 1978).

The origin of the non-covalently bound proteins is not entirely clear. None appear to be immunologically related to capsid or non-structural proteins (Figures 35 and 36, pp. 140 and 142). Mixing experiments with protease treated RF DNA and uninfected cell extracts (Figure 33c, p. 133) suggest that some of these proteins are of cellular origin. The proteins removed by 2-mercaptoethanol treatment (Figure 33b) may be related to proteins with similar properties observed by others (Razin et al., 1982; Lebkowski and Laemmli, 1982a,b) that have been implicated in maintenance of the stability of the nuclear matrix and the binding of cellular DNA

to this structure. In both cases, it is possible that these proteins are not bound to the DNA itself, but rather are bound, via disulfide bridges, to proteins which are bound to the DNA.

The finding that two of the non-covalently bound proteins are immunologically related to nuclear lamina proteins (Figure 38, p. 147) is not surprising since these proteins are known to be rather strong DNA-binding proteins (Lebkowski and Laemmli, 1982a). In HeLa cells, these proteins bind DNA at intervals of approximately 5 kilobase pairs (coincidentally the size of KRV RF) and are thought to form the basis for the commonly observed supervoiled loop domains of cellular DNA (Lebkowski and Laemmli, 1982b).

The possible interaction of KRV RF DNA with the nuclear matrix is particularly interesting in view of evidence that this structure is a site for cellular DNA replication (Pardoll et al., 1980; McCready et al., 1980) and transcription (Ciejek et al., 1983) and that the DNA of a number of viruses can be found tightly associated with it (Nelkin et al., 1980; Buckler-White, 1980; Younghusband and Maundrell, 1982). Binding of KRV RF DNA to the nuclear matrix has not yet been demonstrated, although Lu III DNA has been found associated with non-histone "chromosomal" protein (Gautschi et al., 1976) and Bates et al. have found evidence for the binding of bovine parvovirus DNA to the nuclear matrix (R. C. Bates, personal communication).

In summary, KRV replication appears to make use of a number of structures and processes already present in the uninfected

cell. As stated in the introduction, this should make KRV an excellent model system for analyzing the DNA replication machinery of the eukaryotic cell.

CHAPTER V

SUMMARY AND PERSPECTIVES

The research summarized in this dissertation has covered two rather diverse aspects of the biochemistry of parvoviruses which have not, to date, been explored in great detail: the architecture of the virus capsid and the maintenance of its stability, and the structure and composition of viral DNA. The purpose of this chapter is to briefly review the major conclusions and proposals of these projects separately and speculate on future directions which work in these areas might take.

The unusual stability of the parvovirus capsid to extremes of pH, temperature, detergents and organic solvents suggests that there are very strong interactions among the capsid proteins and between the capsid proteins and the viral DNA. The studies described in Chapter II were undertaken to characterize these interactions and how they contribute to the unusual stability of the virion. Double-shelled capsids, with properties strikingly similar to KRV, have been proposed for a number of other viruses such as tomato bushy stunt virus and related viruses (Jacrot, 1981). At least a superficial similarity exists between KRV and these viruses in terms of shape, genome structure and size, lack of polyamines, and distribution of basic amino acids as described in Chapter II.

An examination of previously published nucleotide sequences for the capsid proteins of two parvoviruses closely related to KRV

revealed that the basic residues of these proteins are highly clustered; in the case of the A protein, the N-terminus is especially basic. It seems reasonable to propose that these domains of high basic amino acid content form the inner shell of the virus. Such clustering of basic amino acids near the N-terminus of capsid proteins appears to be a mechanism used by a number of other viruses (see Chapter II).

It is clear that the presence of DNA noticeably increases the capsid's sensitivity to alkali. It is proposed that this destabilization is due, in large part, to the repulsion of the DNA-phosphate groups, consistent with theoretical arguments discussed previously. Because the virus was shown to lack polyamines, it is possible that the domains of basic amino acids on the capsid proteins perform a charge neutralization function and constitute the inner shell of the virus. The number of basic amino acids in these domains is sufficient to neutralize approximately 30% of the DNA-phosphate and the titration of these groups may be responsible for the alkaline destabilization of full capsids. This ionic interaction of the capsid proteins with the viral DNA could at least partially explain the stability of the virus capsid, particularly under conditions of high temperature, high concentrations of organic solvents, and low pH.

It also appeared from the neutron scattering data that the outer shell of the capsid was rather hydrophobic. This was supported by the finding of a large domain of hydrophobic amino acids in the central portion of the primary sequence deduced for the capsid

proteins of H-1. These observations may further explain the stability of parvovirus capsids and their well-known (and rather annoying) tendency to aggregate (see Figure 2, p. 26), especially at low pH (Johnson and Bodily, 1975).

A number of possible directions for research into parvovirus architecture can be envisioned. The structure of full capsids should be examined by small angle neutron scattering using contrast variation to establish the extent of interaction between DNA and protein. Since neutron scattering is non-destructive, the virus isolated here could be used for higher resolution studies using X-ray diffraction and NMR spectroscopy to examine the structure and dynamics of protein-nucleic acid interactions in the KRV virion on an atomic scale. Starting with DNA clones of parvovirus genomes, deletion of specific regions of the known coding sequences for the capsid proteins should allow the mapping of domains of these proteins within the virion using the techniques mentioned above. Some of the hypotheses regarding the orientation and functions of these domains could then be tested.

From the work on DNA methylation, it can be concluded that both KRV RF DNA and virion DNA lack m^5C, as does the DNA of most other viruses, while both DNAs can serve as a substrate for the host DNA methyltransferase, suggesting that they are either sequestered and thus inaccessible to this enzyme in the cell, or that viral infection in some way results in an inactivation of the host DNA methylation processes. If the DNA is somehow sequestered

from methylation, it would be interesting to know its mechanism, since it could lead to an understanding of how cellular DNA, such as that in active genes, is protected from methylation. Alternatively, it is possible that the rapid encapsidation of viral DNA is in some way responsible for the lack of methylation of the virion DNA. Very little is known about the chromatin structure of the intracellular forms of parvoviral DNA and how it might affect the accessibility of the DNA to various enzymes.

Because KRV DNA normally does not have m^5C, it might be of interest to use restriction methylases and DNA transfection to specifically methylate particular portions (promoters, polyadenylation regions, or coding regions) of the known genes of KRV and determine the effect on the expression of these genes. It would also be of great interest to investigate the methylation state of intracellular parvovirus DNA during latent infections, such as those established by AAV.

The final area of research described in this dissertation, the study of proteins which are tightly or covalently bound to KRV RF DNA, probably leaves open the greatest number of possibilities for future investigation. A number of viral systems were referred to that, like KRV, have protein covalently bound to the nucleic acid at some point. KRV differs from many of these systems in that the DNA in the virion does not appear to have a protein covalently bound and in this regard most closely resembles ØX174.

Based on experiments using antibodies to the known viral proteins, we suggest that the covalently bound proteins are not of viral origin and are, therefore, host proteins. Type II DNA topoisomerases from several eukaryotic sources have been shown to nick duplex DNA and form covalent complexes with the 5' terminus of the DNA substrate as part of their catalytic cycle (Sander and Hsieh, 1983; Tewey et al., 1984), but they have molecular weights far greater than those of the proteins found here (Miller et al., 1981; Sander and Hsieh, 1983). It may be that the RF TP's described are breakdown products of cellular type II topoisomerases, or that they may represent an as-yet uncharacterized class of DNA-binding proteins.

In addition to the RF TP's, a number of proteins were found which are very tightly, but non-covalently, bound to the DNA. Two of these proteins appear to be from the nuclear lamina; the origin of the others is unknown. The possibility was raised that KRV RF DNA may in some way interact with the nuclear matrix, but the indirect and inconclusive nature of evidence in this area and the lack of a clear definition of the nuclear matrix as a physiologically significant entity make an extended discussion of this subject pointless at this time. The most that can be said is that parvoviruses may interact with a group of proteins (a structure?) in the nucleus that have been proposed to be the site of cellular replication and transcription. Alternatively, these proteins may become artifactually bound to the RF DNA during the process of cell

lysis and DNA isolation. Clearly, a great deal of work must be done in other fields before the question of the interaction of KRV with the nuclear matrix can be resolved.

The work described on the RF-binding proteins has provided some answers, and may provide a framework for the formulation of future experiments in this area. If the purification scheme described in Chapter IV were put on a larger scale, it would be possible to isolate microgram quantities of these proteins which could then be used for the production of monoclonal antibodies. With such antibodies in hand, the task of determining the origin and possible functions of these proteins should be made much easier. Antibody affinity chromatography should allow purification of these proteins in native form to determine if they have any enzymatic activities such as site-specific nickase, topoisomerase, DNA polymerase, or primase. An alternative approach to the purification of these proteins would be DNA-affinity chromatography using the cloned DNA of one of the parvoviruses already described. Since at least some of these proteins appear to be of host origin, it should be possible to start the purifications with uninfected cells.

Indirect evidence for the functions of these proteins may come from studies on their role in parvovirus replication. Kinetic labeling studies may make it possible to determine at what point during RF DNA synthesis--initiation, elongation, or termination--the terminal proteins become bound. It would also be useful to

know whether these proteins are found associated with the RF DNA only at specific times during the life cycle of the virus, such as during progeny RF DNA synthesis or encapsidation of viral DNA. The relationship between RF TP-90 and RF TP-40 should be more closely examined either by more detailed peptide analysis or by microsequence analysis. A possible precursor-product relationship between these two proteins could be investigated using pulse-chase experiments with [^{3}H]thymidine and alkaline agarose gel electrophoresis to separate the populations of RF DNA ends having RF TP-90 and 40.

Although the nuclear matrix is a relatively undefined structure within the cell, the nuclear lamina is clearly a distinct cytoskeletal entity (Gerace et al., 1978) and its possible interaction with KRV RF DNA is very intriguing. One way to study this possibility more closely would be to use in situ hybridization of fixed, infected cells with radiolabeled probes specific for parvovirus DNA or proteins (Blum et al., 1983). Coupled with electron microscopy, this technique would provide a powerful means of identifying and localizing parvovirus gene products and DNA within the infected cell. Nuclease protection experiments with the parvovirus DNA in these complexes may provide further insights into the topology and sequence specificity, if any, of this interaction. Since the DNA of several parvoviruses has been sequenced and the locations of the replication origins and trnascriptional promoters are known, it might be possible to evaluate the physiological significance of any sequence-specific interactions uncovered.

Kilham rat virus appears to utilize a number of structure and processes which have already been shown to be utilized by other viruses or the eukaryotic cell. The study of the structure and stability of the virus could conceivably provide a model for the packaging of DNA into any small structure, such as the cell nucleus. Continued studies on DNA methylation and gene expression using KRV may be enlightening, since it is a system where DNA methylation is not normally found. The complete dependence of parvovirus replication on actively growing cells coupled with the isolation of proteins, likely to be of host origin, tightly bound to KRV RF DNA, suggests that these viruses may provide a valuable model system for the study of DNA replication in the eukaryotic cell.

BIBLIOGRAPHY

BIBLIOGRAPHY

Ambros, V., Pettersson, R. F., & Baltimore, D. (1978) Cell 15, 1439-1446.

Ames, B. N., & Dubin, D. T. (1960) J. Biol. Chem. 235, 769-775.

Ames, B. N., Dubin, D. T., & Rosenthal, S. M. (1958) Science 127, 814-212.

Astell, C. R., Smith, M., Chow, M. B., & Ward, D. C. (1979) Cell 17, 691-703.

Astell, C. R., Thompson, M., Chow, M. B., & Ward, D. C. (1982) Cold Spring Harbor Symp. Quant. Biol. 47, 751-762.

Astell, C. R., Thompson, M., Merchlinsky, M., & Ward, D. C. (1983) Nucl. Acids Res. 11, 999-1018.

Bachrach, V., Fischer, R., & Klein, I. (1975) J. Gen. Virol. 26, 287-294.

Banerjee, P. T., Rothrock, R., & Mitra, S. (1981) J. Virol. 40, 118-125.

Banerjee, P. T., Olson, W. H., Allison, D. P., Bates, R. C., Snyder, C. E., & Mitra, S. (1983) J. Mol. Biol. 166, 257-272.

Bates, R. C., Snyder, C. E., Banerjee, P. T., & Mitra, S. (1984) J. Virol. 49, 319-324.

Bergold, P. J., Campbell, G. R., Littau, V. C., & Johnson, E. M. (1983) Cell 32, 1287-1299.

Berns, K. I., & Hauswirth, W. W. (1978) in Replication of Mammalian Parvoviruses, eds. Ward, D. C., & Tattersall, P. (Cold Spring Harbor Laboratory, Cold Spring Harbor, NY) 13-32.

Berns, K. I., & Hauswirth, W. W. (1979) Adv. Virus Res. 25, 407-449.

Blum, H. E., Stowring, L., Figus, S., Montgomery, C. K., Haase, A. T., & Vyas, G. N. (1983) Proc. Natl. Acad. Sci. USA 90, 6685-6688.

Bolden, A., Noy, G. P., & Weissbach, A. (1977) J. Biol. Chem. 252, 3351-3356.

Bourgignon, G. J., Tattersall, P. J., & Ward, D. C. (1976) J. Virol. 20, 290-306.

Bouteille, M., Bouvier, D., & Seve, A. P. (1983) Int. Rev. Cytol. 83, 135-182.

Brown, D. R., Reinberg, D., Schmidt-Glenewinkel, T., Roth, M., Zipurski, S. L., & Hurwitz, J. (1982) Cold Spring Harbor Symp. Quant. Biol. 47, 701-715.

Brown, N. D., Strickler, M. P., & Whaun, J. M. (1982) J. Chromatog. 245, 101-108.

Burnette, W. N. (1981) Anal. Biochem. 112, 195-203.

Buckler-White, A. J., Humphrey, G. W., & Pigiet, V. (1980) Cell 22, 37-46.

Caspar, L. D., & Klug, A. (1962) Cold Spring Harbor Symp. Quant. Biol. 27, 1-24.

Cavalier-Smith, T. (1974) Nature 250, 467-469.

Challberg, M. D., & Kelly, T. J. (1981) J. Virol. 38, 272-282.

Chauvin, C., Witz, J., & Jacrot, B. (1978) J. Mol. Biol. 124, 641-651.

Cheung, M. K., Drivas, D. T., Littau, V. C., & Johnson, E. M. (1981) J. Cell Biol. 91, 309-314.

Ciejek, E. M., Tsai, M. J., & O'Malley, B. W. (1983) Nature 306, 607-609.

Cleveland, D. W., Fischer, S. G., Kirscher, M. W., & Laemmli, U. K. (1977) J. Biol. Chem. 252, 1102-1106.

Clinton, G. M., & Hayashi, M. (1975) Virology 66, 261-267.

Clinton, G. M., & Hayashi, M. (1976) Virology 74, 57-63.

Cohen, S. S., & McCormick, F. P. (1979) Adv. Virus Res. 24, 331-387.

Cole, G. A., & Nathanson, N. (1969) Acta. Virol. 13, 515-520.

Coltmore, S. F., Sturzenbecker, L. J., & Tattersall, P. T. (1983) Virology 129, 333-343.

Davidson, N., & Szybalski, W. (1971) in The Bacteriophage Lambda, ed. Hershey, A. D. (Cold Spring Harbor Laboratory, Cold Spring Harbor, NY) 45-82.

Dobson, P. R., and Helleiner, C. W. (1973) Can. J. Microbiol. 19, 35-41.

Doc-Nguyen, H., Rosenblum, E. N., & Ziegel, R. F. (1966) J. Bact. 92, 1133-1140.

Doerfler, W. (1983) Ann. Rev. Biochem. 52, 93-124.

Engler, W. D., Baer, P. N., & Kilham, L. (1966) Arch. Pathol. 82, 93-98.

Faust, E. A., Gloor, G., Macintyre, M. F., & Nagy, R. (1984) Biochem. Biophys. Acta 781, 216-224.

Feitelson, M. A., Wettstein, F. O., & Stevens, J. G. (1981) Anal. Biochem. 76, 473-479.

Fife, K. H., Berns, K., & Murray, K. (1977) Virology 78, 475-483.

Flanagan, J. B., Pettersson, R. F., Ambros, V., Hewelett, M. J., & Baltimore, D. (1977) Proc. Natl. Acad. Sci. USA 74, 961-965.

Fout, G. S., Medappa, K. C., Mapoles, J. E., & Rueckert, R. R. (1984) J. Biol. Chem. 259, 3639-3643.

Frankel-Conrat, H., & Wagner, R. R. (1974) in Comprehensive Virology I (Plenum Press, NY), p. 37.

Frearson, P. M., & Crawford, L. V. (1972) J. Gen. Virol. 14, 141-155.

Fujisawa, H., & Hayashi, M. (1977) J. Virol. 24, 303-313.

Gautschi, M., Siegel, G., & Kronauer, G. (1976) J. Virol. 20, 29-38.

Gerace, L., Blum, A., & Blobel, G. (1978) J. Cell Biol. 79, 546-566.

Gibson, W., & Roizman, B. (1971) Proc. Natl. Acad. Sci USA 68, 2818-2821.

Gocke, E., Bonven, B. J., & Westergaard, O. (1983) Nucl. Acids Res. 11, 7661-7678.

Gosule, L. C., & Schellman, J. A. (1976) Nature 259, 333-335.

Guinier, A., & Fournet, G. (1955) Small Angle Scattering of X-Rays (Wiley, NY).

Hammer, S. M., Richter, B. S., & Hirsch, M. S. (1981) J. Immunol. 127, 144-148.

Handa, H., Shiroki, K., & Shimojo, H. (1977) Virology 82, 84-92.

Harding, N. E., Ito, J., & David, G. S. (1978) Virology 84, 279-282.

Harrison, S. C., Olson, A. J., Schutt, C. E., Winkler, F. K., & Bricogne, G. (1978) Nature 276, 368-373.

Hermondson, M. A., Abad-Zapatero, C., Abdel-Meguid, S. S., Pundak, S., Rossman, M. G., & Tremaine, J. H. (1982) J. Virol. 119, 133-149.

Jacrot, B. (1976) Rep. Prog. Physics 39, 911-953.

Jacrot, B. (1981) in Comprehensive Virology 17, eds. Fraenkel-Conrat, H., & Wagner, R. R. (Plenum Press, NY) 129-181.

Jacrot, B., & Zaccai, G. (1981) Biopolymers 20, 2413-2426.

Jahn, R., Schiebler, W., & Greengard, P. (1984) Proc. Natl. Acad. Sci. USA 81, 1684-1687.

Johnson, F. B., & Bodily, A. D. (1975) Proc. Soc. Exp. Biol. Med. 150, 585-590.

Kaper, J. M. (1975) The Chemical Basis of Virus Structure, Dissociation and Reassembly (American Elsevier, NY).

Karasaki, S. (1966) J. Ultrastruc. Res. 16, 109-122.

Kelly, D. C., & Elliott, R. M. (1977) J. Virol. 21, 408-410.

Kilham, L., & Oliver, L. J. (1959) Virology 7, 428-437.

Koczot, F. J., Carter, B. J, Garon, C. F., & Rose, J. A. (1973) Proc. Natl. Acad. Sci. USA 70, 215-219.

Koehler, W., Hendricks, R. W., Child, H. R., King, S. R., Lin, J. S., & Wignall, G. D. (1981) in Scattering Techniques Applied to Supramolecular and Non-Equilibrium Systems, eds. Chen, S. N., Chu, B., & Nossal, R. (Plenum Press, NY), 75-80.

Kolleck, R., Tseng, B. Y., & Goulian, M. (1982) J. Virol. 41, 982-989.

Lanzer, W., & Holowczak, J. A. (1975) J. Virol. 16, 1254-1268.

Lavelle, G., & Mitra, S. (1978) in Replication of Mammalian Parvoviruses, eds. Ward, D. C., & Tattersall, P. T. (Cold Spring Harbor Laboratory, Cold Spring Harbor, NY), 219-229.

Lauer, W. G. (1970) Virology 41, 488-500.

Lebkowski, J. S., & Laemmli, U. K. (1982a) J. Mol. Biol. 156, 309-324.

Lebkowski, J. S., & Laemmli, U. K. (1982b) J. Mol. Biol. 156, 325-344.

Lepine, P., & Pavilanis, V. (1948) Ann. Inst. Pasteur (Paris) 74, 155-156.

Li, A. T. (1977) Ph.D. Dissertation, University of Tennessee.

Lichy, J. H., Nagata, K., Friefeld, B. R., Enamoto, T., Field, J., Guggenheimer, R. A., Ikeda, J. E., Horwitz, M. S., & Hurwitz, J. (1983) Cold Spring Harbor Symp. Quant. Biol. 47, 731-740.

Maniatis, T., Fritsch, E. F., & Sambrook, J. (1982) Molecular Cloning, (Cold Spring Harbor Laboratory, Cold Spring Harbor, NY), 156.

Margolis, G., & Kilham, L. (1970) Lab. Invest. 22, 478-488.

Margolis, G., & Kilham, L. (1975a) Prog. Med. Virol. 20, 113-143.

Margolis, G., & Kilham, L. (1975b) Prog. Med. Virol. 20, 144-179.

Marquardt, D. W. (1963) J. Soc. Ind. Appl. Math. 11, 431-441.

Marx, J. L. (1984) Science 223, 152-153.

Mayor, H. D., & Melnich, J. C. (1966) Nature 210, 331-332.

Mayor, H. D., & Kurstak, E. (1974) Viruses, Evolution and Cancer, eds. Kurstak, E., & Meramorosch, J. (Academic Press, NY), 55-78.

McCready, S. J., Godwin, J., Mason, D. W., Brazell, I. A., & Cook, P. R. (1980) J. Cell Sci. 46, 365-386.

Merchlinski, M. J., Tattersall, P. T., Leary, J. J., Cottmore, S. F., Gardiner, E. M., & Ward, D. C. (1983) J. Virol. 47, 227-232.

Meyndier, G., Vago, C., Planteion, G., & Atger, P. (1964) Rev. Zool. Agr. Appl. 63, 207-212.

Mitra, S. (1980) Ann. Rev. Genet. 14, 347-397.

Mitra, S., & Kaesberg, P. (1965) J. Mol. Biol. 14, 558-571.

Mitra, S., Snyder, C. E., Bates, R. C., & Banerjee, P. T. (1982) J. Gen Virol. 61, 43-54.

Moore, P. B. (1980) J. Appl. Cryst. 13, 168-175.

Muller, D. E., & Siegl, G. (1983a) J. Gen. Virol. 64, 1043-1054.

Muller, D. E., & Siegl, G. (1983b) J. Gen. Virol. 64, 1055-1067.

Myers, M. W., & Carter, B. J. (1981) J. Biol. Chem. 256, 567-570.

Nass, J. G. (1973) J. Mol. Biol. 80, 157-175.

Nelkin, B. D., Pardoll, D. M., & Vogelstein, B. (1980) Nucl. Acids Res. 8, 5623-5633.

Nickerson, K. W., & Lare, L. C. (1977) Virology 81, 455-473.

Nomoto, A., Detjen, B. M., Pozzatti, R., & Wimmer, E. (1977) Nature 268, 208-213.

Olson, A. J., Bricogne, G., & Harrison, S. C. (1983) J. Mol. Biol. 171, 61-94.

Paradiso, P. R. (1983) J. Virol. 46, 94-102.

Paradiso, P. R. (1984) J. Virol. 52, 82-87.

Paradiso, P. R., Williams, K. R., & Constantino, R. L. (1984) J. Virol. 52, 77-81.

Pardoll, D. M., Vogelstein, B., & Coffey, D. S. (1980) Cell 19, 527-536.

Penalva, M. A., & Salas, M. (1982) Proc. Natl. Acad. Sci. USA 79, 5522-5526.

Pintel, D., Dadachanji, D., Astell, C. R., & Ward, D. C. (1983) Nucl. Acids Res. 11, 1019-1038.

Prage, L., & Pettersson, V. (1982) Virology 45, 364-373.

Pritchard, C., Stout, E. R., & Bates, R. C. (1981) J. Virol. 37, 352-362.

Razin, S., Chernokhvostov, V. V., Roodyn, A. V., Zbarsky, I. B., & Georgiev, G. P. (1981) Cell 27, 65-73.

Reimer, S. G., & Bloomfield, V. A. (1978) Biopolymers 17, 785-794.

Rekosh, D.M.K., Russell, W. C., Bellet, A.J.D., & Robinson, A. J. (1977) Cell 11, 283-295.

Revie, D., Tseng, B. Y., Grafstrom, R. H., & Goulian, M. (1979) Proc. Natl. Acad. Sci. USA 76, 5539-5544.

Rhode, S. L. (1973) J. Virol. 11, 856-861.

Rhode, S. L. (1974a) J. Virol. 13, 400-410.

Rhode, S. L. (1974b) J. Virol. 14, 791-801.

Rhode, S. L. (1976) J. Virol. 17, 659-667.

Rhode, S. L. (1977a) J. Virol. 21, 694-712.

Rhode, S. L. (1977b) J. Virol. 21, 446-453.

Rhode, S. L. (1978) J. Virol. 25, 215-223.

Rhode, S. L. (1982) J. Virol. 42, 1118-1122.

Rhode, S. L., & Klaassen, B. (1982) J. Virol. 41, 990-999.

Rhode, S. L., & Paradiso, P. R. (1983) J. Virol. 45, 173-184.

Richards, R., Linser, P., & Armentrout, R. W. (1977) J. Virol. 22, 778-793.

Ruffolo, P. R., Margolis, G., & Kilham, L. (1966) Amer. J. Rathol. 49, 795-824.

Salzman, L. A. (1977) Virology 76, 454-461.

Salzman, L. A., & White, W. (1973) J. Virol. 11, 299-305.

Salzman, L. A., White, W., & McKerle, L. (1972) J. Virol. 10, 573-577.

Shortridge, K. F., & Stevens, L. (1973) Microbios 7, 61-72.

Siegl, G. (1976) Virol. Monogr. 15, 1-109.

Siegl, G., & Gautschi, M. (1976) J. Virol. 17, 841-853.

Simon, D., Grunert, F., Acken, U. V., Doring, H. P., & Kroger, H. (1978) Nucl. Acids Res. 6, 2153-2167.

Sims, J., Koths, K., & Dressler, K. (1978) Cold Spring Harbor Symp. Quant. Biol. 43, 349-365.

Singer, I. I., & Rhode, S. L. (1977a) J. Virol. 21, 713-723.

Singer, I. I., & Rhode, S. L. (1977b) J. Virol. 21, 724-731.

Singhal, R. P. (1974) Sep. Purif. Meth. 3, 339-398.

Snyder, C. E., Schmoyer, R. L., Bates, R. C., & Mitra, S. (1982) Electrophoresis 3, 210-213.

Stillman, B. W. (1983) Cell 35, 7-9.

Szostak, J. W., & Blackburn, E. H. (1982) Cell 29, 245-256.

Tattersall, P. (1978) in Replication of Mammalian Parvoviruses, eds. Ward, D. C., & Tattersall, P. (Cold Spring Harbor Laboratory, Cold Spring Harbor, NY), 53-72.

Tattersall, P., & Ward, D. C. (1976) Nature 263, 106-109.

Tattersall, P., & Ward, D. C. (1978) in Replication of Mammalian Parvoviruses, eds. Ward, D. C., & Tattersall, P. (Cold Spring Harbor Laboratory, Cold Spring Harbor, NY), 3-12.

Tattersall, P., Caute, P. J., Shatkin, A. J., & Ward, D. C. (1976) J. Virol. 20, 273-289.

Tattersall, P. T., Shatkin, A. J., & Ward, D. C. (1977) J. Mol. Biol. 111, 375-394.

Tennant, R. W., & Hand, R. E. (1970) Virology 42, 1059-1067.

Tennant, R. W., Layman, K. R., & Hand, R. E. (1969) J. Virol. 4, 872-879.

Tijssen, P., Van der Hurk, J., & Kurstak, E. (1976) J. Virol. 17, 686-691.

Vasquez, C., & Brailovsky, C. (1965) Expt. Mol. Pathol. 4, 130-140.

Virudachalam, R., Sitarman, K., Heuss, K., Argos, P., & Markely, J. L. (1983a) J. Virol. 130, 351-359.

Virudachalam, R., Sitarman, K., Heuss, K., Argos, P., & Markely, J. L. (1983b) J. Virol. 130, 360-371.

Vogt, V. M., & Braun, R. (1977) Eur. J. Biochem. 80, 557-566.

Vriend, G., Hemminga, M. A., Verdin, B.J.M., Dewit, J. L., & Schaafsma, T. J. (1981) FEBS Lett 134, 167-171.

Ward, D. C., & Dadachanji, D. (1978) in Replication of Mammalian Parvoviruses, eds. Ward, D. C., & Tattersall, P. (Cold Spring Harbor Laboratory, Cold Spring Harbor, NY), 297-313.

Werner, D., & Petzelt, C. (1981) J. Mol. Biol. 150, 297-302.

Werner, D., Zimmerman, H., Rauterberg, E., & Spalinger, J. (1981) Expt. Cell Res. 133, 149-157.

Willis, D. B., & Granoff, A. (1980) Virology 107, 250-257.

Younghusband, H. B., & Maundrell, K. (1982) J. Virol. 43, 705-713.

Youssoufian, H., Hammer, M. S., & Mulder, C. (1982) Proc. Natl. Acad. Sci. USA 79, 2207-2210.

VITA

Clarence Richard Wobbe was born in Marianna, Florida on October October 30, 1957. In 1958, his family moved to Springfield, Ohio, where he attended public schools and graduated with honors from Springfield Shawnee High School in June 1975. After completing a Bachelor of Science degree, with distinction, in Biochemistry at Centre College of Kentucky in June 1979, he enrolled in the doctoral program at The University of Tennessee-Oak Ridge Graduate School of Biomedical Sciences at the Biology Division of Oak Ridge National Laboratory. He received his Doctor of Philosophy degree, with a major in Biomedical Sciences with an emphasis in Biochemistry, in December 1984 and will begin post-doctoral study with Dr. Jerard Hurwitz of the Memorial Sloan-Kettering Cancer Research Center in New York City. He is a member of Phi Beta Kappa, Omicron Delta Kappa, and Phi Kappa Phi honor societies and has been a student affiliate with the American Chemical Society.